Structural Adhesive Bonding for Marine Applications

by

Koh Chun Li, Julie

Thesis submitted to the Faculty of Engineering, University of Glasgow, for the Degree of Master of Science

December, 1997

ACKNOWLEDGEMENT

I would like to take this opportunity to express my sincere gratitude to my supervisor, Professor M.J. Cowling for his instruction, guidance and patience throughout this project and Dr. Esther Knox for her useful discussions. I would also like to thank laboratory technicians, Mr. Alexander Torry for his assistance and advice during all experiments and Mr. Denis Kearns for his help in preparing the specimens and guidance in bonding the specimens. Also my family members for their support and encouragement throughout my course in the University of Glasgow. And lastly to all others who have helped in one way or another in the project.

ABSTRACT

In this present study, four cold curing adhesives, namely, F241, Redux 420, Araldite 2013 and XD 4416 were evaluated for bonding steel tapered double cantilever beams (TDCB) specimens. Fracture toughness of the adhesives were compared and evaluated at temperature range of -40 °C to 60 °C. From the results obtained, F241 bonded joints exhibited the best fracture strength at ambient temperature. Relatively good results were achieved at both high and lower temperature compared to Araldite 2013 and XD4416. It was also observed that XD4416 must be post cured in order to exhibit its full strength.

Fatigue tests in a 'dry' environment were also performed on the bonded joints. R ratio ranging from 0.13 to 0.17 was studied. From the results it is clear that R ratio and maximum load is of considerable importance in influencing fatigue crack growth rate. Fatigue crack growth rate was observed to undergo a number of transitions in a nominally constant compliance test piece subjected to constant load ranges.

The joint fracture strength was improved by incorporating primers. Two primers namely Permabond SIP and A-187 were studied on F241 bonded joints. Since SIP is recommend for F241 by the manufacturer, the highest strength was obtained. Relatively high fracture strength was also obtained with a 5% solution of A-187, in water.

Contents

Chapter 1

INTRODUCTION

Adhesive bonding is a technique for joining materials which, in recent years, has shown itself capable of replacing or supplementing conventional methods such as riveting, welding and mechanical fastening in a variety of applications. The growth in the use of adhesives, especially in technically demanding applications has been rapid and many major developments in the technology of adhesives have been reported. Such developments include the greater use in the automotive and aircraft industries as well as marine industries. Particularly, as marine technology moves towards the design and construction of hydrofoil fast craft and other advanced ships, there is a growing awareness that in order to obtain the requisite high strength, lightweight structures, it will be necessary to adopt many aerospace materials and design concepts. However, the effective use of adhesives in advanced ships depends upon developing adequate design criteria.

One of the significant events of recent years in the adhesives industry has been the development of toughened epoxies and acrylics. These provide properties such as tolerance to oily surfaces, the ability to bond dissimilar surfaces over a wide temperature range, high peel strength and impact resistance for both systems. Such acrylic or epoxy systems, provide good gap filling which also acts as a sealant within a joint enabling the creation of complex joints that are essential for marine applications. In addition, they also offer the ability to dissipate the applied stress over the whole bond area. The toughening mechanisms in the adhesives mean that a crack propagating through the hard phase is stopped on reaching a rubber microsphere[1-6].

Long term durability for adhesively bonded structures under severe service conditions is uncertain due to a shortage of data at present. Thus it is important to note that in order to design adhesively bonded structures there is a need to develop reliability criteria for adhesive joints. The peel and lap shear tests normally used to characterise adhesive strengths are too dependent on specimen geometry to be useful for design purposes. Instead it is judged that fracture toughness is the appropriate criteria for adhesive failure, for essentially two reasons. Firstly, adhesive resins are generally brittle materials that fail by crack initiation and propagation rather than by gross yielding and flow. Secondly, even if the adhesive resin does exhibit yielding, it does so with the confines of a thin bond line that is small compared to the overall joint dimensions, so that the joint as a whole fails in a linear elastic, brittle fashion[7].

Flaw resistance is thus important in the design and analysis of adhesive joints, since it is directly responsible for the reliability and integrity of adhesively bonded structures. The current study incorporated a fracture mechanics approach to examine the flaw tolerance of adhesively bonded connections, using Tapered Double Cantilever Beam (TDCB) test pieces. The TDCB specimen was developed by Mostovoy and Ripling[8,9] consisting of high modulus contoured metal (steel) adherends bonded together by a thin layer of adhesive. A cohesive crack was introduced in the low modulus adhesive layer of the joint and the associated energy release rate was evaluated. The shape of the adherend is designed to give an approximately linear compliance during the course of crack growth.

The current study involved the use of cold-curing structural adhesives only. They were Permabond F241 Toughened Acrylic, Ciba Polymers XD4416 and Araldite 2013 two-part cold-curing Epoxy Adhesives. All of the test specimen specifications used for temperature testing were reduced to half the original specification and fabricated in accordance to the ASTM D3433-93[10], except for fatigue specimens. This was because the original full size specification was unable to fit into the temperature testing chamber. A correlation of the fracture energy release rate between the original and half size specimen was carried out before temperature testing. The results show that, with the compliance changed for the reduced size, the fracture energy release rates obtained were similar to that of original size specification.

In order to reduce uncertainty of using adhesive bonding it is necessary :

(1) To study the fracture strength of adhesively bonded connections

The fracture strength of steel connections bonded by the different adhesives was compared in the current study. Previous observations by M. Fernando, W.W. Harjoprayitno and A.J. Kinloch[11], using aluminium-alloy TDCB joints bonded with toughened epoxy structural adhesives, showed that there was no dependence of the value of the adhesive fracture energy upon the type of surface pre-treatment employed for the substrates prior to bonding at room temperature. Thus in this present study, only grit blasting was used for pre-treatment.

(2) To study the effect of temperature on fracture strength

It was shown that the thermal effect on the adhesives leads to significant changes in the toughness of the joints. It was found that at lower temperatures, the adhesives became brittle, leading to a reduction in strength but less scatter in the results. At high temperatures, the adhesives softened and could not sustain the load, thus leading to failure by plastic yielding in the joint bond line and creating greater scatter in the results[9,12].

(3) To study the effect of using coupling agents to improve durability

The use of primers was examined to improve on the durability of bonded joints. It has been shown elsewhere that a primer can make an essential contribution to the strength and durability of adhesively bonded joints[13,14]. Two different silane coupling agents were used in the current study to improve the adhesion between the acrylic adhesives and steel substrate. The fracture strength of the acrylic/silane coupling agent treated steel joints was investigated. The highest fracture strength was obtained with Permabond SIP, Self-indicating Pre-treatment, when compared with A187 (gamma-Glycidoxypropyltrimethoxysilane). An optimum concentration of the A187 coupling agent was also determined.

(4) Fatigue behavior of bonded joints

Cyclic fatigue behaviour of the TDCB bonded with F241 was examined. The early work by Mostovoy and Ripling[8] clearly established the validity of using a linear-elastic fracture-mechanics (LEFM) approach for describing the fatigue crack growth behaviour. In the current study the effects of varying R ratio on the crack propagation rate were studied in a dry environment.

Chapter 2

LITERATURE REVIEW AND BACKGROUND

2.1 Acrylic And Epoxy Adhesives

Acrylic

This is a rapidly developing group of toughened adhesives based on a variety of acrylic monomers. They contain a dispersed, physically separate, though chemically attached, resilient rubbery phase which "toughens" them. Their viscosity is fairly readily modified and they are available in the form of thin liquids, syrupy resins and thixotrope semi-solids. The curing process of the whole family is based on the radical polymerisation of the acrylic vinyl group giving, as a consequence, a 100% liquid to solid conversion.

Polymerisation is normally induced by one of two methods. In the first, a catalytic hardener may be applied separately to the surface to be bonded, and prior to the application of the adhesive to either surface, or it may be mixed directly into the adhesive just before use. The former technique is very convenient but where larger gaps are involved the second technique is unavoidable.

All these adhesives are intended to cure at room temperature. Some of them should not be heated in the uncured state, while others may be heated or warmed in order to speed the process. The group as a whole copes well with oily surfaces, they are simple to use, robust and some versions are capable of filling large gaps. A variety of cure speed is also available.

Taken as a whole the group has proved to be particularly reliable, even on oily and contaminated surfaces, although some forms appear to be more subject than others to polymerisation inhibition induced by chemical contamination. The properties possessed by the group give the designer enormous freedom. The materials available possess extremely high strength, impact and peel resistance, Fig.1 shows the family of acrylic adhesives used for structural and semi-structural application. One disadvantage is that, by comparison with the epoxides, only a relatively limited number of individual formulations have been developed. However, they can meet many demands and should be considered whenever a robust performance is required[15-17]

The earliest published durability test results involving aluminium adherends was by Zalucha in 1972[18] whereas Minford[19] has also been accumulating extensive weathering data at the Alcoa Labs on the same Hughson chemical adhesive formulation[19]. It seems quite clear from the durability test results that the performance on acetone degreased adherends is much inferior to that found on acidic deoxidised adherends even with the present state of the art high performance designed acrylic. Even so, the usual formulator of acrylic continues to recommend that these structural acrylics can bond effectively to non-cleaned joint surface.

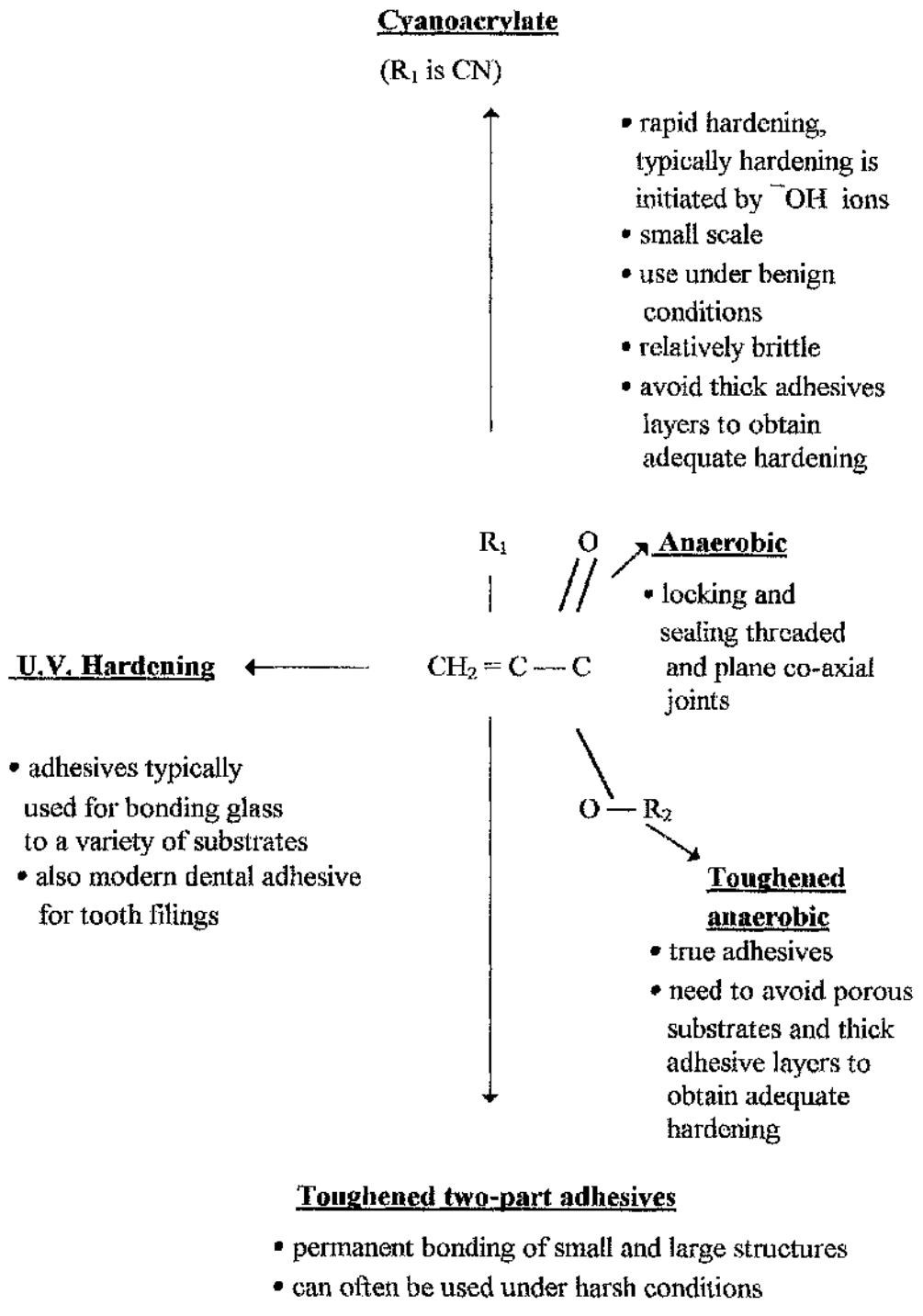

Fig. 1 The family of acrylic adhesives used for structural and semi-structural applications; R_1 and R_2 represent various organic groups[15]

Epoxides

Epoxy adhesives are the most widely used of all structural adhesives. They are available in film form, as liquids, and as pastes. They are among the easiest of all adhesives to process. Cure temperatures vary from ambient to almost 200 °C and bonding pressures with some systems can be little more than contact pressure.

Epoxy adhesives are thermosetting resins which solidify by polymerisation. Like acrylics, the toughened versions contain a dispersed rubbery phase. Once set, they will soften on heating but will not melt. Two-part resin and hardener systems solidify on mixing (sometimes accelerated by heat), while one-part materials require heat to initiate the reaction of a latent catalyst. The properties of the epoxies vary with the type of the curing agent and the type of resin used. Epoxies generally have high cohesive strength, are resistant to oils and solvents and exhibit little shrinkage during curing. They provide strong, durable joints and the excellent creep, fatigue and impact resistance of the toughened versions makes them particularly suitable for structural applications. Table 1 shows the compatibility of the principal structural adhesives with a variety of materials[15-17]. Excellent compatibility was found to be metals except zinc bonded with acrylic and epoxies.

From the data of Minford[20], it is seen that a variety of unfilled and filled room temperature curing, two part epoxy joints had excellent durability in 2 years hot humidity. This performance is predicted, however, on the use of a good surface pre-treatment. In Fig.1a, we see 3 of 5 commercial epoxy produced joints showing only minor change in joint strength after 2 years in an industrial atmosphere.

Table 1 Compatibility of the principle structural adhesives with a variety of composite and associated material[16]

Material to be bonded	Acrylic		Epoxy		PU
	Pseudo 1 Part	Two Part	One part (heat cured)	Two Part	Two Part
Metal					
- Aluminium	1	1	1	1	4
- Steel	1	1	1	1	4
-Zinc	2	2	2	2	4
Thermoplastic					
-Polyamide (Nylon)	2	2	3	2	2
-Polyphenylene	3	3	3	2	1
- Polypropylene	2	2	4	3	1
Thermoset					
- Epoxy	2	2	1	1	2
- Phenolic	2	2	1	1	2
- Polyester hand lay	1	1	2	1	1
- VARI	1	1	2	1	1
- SMC	1	1	2	1	1
- Cold Press	1	1	2	1	1
- Polyurethane -RIM	3	3	4	2	1
Paint					
- Cataphoretic	1	1	1	1	1

Scale :

1 Excellent
2 Good
3 Good but possible problem
4 Unsuitable

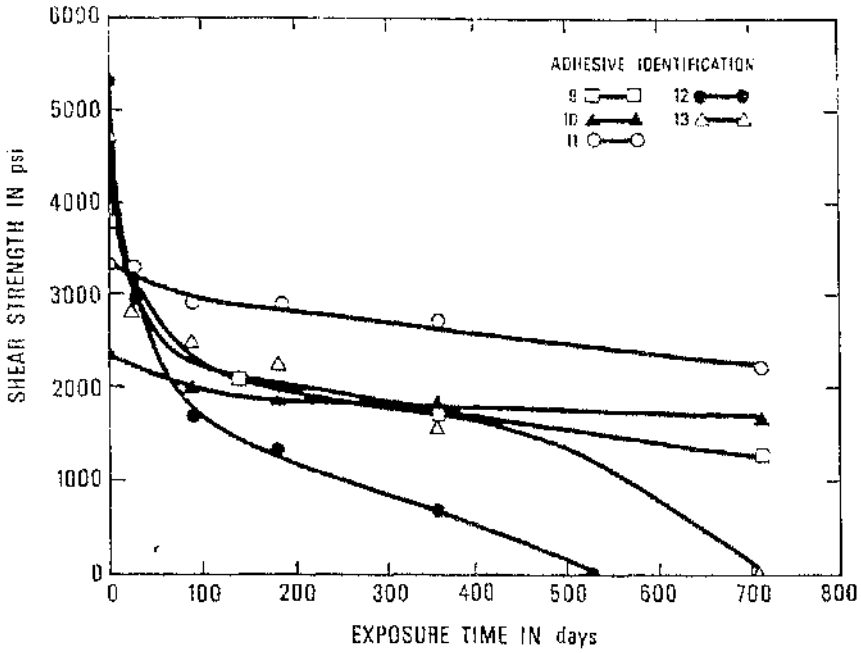

Fig. 1a Epoxy joint- water immersion cycle[21]

2.2 Mechanisms of Adhesion

Joint strength is dependent on the force with which the adhesive and adherends cohere and on the area of the bonding surfaces over which adhesion takes place. Adhesion occurs within an interfacial region of molecular dimensions where the adhesive meet the adherend, and can be reduced where weakly adherend surface layers or contamination are present. Therefore the surfaces to be bonded must be thoroughly cleaned and modified to a suitable condition before joining. Surface pre-treatment may be critical for the durability of bonds even though initial joint strengths with untreated surfaces are satisfactory.

The choice of treatment will be determined by the nature and condition of the adherend materials, and the type of adhesive, the joint function and loading requirements, environment conditions, and economic factors. Rapid solvent cleaning is sometimes sufficient, although a lengthy multiple cleaning and chemical treatment process may be required. In general, the purpose of surface preparation is to ensure joint reliability and prevent premature failure[22].

An initial step towards good adhesion is to ensure that the surface of the adherend is free from dirt, dust, grease, moisture, corrosion products and other contaminates. Surface uniformity should also be ensured. Non-absorbent materials such as metals are often degreased first by solvents and then given further treatment such as grit blasting or chemical etching.

Degreasing is usually adequate for low strength adhesives but further treatment is vital for the high strength bonds associated with structural adhesives. One approach involves increasing the surface area by abrasion with or preferably impact blasting with a shot or grit-blasting processes, the choice being dependent on the materials for treatment and the equipment available. Alumina, quartz and carborundum grit are suitable for steels and light alloys. Dry abrasive processes invariably produce dust on the surface which must be removed before bonding[5,6,17].

Fig.2 shows an interface in which the adherend is pre-treated by shot or grit blasting into which the adhesive can flow. If it can displace the air pockets on the surface, the two materials are in intimate contact along a tortuous path. Fig.3 shows loading which is known as mode I and results in movement of the adherend as shown by the dotted lines in the figure. Little energy dissipation is required to separate the adherends and a clean separation of the adherends is possible[12]. If a wedge is driven into the edge of this bond we can see no abrupt plane of stress transfer. Rather, for the crack to propagate across the bond, the line of force has to take detours as shown in Fig.4 by the series of arrows. Some detours go into the adhesive. In most cases, the adhesives can deform more than the adherend.

Another reason surface roughness aids adhesive bonding is the interlocking effect. When Mode I loading is applied to the situation in Fig.4, the applied force cannot cleanly follow the path between the two adherends, but rather must make excursions. As excursions are made into either adherend, energy can be dissipated by plastic deformation.

Note also the possibility of a "lock and key site" at which the adhesive would have to physically pass through the material of the adherend in order for separation to take place[12]. In Fig.4, a segment of the surface is indicated by arrows. In this segment, the adhesive has completely filled a pore on the surface. At this pore, the exit of the adhesive is partially blocked by part of the adherend . This place in the inter-phase may exhibit the so-called " lock and key" effect. A key, when turned into the tumblers of a lock, cannot be removed from the lock because of the physical impediment provided by the tumblers.

In the same way, a solid adhesive in a pore such as that shown in Fig.4 , cannot move past the "overhang" of the pore without plastically deforming. Plastic deformation acts as an energy absorbing mechanism and the strength of the adhesive bond appears to increase. Maxwell[23] made measurements of the effect of different degrees of surface roughness using maple wood adherends, Boroff and Wake[24] related bond strength of rubber to textiles to the degree of penetration of fibre ends into the rubber. Perrins and Pettett[25] showed the coating strengths of plastics on metals appeared to involve both a mechanical interlocking and other interaction dependent on the surface chemistry of plastic polymer. Investigations of Packham[26] on the adhesion of polyethylene to aluminium surface (variously treated, including anodising) demonstrated the importance of mechanical interlocking components to bond strength. The opportunity for mechanical interlocking can range from the presence of macroscopically rough surface texture to microscopically rough surface condition, as shown by Chen *et al.*[27] and White *et al.*[28]. The significant increased surface roughening of the adherend has been studied by Evans and Packham[29], whereas Eich *et al.*[30] as early as 1971, evaluated the highly

significant influence of surface roughness on both wetting and adhesion in dental adhesive application.

Another reason surface roughness improves adhesion is purely a matter of physical area of contact. Fig.3, shows a situation where the contact between the two materials is in a plane, the minimum possible contact area between two rectangular bodies. If this is imagined in three dimensions, the surface area is increased substantially. If interfacial interactions scale as the area of contact then the total energy of surface interaction increases by an amount proportional to the surface area.

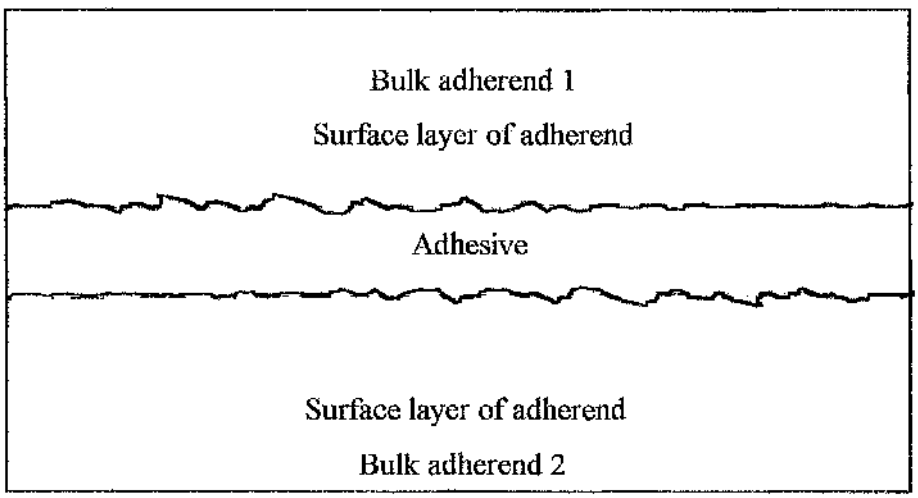

Fig.2 Cross-section of a typical joint surface treated with shot or grit blasting. The surface roughness of the adherend creates an interlocking between the adhesive and adherend[12]

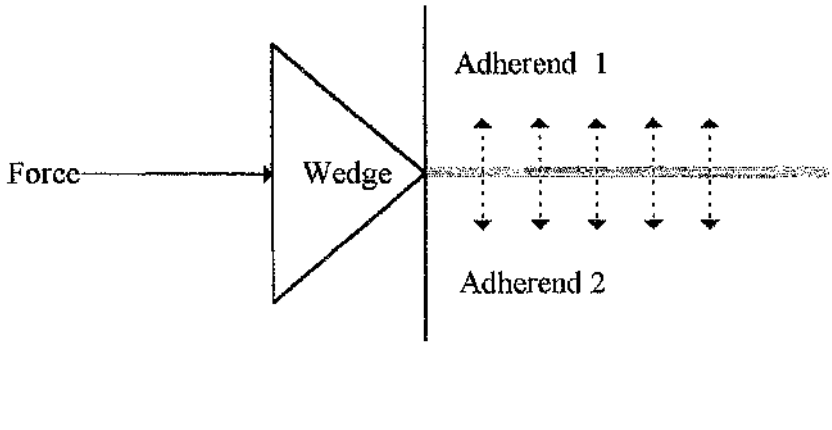

Fig.3 A wedge is driven into the edge of sharp interface between adherends 1 and 2[12] .

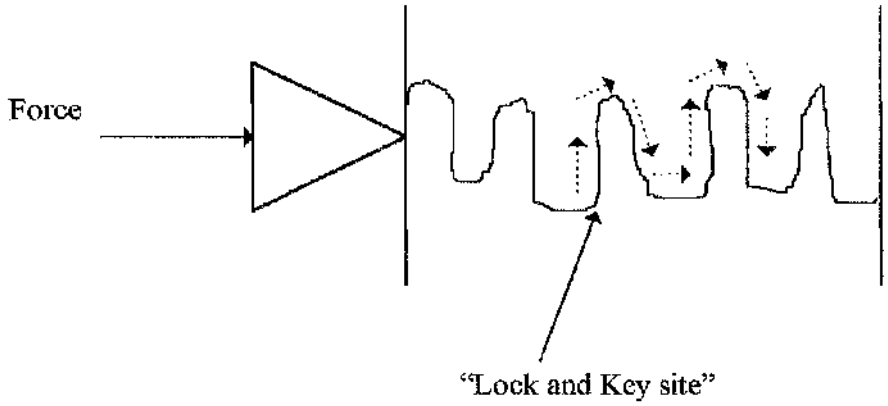

Fig.4 Schematic showing a tortuous interface between two adhering materials[12].

2.3 Fracture Mechanics of Adhesive Joints

Adhesive joints usually fail by the initiation and propagation of flaws and since the strength of most real solids is governed by the presence of flaws, resistance to flaws is important in the design and analysis of adhesive joints. It is directly responsible for the reliability and integrity of adhesively bonded structures, which are used increasingly in many advanced engineering applications. The main aims of the various theories are to analyse mathematically the loads at which the flaws propagate and describe the manner in which they grow. The source of naturally occurring flaws may be voids, cracks, dirt particles, additive particles, inhomogeneities in the adhesive, etc. which may be initially present at a critical size to develop during the fracture test.

Essentially, fracture mechanics is the study of the strength of a structure which contains a flaw, usually considered as an elliptical crack. The theories were originally developed for cohesive fracture of materials[31,32] but have been extended to adhesive joints[33-35].

Fracture mechanics has proved to be particularly useful for characterising the toughness of adhesives, identifying mechanism of failure and estimating the service life of 'damaged' structures - the 'damage' being in the form of cracks, air-filled voids, de-bonds, etc. having arisen from manufacturing, environmental attack, fatigue loading, sub-critical impact loads, etc.

Fracture mechanics is based on G. R. Irwin's[36] first observation that the stress field in the vicinity of a crack tip can be adequately defined by studies of crack extension and by a single parameter, K, the stress intensity factor. Since the parameter is a function of the applied load and crack size, K increases with load. When the intensity of the local tensile stresses at the crack tip attains a critical value, K_c, a previously stationary or slow moving crack propagates abruptly.

The value of K_c defines the "critical fracture toughness" and is a measure of a material property. Under carefully controlled conditions, it is constant for a particular material, since cracking always occurs at a given value of local stress intensity regardless of the structure in which the material is used. Secondly, the energy criterion arising from Griffiths[37] and later Orowans's[38] work, supposed that fracture occurs when sufficient energy is released (from the stress field) by growth of the crack to supply the requirements of a new fracture surface. The energy release comes from stored elastic or potential energy of the loading system and can be calculated for any type of test piece. The approach, therefore, provides a measure of the energy required to extend a crack over unit area, and this is termed the fracture energy. When plane strain and tensile opening mode prevails it is denoted G_{IC}. The pioneering work in the application of continuum fracture mechanics to the failure of adhesive joints was undertaken by Mostovoy and Ripling and co-workers[39]. They developed the tapered double cantilever beam joint geometry, shown in Fig.5 which is a constant compliance geometry. The results in the adhesive fracture energy being independent of crack length. Thus this geometry is well suited to environmental studies where velocity will be a function of the applied load and environment.

Studies by various workers[34,48] have demonstrated the pronounced effect of bond thickness on adhesive fracture energy for rubber modified epoxy adhesives. Bascom *et al.*[48] observed the effect shown in Fig.4a, for a CTBN-modified piperidine cured epoxy adhesive using a TDCB specimen. As shown, adhesive fracture energy fracture energy passes through a maximum, designated G_{IC}, at a specific bond thickness, tm. At thickness beyond tm, fracture energy decline until a value is reached which remains essentially constant with increased thickness.

Further investigations by Bascom and Cottington[7] and more recently Kinloch and Shaw[34] have shown that the general bond thickness adhesive fracture energy relation shown in Fig.4a is maintained over a wide range of temperatures and displacement rates. Furthermore, an increase in temperature was found to have an effect similar to a reduction in rate, i.e. increases in the values of both G_{IC} and tm. This demonstrates clearly the practical consequences of the bond thickness effect.

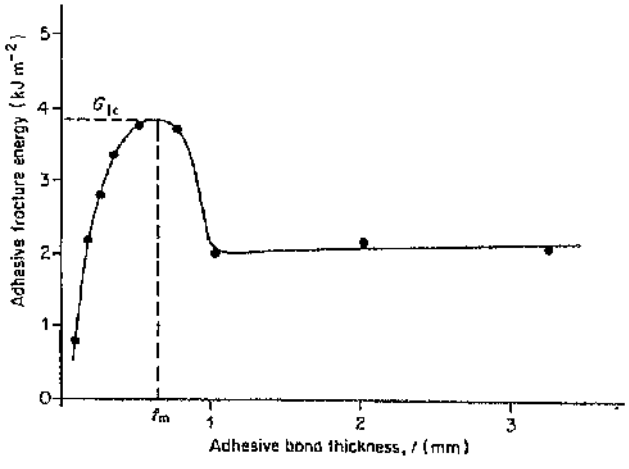

Fig.4a Effect of adhesive bond thickness on fracture energy[48]

Stress Intensity Approach

A sharp crack in a uniformly stressed infinite homogeneous lamina of a bulk adhesive is shown in Fig.6. Assuming Hookean behaviour and infinitesimal strains, i.e. linear elastic consideration, Westergaard[40] has developed certain stress functions solutions which relate the local stress concentration of stresses at the crack tip to the applied stress, σ_o. For regions close to the crack tip, equation 1.

$$\sigma ij = \sigma_o \left(\frac{a}{2r}\right)^{\frac{1}{2}} fij(\theta) \qquad (1)$$

Irwin[36] modified the equation to give the stress distribution in the vicinity of a crack tip in an infinite sheet under opening mode loading to take the form

$$\sigma ij = \frac{K_I}{\sqrt{2\pi r}} fij(\theta) \qquad (2)$$

Where r and θ are polar co-ordinates with their origin at the crack tip. He[36] relates the magnitude of the stress intensity local to the crack in terms of the applied loading and geometry of the structure in which crack is located. The parameter K is the stress intensity factor for linear elastic fracture mechanics (LEFM) and is defined as

$$K_I = \sigma_o Y \sqrt{a} \qquad (3)$$

where

σ = applied stress

a = crack length

Y = geometry constant

Values of Y may be obtained experimentally or theoretically. A crack may be stressed in three different modes, denoted by I, II, III as depicted in Fig.7. In this study, only mode I loading is considered.

Determination of Adhesive Fracture Energy

For isotropic, monolithic plane strain cases, the associated strain energy release rate, G_{IC}, is related to K_I by

$$G_{IC} = \frac{K_I^2}{E_a}(1 - \upsilon a^2) \qquad (4)$$

where E_a is the Young's modulus of adhesive and ν_a is Poisson's ratio of adhesive.

The direct application of equations 1-4 to multiphase adhesive joints has been assumed and used to measure G_{IC}[41-44] but these fundamental relationships and the validity of this toughness evaluation for fracture design of the joints have not been fully addressed. It is not quite clear as to what extent the crack tip field follows the classical fracture mechanics requirements and whether the G-K relationship in equation 4 is implied in the adhesive fracture. While an exact

analysis of the fracture of the adhesive joints is absent at the present time, efforts towards understanding the fundamental behaviour of this kind of fracture problem have led to the establishment of some useful analytical expressions for the commonly used specimens. The earliest and most widely employed analysis for the DCB specimen was based on a simple one-dimensional monolithic beam theory[45,46]. Solutions for the monolithic beams have been assumed to hold for general cases, and fracture strength for the test is related to the specimen compliance, C by

$$G_{IC} = \frac{P^2}{2b}\frac{dC}{da} \qquad (5)$$

where P is the applied force. Assuming that each flank behaves as a cantilever beam and that the compliance is not affected significantly by the presence of the thin adhesive, fracture strength may be approximated by

$$G_{IC} = \frac{4P^2}{Eb^2}\left[\frac{3a^2}{h^3} + \frac{1}{h}\right] \qquad (6)$$

where E is the elastic modulus of adherend, a, is the crack length, and h is the beam height measured normal to the crack tip.

This relationship is employed in the design of the approximately linear compliance test compliance test specimen. To construct a specimen in which the crack would propagate at a constant load, the shape of the adherend (variation of h and a) is designed so dC/da has a constant value, that is

$$m = \frac{3a^2}{h^3} + \frac{1}{h} \qquad (7)$$

where m is called the shape factor and has a dimension of $mm^{-1}(inch^{-1})$. Within the accuracy of the simple beam theory used to derive equation 6, such a specimen should display a constant crack propagation force, P, regardless of the crack length. Thus the crack length does not need to be measured during the test. Substituting equation 7 to 6 gives fracture strength for the TDCB specimen as

$$G_{IC} = \frac{4P^2m}{Eb^2} \qquad (8)$$

Fig.5 shows a standard fracture test of adhesive joint TDCB with specific m = 3.54 mm^{-1} (90 $inch^{-1}$)[10].

The earliest investigations into crack propagation in epoxy resins were by Broutman and McGarry[47] and Mostovoy and Ripling[39]. A feature that became immediately apparent from these investigations was the observation that the crack propagation tends to take place in epoxy resins by means of a discontinuous 'stick-slip' mechanism. Broutman and McGarry[47] found that crack propagation was usually of a continuous type in brittle thermoplastics but tended to be discontinuous in thermosets. Mostovoy and Ripling[39] examined the behaviour of epoxy resins so that they could compare it with crack propagation in adhesive joints. They pioneered the use of the tapered double cantilever beam specimens for this type of investigation. The main advantage of the tapered double cantilever beam in the study of the stability can be appreciated from the schematic load displacement curve in Figs.8-10. When propagation takes place in a continuous manner, cracks grow at a constant load as in Fig.8. However, if the cracks propagate in a stick-slip manner the load displacement curves takes on a see-saw appearance, as in Fig.9. The load at which a crack jumps is P_i and the load at which it arrest is P_a. These are approximately constant at all crack lengths.

Sometimes, the crack grows steadily in a controlled manner with the load for crack propagation remaining constant. However, unlike stable brittle propagation, a relatively high value of fracture strength is now required and the fracture surface is rougher and torn in appearance, indicating a more ductile fracture process. Therefore, this type of crack growth, seen in Fig.10, is often observed at the highest test temperatures when the yield stress of the adhesive is relatively low, with severe crack tip plasticity and blunting which gives rise ductile failure and stable the crack growth.

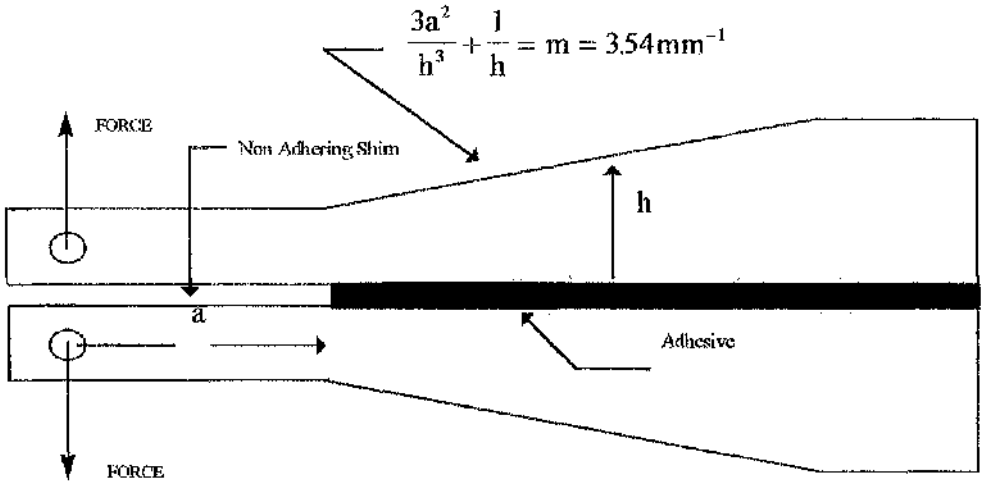

Fig.5 Contour Double-Cantilever Bean Specimen

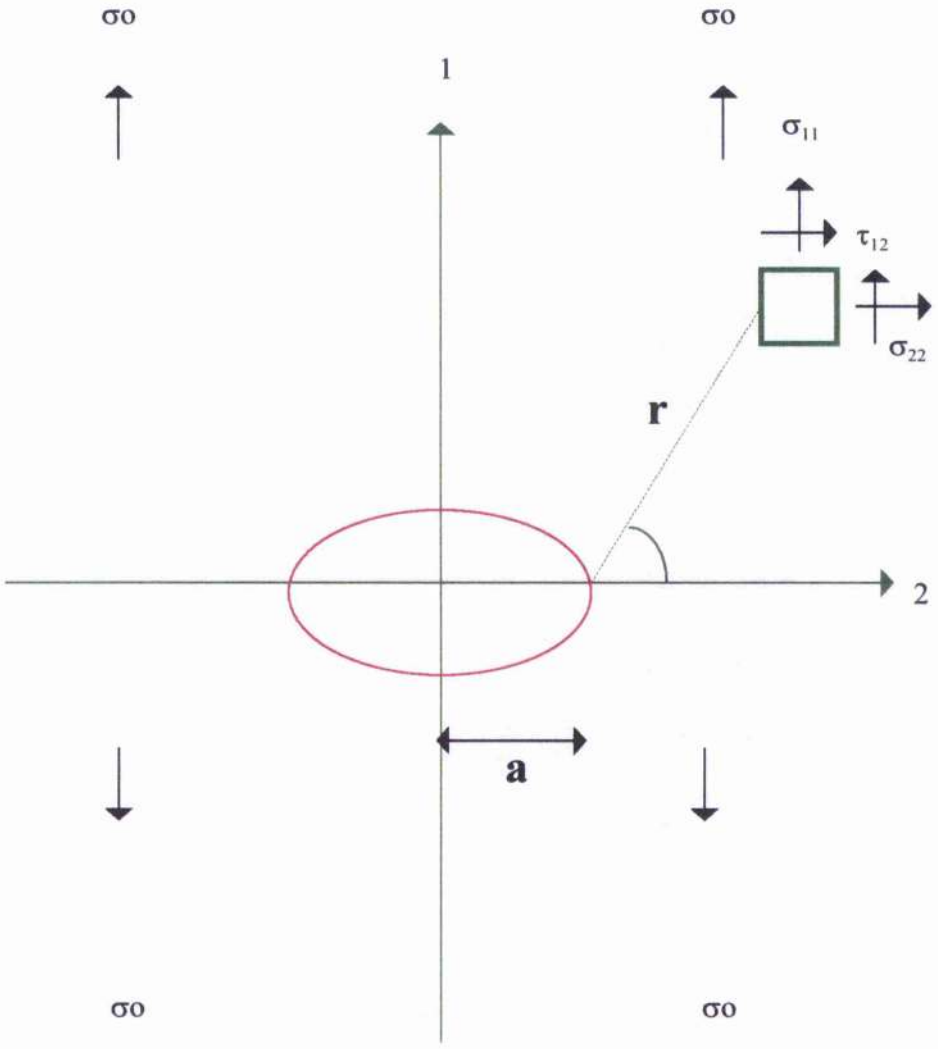

Fig.6 Sharp crack in a uniformly stressed, infinite lamina[15]

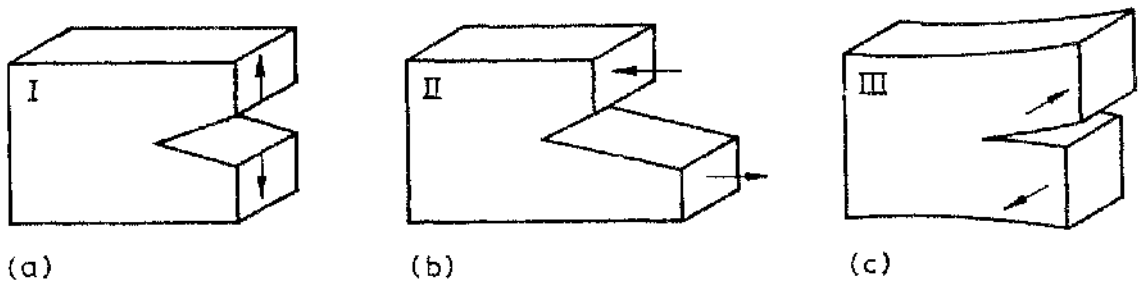

Fig.7 Modes of loading (a) Cleavage or Tensile-opening mode - mode I. (b) In plane shear mode - II. (c) Anti plane shear mode - mode III

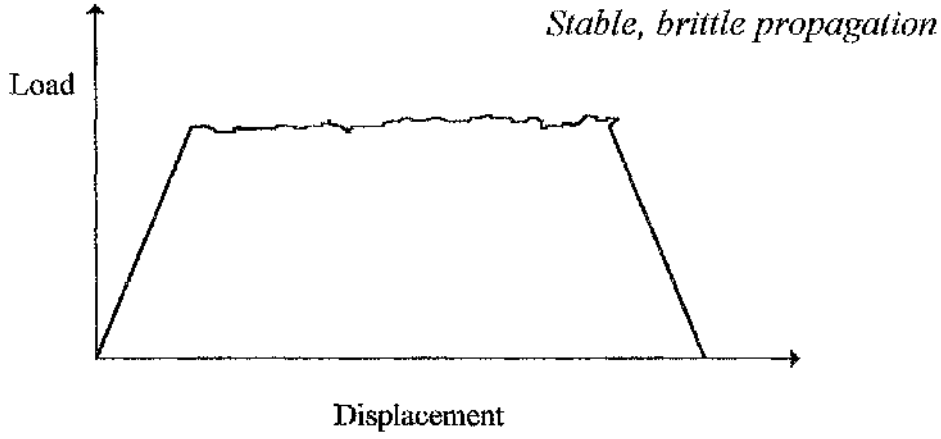

Fig.8 Load displacement for stable, brittle crack propagation of tapered double cantilever beams[48]

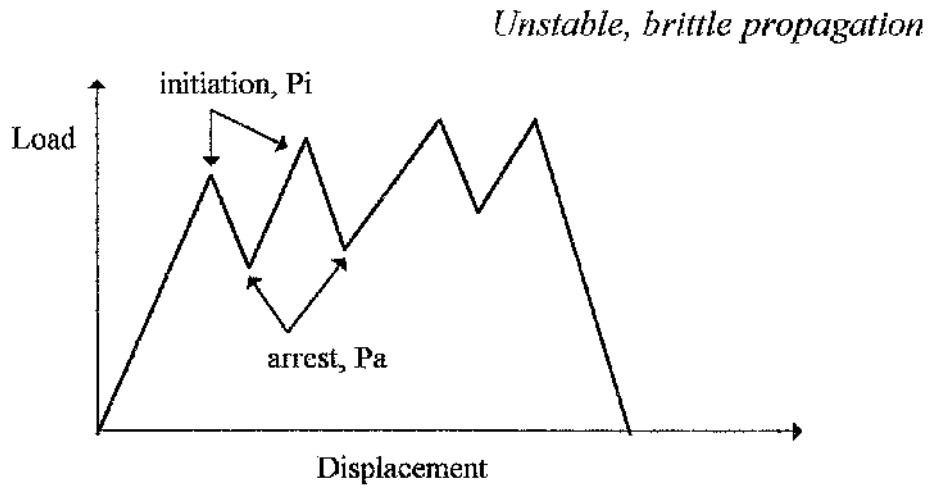

Fig.9 Load displacement for unstable, brittle crack propagation of tapered double cantilever beams[48]

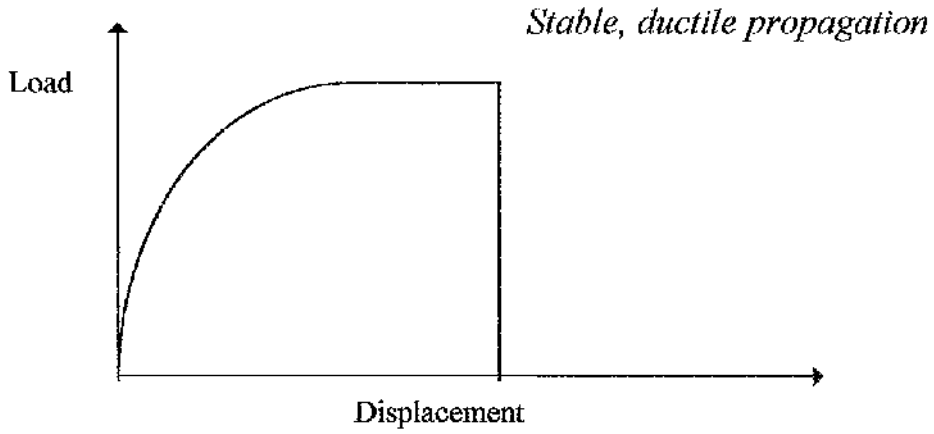

Fig.10 Load displacement for stable, ductile crack propagation of tapered double cantilever beams[48]

2.4 Fatigue Behaviour of Adhesive Joints

The effective use of adhesives in structural applications such as an advanced ship depends upon developing adequate design criteria. Thus adhesive joints are expected to perform satisfactorily under service conditions which include dynamically and statically applied loads and exposure to hostile environments. It is, therefore, of importance to use the appropriate adhesive systems which will possess adequate service life under the operating conditions which are to be experienced by the bonded structure. This, in turn, leads to the need to understand the mechanism of failure and to be able to predict quantitatively, the expected service life. In this section, only the service life of the adhesive joints subjected to dynamic fatigue will be considered.

Dynamic fatigue is the phenomenon of failure or fracture of a joint under repeated or oscillatory loading. The importance of dynamic fatigue is that under cyclic loads, joints will fail at stress levels much lower than they can withstand under monotonic loading. Also, for a given alternating stress amplitude, they will fail in a much shorter time than the static fatigue time where a constant stress of the same magnitude has been applied. Most jointed structures are liable to dynamic loading, and it accounts for large number of service failures. Compared to other methods of fastening such as rivets, spot welds and mechanical fasteners, adhesively bonded joints are generally regarded as possessing good dynamic fatigue properties shown in Fig.11. This essentially arises from the adhesive, giving a more even stress distribution in the joint compared to other methods[15] and imparting a lower stress concentration factor[49]. Data obtained by Knox *et al.*[49] shown in Fig.12 are the fatigue results for two types of loading. In the high cycle, low stress, regime both types of adhesive perform better than the welded equivalent.

Albrecht[50] has shown that the fatigue life of adhesively bonded cover plates on the tension range of a steel girder can be hugely greater than that of welded cover plates provided that the plate ends are bolted to prevent de-bonding. Also, Martin[51], has demonstrated a similar superiority of the adhesively bonded web stiffeners.

An important reason for the scarcity of uses of the adhesives in heavy structural engineering is a lack of information about the long term properties of appropriate types of adhesive in adverse environmental conditions and stress regimes. This has prompted extensive studies of adhesively bonded joints.

The fatigue life of structural components subjected to cyclic loads can be divided into three stages : initiation (region I), propagation (region II) and fast fracture (region III). The total fatigue life is governed by factors such as fatigue and fracture characteristics of the material, applied load, geometry of the component and environment. Fatigue crack initiation and propagation can alternatively be divided into threshold and finite life regions.

The threshold behaviour for initiation and propagation is an important consideration in design because a large portion of the fatigue life of a structural component may be expended in the near threshold region. If the applied stress is below the endurance (threshold) limit for the fatigue crack initiation, the crack may not initiate. After the crack initiates and the fatigue crack driving force is lower than the threshold value for crack propagation, the crack may not grow or only grow at an extremely slow rate. Thus, the threshold behaviour for crack initiation and propagation is an important consideration for structural integrity evaluation.

Determination of Adhesive Fracture Energy from Fatigue Test

A fracture mechanics approach to describe fatigue crack growth in adhesive joints is reported by Mostovoy and Ripling[8] . They employed a tapered double cantilever beam to obtain the value of da/dN as a function of the maximum fracture energy release rate, Gmax, applied in the fatigue cycle. A sine wave loading form was used at a frequency of 2 Hz.

From equation 5, the maximum value of the fracture energy release rate, Gmax, applied during a fatigue cycle may be deduced using

$$G\max = \frac{(P\max)^2}{2b}\frac{dC}{da} \qquad (9)$$

Where Pmax is the maximum load applied during the fatigue cycle. Alternatively, the value of dC/da may be describe using beam theory, seen equation 7. Thus the value of Gmax may be deduced :

$$G\max = \frac{4(P\max)^2}{Eb^2}\left[\frac{3a^2}{h^3}+\frac{1}{h}\right] \qquad (10)$$

If the fatigue data are plotted in the form of Gmax versus da/dN, using logarithmic axes for both parameters, then a major portion of the relationship so obtained is often linear and the region may be described by a form of the Paris equation, namely

$$\frac{da}{dN} = D(G\,max)^n \qquad (11)$$

Where the parameters D and n are constants but their values typically depends upon the materials variables, temperature, frequency, stress ratio and environment.

A typical graph of da/dN versus Gmax is shown in Fig.13 using logarithmic scales. The fatigue data reveal a curve which is sigmoidal in shape with three distinguishable regions mention earlier :

(1) Region I - the threshold region associated with low values of da/dN and Gmax.
(2) Region II - the linear portion.
(3)Region III - the value of Gmax starts to approach that of critical fracture energy, Gc

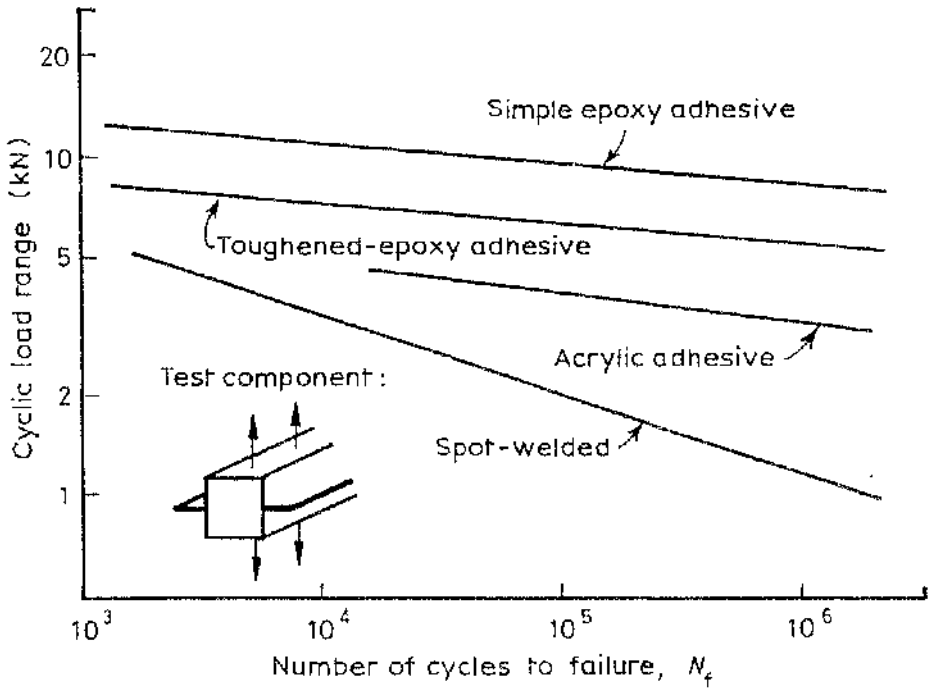

Fig.11 Dynamic fatigue properties of steel double-box hat structures either adhesively bonded or spot welded[15]

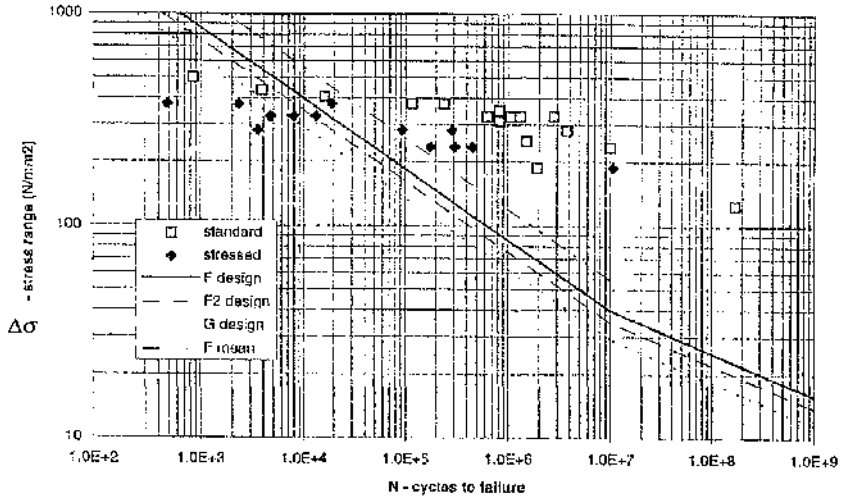

Fig.12 S-N data adhesively bonded joints[49]

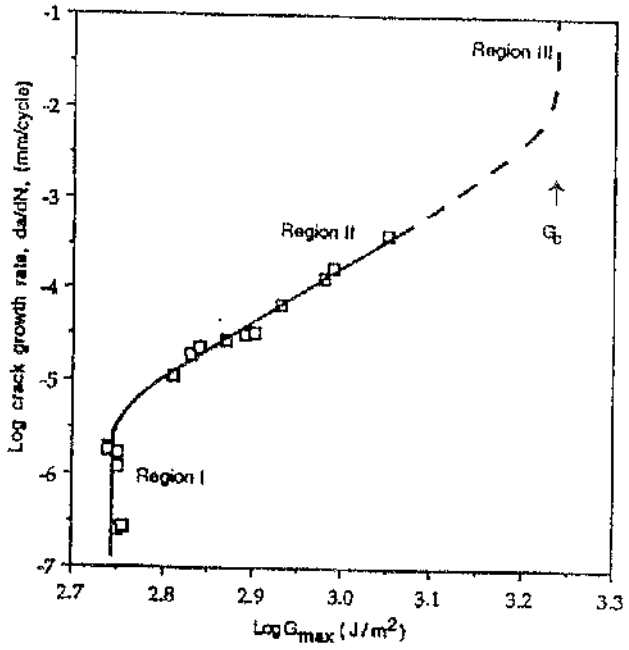

Fig.13 Crack growth rate per cycle, da/dN, versus Gmax for TDCB specimens prepared using the CAE pre-treated substrates. The fatigue tests were conducted in the 'dry' environment.[11]

2.5 Silane Coupling Agents

A great many adhesive bonding applications employ some type of coating applied to the treated adherend surface, which usually can be described as primers or coupling agents. The former have the function of serving as adhesion promoters and protective coatings, whereas the latter serve to create a chemical bonding between the adhesive and the adherend. This distinction is not always as clear as described, however, and situations arise where primers end up acting more like a coupling agents, and conversely, coupling agents often are serving distinctly as primers in the overall joint.

Primers are important for a number of reasons. First, they protect a freshly prepared adherend surface from contamination or changes which might otherwise occur as a result of contact of the surface with its environment. The primer is especially useful when it can penetrate to create mechanical interlocking. A related function of protection against the corrosive effects of the service environment is provided when special corrosion inhibiting primers are used. A second function is to penetrate any surface roughness or porosity.

The low viscosity of most primers, as compared with the primary adhesive formulation in the bond line, permits ready application by different methods such as spraying, dipping, brushing, or roll coating. This is applied as early as possible to the pre-treated surface, for example, after acetone cleaning and grit-blasting. Falcon and Miller[52] considered the benefit of a special primer for making repairs on the main rotors in helicopters in 1977.

In addition, there can be enhanced joint durability where better wetting of the adherend surface by the primer is achieved than would result from the use of the adhesive alone. Not only the adhesive but the primer solution as well may contain special wetting agents, flow-control agents, elastomeric toughening additives, and corrosion-inhibiting additives.

The low molecular weight of most primers obviously is able to create the distinct opportunity to flow, wet, and develop more intimate and complete surface contact with the varying geometries of the treated surface. There always needs to be some testing of any primer with a suggested adhesive where this information is not already available to make sure the primer adequately wets the adhesive. Herczeg *et al.*[53] have pointed out that if epoxy primers are not properly formulated, the surface energy level of the cured epoxy primer coat can be reduced so the adhesive will not wet out the primer.

Bishop *et al.*[54] has recently offered an interesting examination of the bonding between metal surface with an epoxy with and without a primer. They sectioned across the bond line with an ultramicrotome and viewed the sections using transmission electron microscopy (TEM). In the absence of a primer, it was possible to observed trapped air in the adherend surface roughness created by light abrasion. Much porosity was apparently eliminated when metal adherends were primed.

The Chemistry of Silanes

Organofunctional silanes are bifuntional molecules in that they usually have two types of reactivity built into single structure. Fig.14 shows the common elements of a typical organofunctional silane. Most commercially available organosilane coupling agents are based on following generalised anatomy structure in Fig.14. The organofunctional side (Y) is designed for reactivity with a chosen organic resin.

Organofunctional groups now include a range of aminos, epoxies, methacryls, vinyls, mercaptos, ureas, isocyanates and isocyanurates. As an additive, the organofunctional group is selected to take part in the cure reaction of the coating system. As an intermediate, the silane may be used initially to modify the resin and then cross-link when the coating is exposed to ambient moisture.

Between the organic functional group and the silicon atom there is a linking group, most commonly a proply chain. The silicon-carbon bond of the linking group is stable under most environmental conditions. The 'silane' side of the molecule offers inorganic reactivity through hydrolyzable groups attached to silicon (X). The hydrolyzable groups are usually alcohol residues, such as methoxy and ethoxy. Each hydrolyzes at a different rate and releases a different alcohol upon reaction with ambient moisture. In some cases, only two hydrolyzable groups are present, although three are more convenient synthetically and usually provide more moisture resistant bonds. Most coupling agents have only one silicon atom, but some silanes are now available with multiple silicon. Fig.15 shows many of the organic functional groups available, emphasising those typically used in coatings.

Hydrolysis Chemistry

The reaction of the silicon end of the molecule, as depicted in Fig.16, is initiated by hydrolysis of the alkoxy group, usually after exposure to ambient moisture. The result of this reaction is the release of an alcohol and the formation of a silanol. The speed with which this reaction occurs depends upon the pH of the formulation (slowest at pH 7) and upon the steric bulk and polarity of the alcohol residue (methoxy>ethoxy>methoxyethoxy>t-butoxy). Catalysts for the hydrolysis include not only hydronium and hydroxide ions, but other bases (such as organic amines) and metals (such as tin). In order to become "active" the silane must first hydrolyze.

Silane Condensation on a Surface

The naturally occurring acidity or alkalinity of most inorganic surfaces is usually sufficient to catalyse silane hydrolysis. The absorbed water found on these surfaces generally is enough to complete hydrolysis of the silane. Once in the silanol state, the silane can proceed to condense with a mineral surface. This is the first step in the actual coupling process. The silane migrates to the surface, hydrolzes, hydrogen-bonds with the surface and, upon release of water, forms a direct covalent bond with the surface. Condensation proceeds most slowly at pH 4-5 and is catalysed by hydronium and hydroxide ions. Other bases and metals also catalyse the condensation reaction.

Each silicon atom has three hydrolyzable sites, but it is unlikely all three sites will bond with the surface. The silanols that do not react with the surface can condense with themselves, forming an Si-O-Si network on the substrate surface. To complete the adhesion process, the organofunctional group on the silane reacts with the resin or binder of the coating.

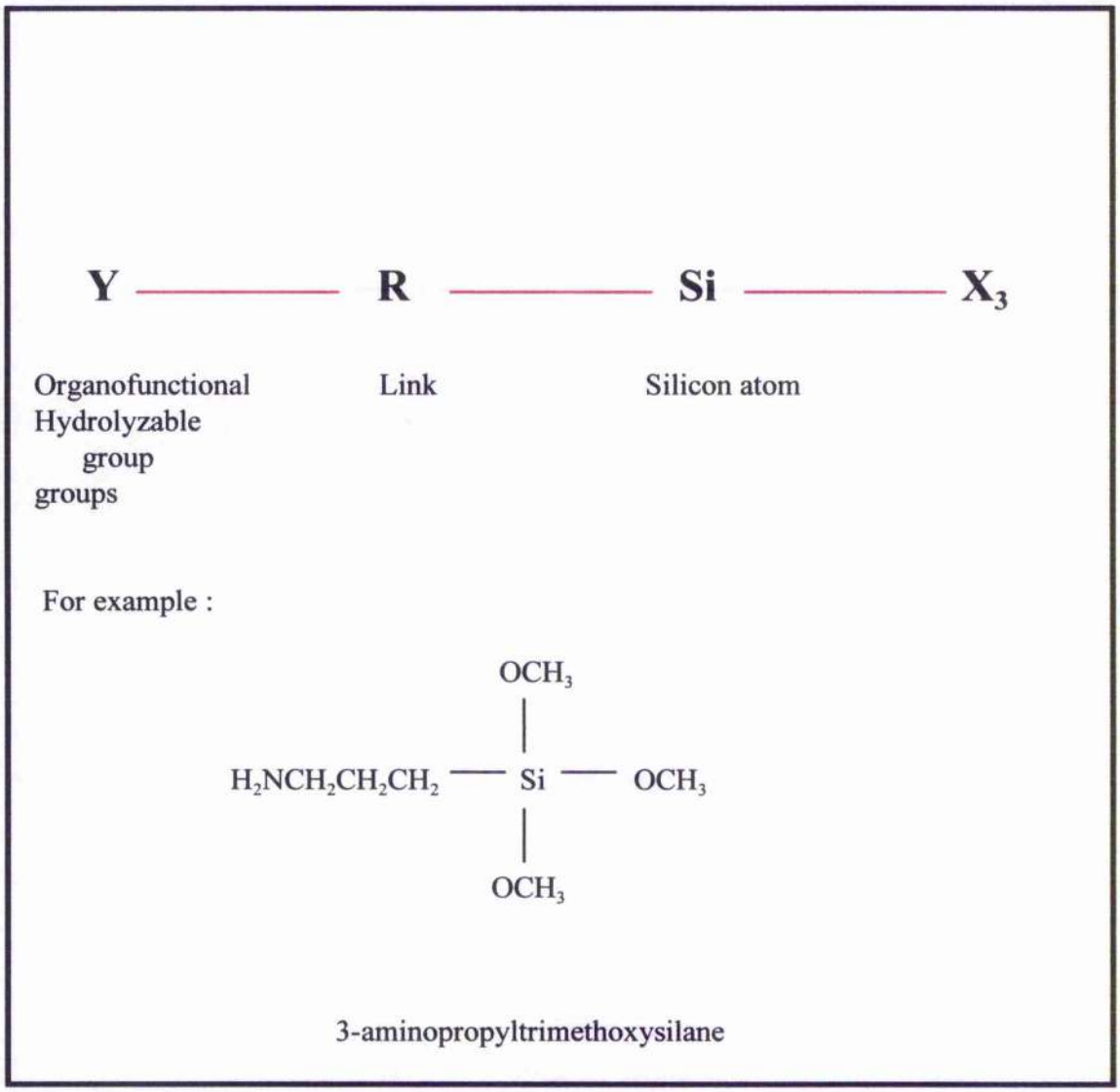

Fig.14 Anatomy of a typical organofunctional silane[55]

Functional group	Representative structure	Typical use
Alkyl	$C_8H_{17} - Si - (OCH_2CH_3)_3$ n-octyltriethoxysilane	Waterproofing, dispersant
Vinyl	$CH2 = CH - Si(OCH_3)_3$ vinyltrimethoxysilane	Latexes
Methactyl	$CH_2 = C(CH_3)\overset{O}{\overset{\|}{C}}O(CH_2)_3Si(OCH_3)_3$	Arcylic
Epoxy	$H_2C - \underset{O}{CH} - CH_2O(CH_2)_3Si(OCH_3)_3$	Epoxy resins
Primary amino	$H_2N - (CH_2)_3Si(OCH_2CH_3)_3$ aminopropyltriethoxysilane	Epoxies, urethanes
Secondary amino	 $-HN-(CH_2)_3Si(OCH_2CH_3)_3$ phenylaminopropyltrimethoxysilane $H_2N-[CH_2CH_2CH_2Si(OCH_2CH_3)_3]_2$ bis(trimethoxysilylpropyl)amine	Urethanes, phenolics

Fig.15 Selected Commercial Organofunctional Silanes[55]

Polyamino	$H_2N - CH_2CH_2NHCH_2CH_2CH_2 - Si(OCH_3)_3$ aminoethylaminopropyltrimethoxysilane	Epoxies
Mercapto	HS – (CH2)3Si(OCH3)3 mercaptopropyltrimethoxysilane	Rubber, urethanes
Ureido	$H_2NCNH - (CH_2)_3Si(OCH_2CH_3)_3$ ureidopropyltrimethoxysilane	Phenolics urethanes
Isocyanato	$O = C = N - (CH_2)_3Si(OCH_2CH_3)_3$ isocyanatopropyltriethoxysilane	Polymer modification
Polyether	Polyether – $(CH_2)_3Si(OCH_2CH_3)_3$ polyethersilane	Dispersant

Fig. 15 Selected Commercial Organofunctional Silanes (continued)

Hydrolysis :

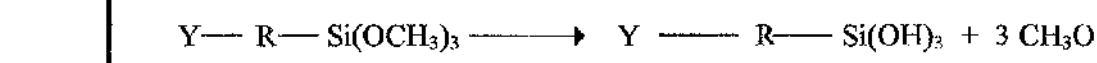

Condensation to a surface - adhesion :

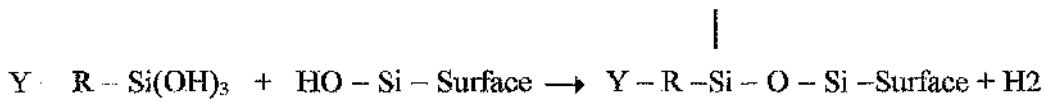

Condensation with another silane - crosslinking :

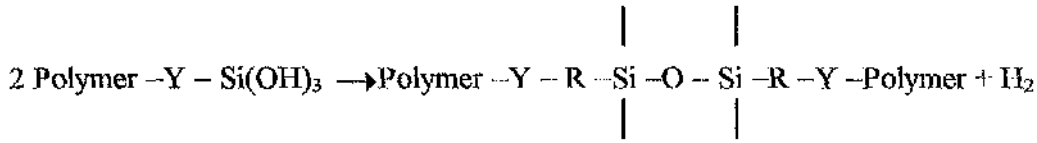

Fig.16 Hydrolysis and Condensation of Organofunctional Silanes[55]

It is important, however, to apply the silane in the correct way. The silane must have time to react with the steel surface before the adhesive is applied. If such time is not allowed, perhaps by accelerated drying of the silane coated surface, than little durability improvement will be seen. Three parameters affect the silane priming process. There are (i) the age of the silane priming process, (ii) the age of the silane solution,(iii) the solvent used for the silane and (iv) the drying time/temperature. Only by optimising these conditions can the best durability be obtained[56]. When this is done, there is a very good chance that the performance of the coatings in aggressive environments will be significantly improved.

The age of the silane solution when applied to the substrate critically influence the eventual durability. The durability of the joints improves with age so that it reaches the maximum about one hour after the silane is mixed with water. When majority of the water is replaced by ethanol there is little change in silane efficiency with time and the eventual durability is significantly lower than with the water system[13]. An equally important parameter is the drying temperature used on the substrates after priming. Higher temperatures reduce the effectiveness of the silane, probably by not allowing the silane complex to react with the substrate, see Table2.

Table 2 Joint strength in MNm^{-2} after immersion in water at 60 °C for 1500 hours[57]

Solution age (min)	**Drying Temperature (°C)**		
	20	40	60
30	34.23	26.72	25.05
60	34.38	21.98	22.93
90	33.72	19.25	18.40

Chapter 3

EXPERIMENTAL DETAILS

3.1 Tapered Double Cantilever Beam Specimens

The tapered double cantilever beam was designed to measure the resistance to opening mode (mode I) fracturing. The adherend for all the tests in this study were fabricated from mild steel with specification of all dimensions in accordance to ASTM standard D3433-93[10], see Fig.17. In monotonically increasing load tests, where cracking occurs rapidly, the fracture proceeds cohesively, in the centre of the bond. Fractures of this type are independent of the adherend material so that the data collected with the mild steel adherend should be applicable to different adherends with well made joints.

The cleaning procedure for the mild steel adherends consisted of degreasing and grit blasting the adherends prior to bonding the surface, which is described in a simple flow chart, in Fig.18. If silane primer was required to enhance the joint strength, the silane solution must be prepared in the correct proportion and left to react for at least 60 minutes before applying as a thin film on the cleaned and degreased surface[13]. The primed surface must be left to dry completely. This drying process can also be accelerated by blow drying the surface with air. Once the adherends were degreased, cleaned and primed, the required crack length on the adherends was marked and P.T.F.E was sprayed on the marked portion only to prevent bonding of the shim and adherends. This was done by masking the unmarked portion of the adherends. Adhesive was then applied on the surface according to instructions given by the manufacturer.

The adherends were clamped together and were separated by shims of the size required. In order to obtain the proper bond-line thickness, the sharp edged shims, were placed in-line with the marked adherend, sprayed with P.T.F.E, to act as a starter crack. This resulted in an initial crack length of approximately 48mm. The bonded joints were then cured at room temperature for at least 24 hours. Once the cure cycle was completed, the clamps and shim were removed. The bonded specimens were then cleaned thoroughly at both sides to remove any burrs present prior to testing.

Fracture Testing

Tests on the TDCB specimens were conducted at a constant rate of displacement of the cross-head of the Lloyd tensile machine in order to ascertain the value of the adhesive fracture energy, G_{IC}. The rate of displacement used for these monotonically loaded tests was 0.5mm min^{-1}. Fig.19 shows the set-up of the Lloyd machine for testing at ambient temperature. Fig.20 shows the set-up of the Lloyd machine incorporated with a chamber for testing bonded joints at temperatures of 60 °C and -40 °C. The load-displacement characteristics were recorded and from these G_{IC} values were derived.

Fatigue Testing

The fatigue tests were carried out on a Dartec machine as shown in Fig.21. The tapered double cantilever beam was used to obtain the values of da/dN as a function of the fracture energy release rate, applied in the fatigue cycle. A sine wave loading form was employed at a frequency of 2 Hz at ambient temperature. The TDCB specimen was loaded in transverse tension through a pair of loading pins. The crack length as a function of the number of cycles was determined by utilising a 40X travelling microscope. To improve the monitoring of the crack length, one side of the TDCB specimens was painted with ink and marked with equally spaced lines, see Fig.22.

All of the fatigue tests were carried out with constant load ranges. The R ratio was varied by keeping the minimum load (0.2 KN) constant and varying the maximum cyclic load value. Test results are shown in Appendices.

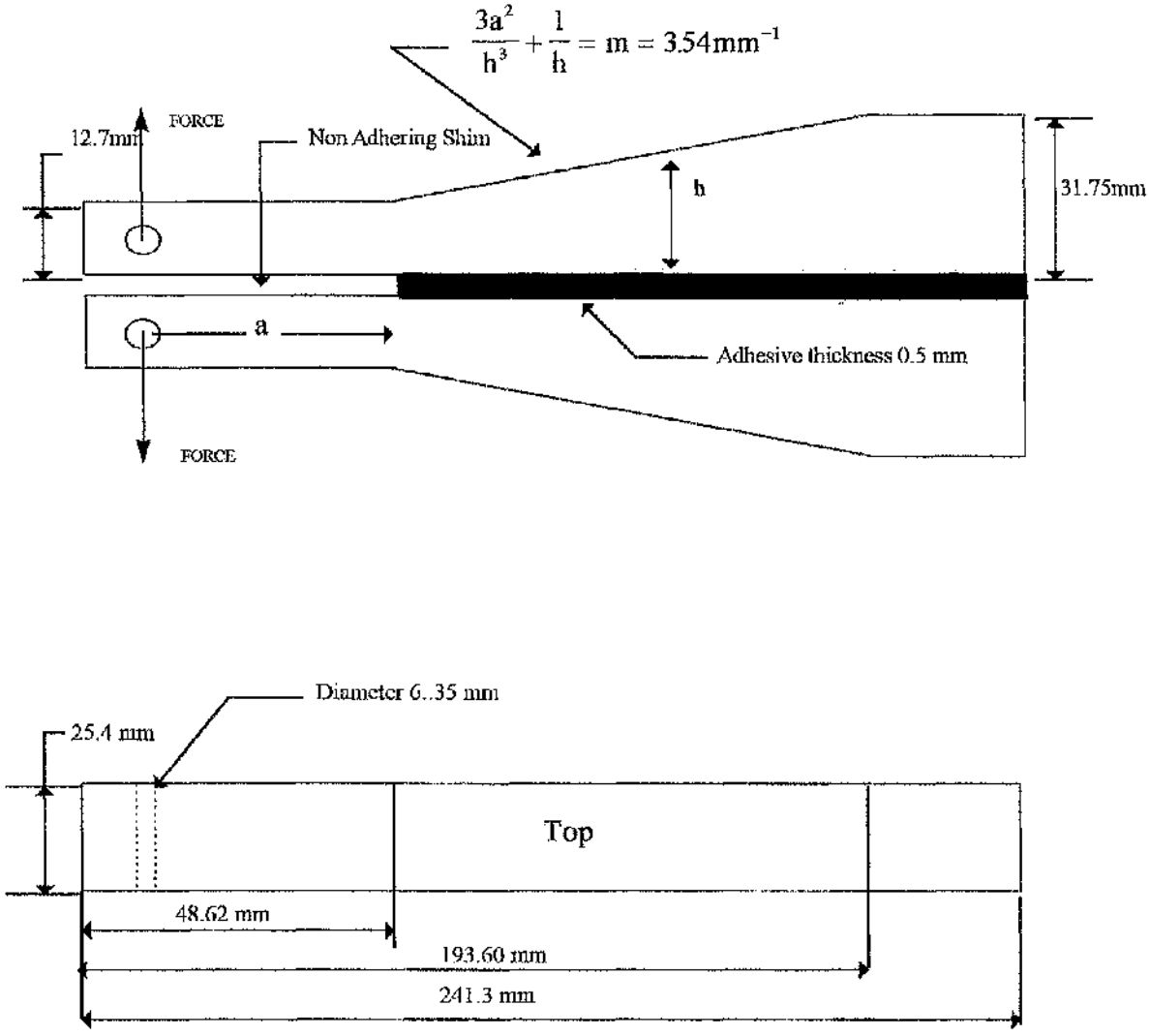

Fig.17 Tapered Double-Cantilever Beam Specimen

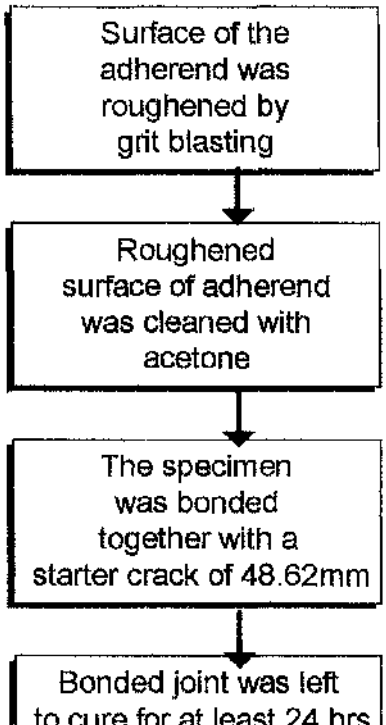

Fig.18 Flow chart of specimen preparation

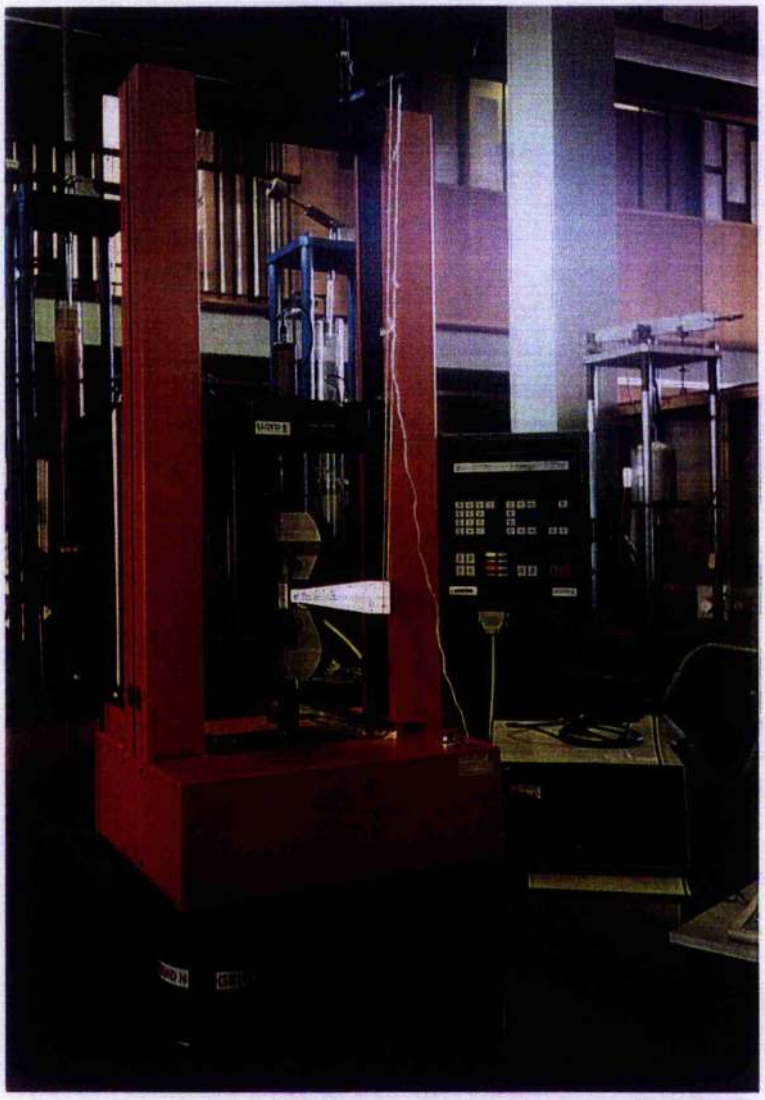

Fig. 19 Set-up of the Lloyd machine for testing bonded joints at ambient temperature

Fig.20 Set-up of the Lloyd machine incorporated with a chamber for testing bonded joints at both 60 °C and -40 °C

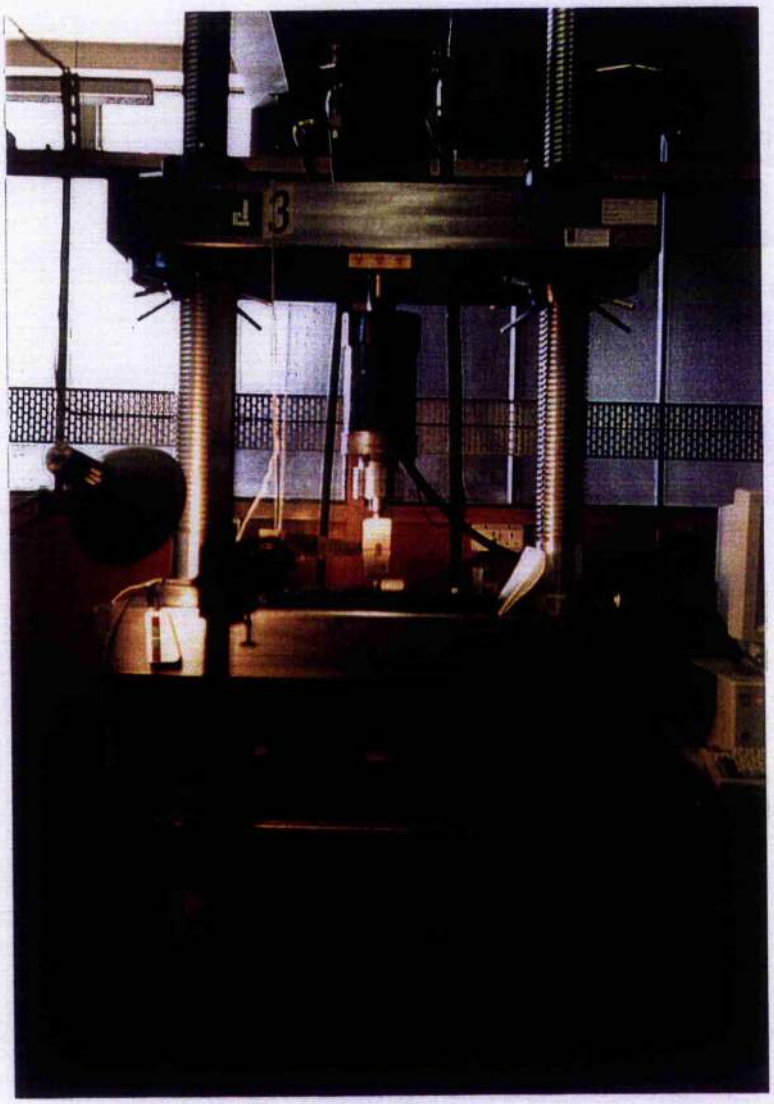

Fig.21 Dartec electro-hydraulic testing machine with controller and computer system to monitor the fatigue cycles

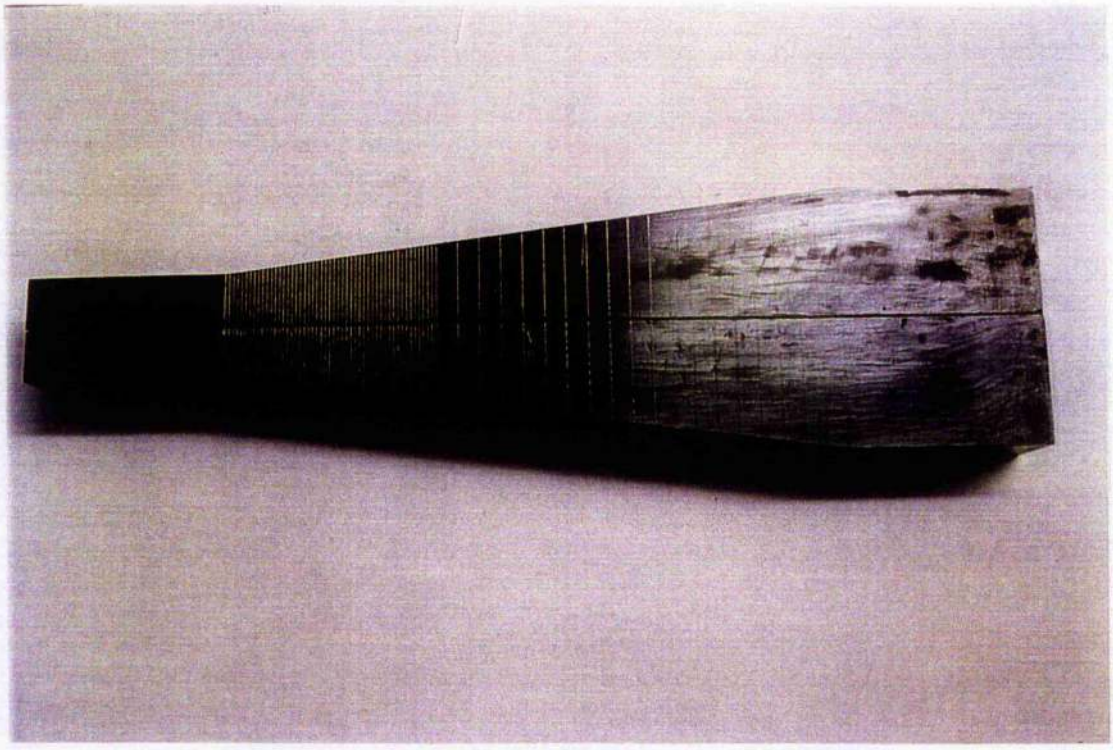

Fig.22 Bonded joint painted one side with ink and equally marked lines inscribed

3.2 Adherend

In order to compare the strength of various adherend materials it is necessary to carry out some standard form of test to establish their relative properties. The tensile properties of the adherend material were determined by using a standard tensile test piece for the purpose of determining the following properties : yield strength; proof strength; tensile strength; elongation; reduction of area. Circular machined test pieces with dimensions complying with BS 18:1987 British Standard - Method for tensile testing of material[58] were used as shown in Fig.23. These incorporated a transition curve between the gripped ends and the parallel length and were subjected to a gradually increasing tensile load until failure occurred. Measurement of the change in length were recorded throughout the loading operation by means of extensometers.

3.3 Bulk Adhesive

Adhesives, in general, have very much lower yield strengths than mild steel. The very strongest are less than half the strength of mild steel. In a tensile test, at room temperature, the bulk adhesive fractured in a brittle manner when compared to the mild steel which fractured in a ductile manner. Nevertheless, there remains enormous potential for adhesive usage in structural applications and improvements of the adhesives properties to supply to specific industries are constantly being developed by adhesives manufacturers.

The specimens and test methods were comparable to those used for plastic materials. Properties determined are intrinsic to the material: they were obtained under a uniform and uniaxial state of stress with no influence of the adherends.

Deformation of the bulk specimen was easily measured using an extensometer or strain gauges. The main difficulty was to produce specimens without defects such as voids and porosity. A technique to produce 200mm x 200mm plates with thickness of 2mm was used and gave excellent quality with an absence of voids. The technique used for producing flaw free specimens consisted of curing plates of bulk adhesive in a mould under pressure. This method has been used successfully with epoxides[59]. A slightly different method was used to obtained bulk acrylic specimens. Two Teflon coated nylon plates were used. However, one plate was surrounded with 3mm thickness nylon strips to achieve the adhesive thickness. The adhesive and initiator were applied on the plates and clamped together, according to manufacturer's recommendation. The adhesive was then left to cure at room temperature. The cured adhesive was removed and screwed onto a piece of wood for extra support. Specimens were then obtained by machining the blanks to the required shape, as shown in Fig.24.

All specifications were according to BS 2782 : Part 3 : Method 322 : 1994 : Plastics- Mechanical properties[60].The Young's modulus, Poisson's ratio, elastic limit and failure characteristics were derived from the stress-strain curve.

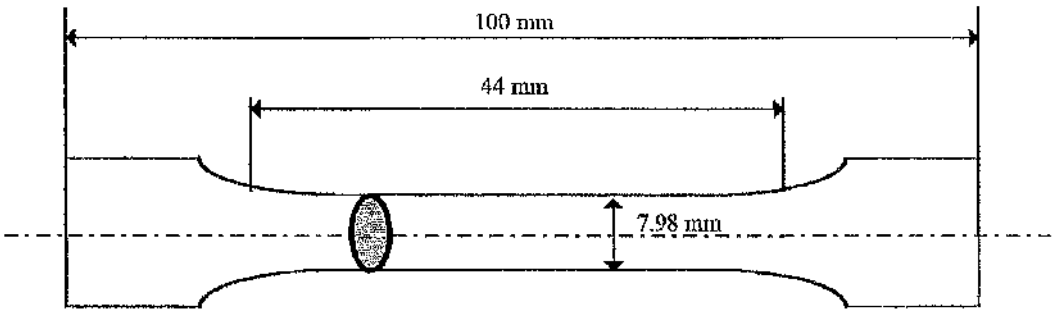

Fig.23 Specimens used for the adherend mechanical properties.

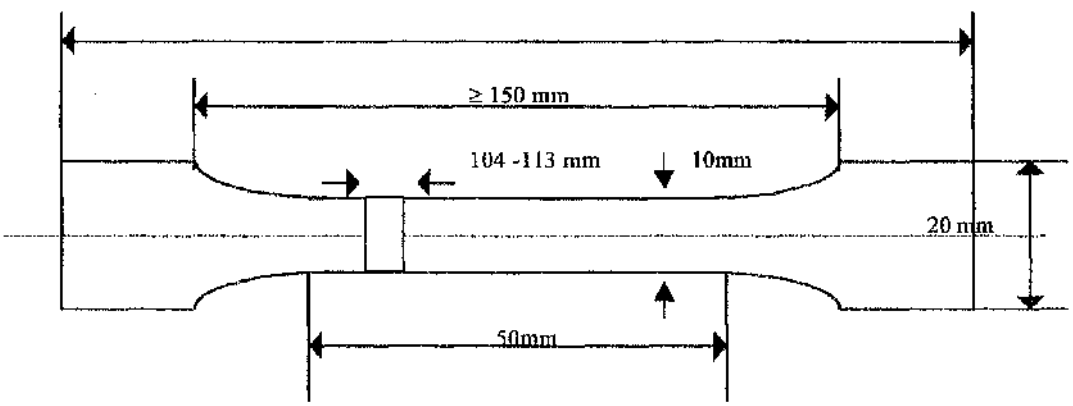

Fig.24 Specimens used for the adhesive mechanical properties.

3.4 Structural Adhesives Used

Permabond F241 Toughened Acrylic

Permabond F241 is a toughened acrylic adhesive which is used in conjunction with an initiator to give a rapid, room temperature curing system. This adhesive has an outstanding resistance to peel, impact and shear forces; excellent durability and the ability to bond a wide variety of materials including oily steel. Table 3 shows the physical properties of the adhesive.

Table 3 Physical Properties of Permabond F241 Toughened Acrylic

	F241
Appearance	Viscous off-white
Specific Gravity	1.0
Viscosity (cP)	30,000
Shelf Life (stored at 5 to 25 °C)	1 year

Ciba Polymers Redux 420 A/B

Redux 420 A/B is a two component, room-temperature curing paste adhesive of high strength and toughness. It is suitable for a wide variety of metal, honeycomb and fibre reinforced composite bonding applications. It has a very high shear strength even at temperatures up to 70 °C and a good peel strength. Table 4 shows the physical properties of this adhesive.

Table 4 Physical Properties of Redux 420 A/B

	Redux 420 A	Redux 420 B	Redux 420 A/B
Appearance	Yellow	Blue/Green	Green
Specific Gravity	1.1-1.2	0.95-1.05	1.1-1.2
Viscosity (Pa s)	90-130	0.8-1.6	35-45
Pot Life	-	-	1 hour
Shelf Life (stored at 18 to 25 °C)	3 Years	3 Years	-

Ciba Polymers Araldite 2013 (AV144-2 / HV997)

Araldite 2013 is a two component, room-temperature curing paste adhesive of high strength and toughness. It is thixotropic with good environmental and chemical resistance. Although it is designed as a metal bonding adhesive it is also suitable for bonding other materials such as ceramics, glass, rubbers, rigid plastics and most other materials in common use. Table 5 shows the physical properties of the adhesive.

Table 5 Physical Properties of Araldite 2013

	2013 A	2013 B	2013 A/B
Appearance	Grey soft paste	Beige soft paste	Grey paste
Specific gravity	1.14	0.9	1.2
Viscosity (Pa s)	50-95	thixotropic	thixotropic
Pot Life	-	-	50-80 minutes
Shelf Life (stored at 18 to 25 °C)	3 years	3 years	-

XD 4416

XD4416 is a two component, room-temperature curing paste adhesive of high strength and toughness. It is designed for bonding composite pipes but it is also suitable for bonding other materials such as metals. Table 6 shows the physical properties of the adhesive.

Table 6 Physical Properties of XD 4416

	Araldite AV 4415	Hardener HV 4416	Mixed
Appearance	White-beige paste	Black paste	Dark grey paste
Density (Mg/m^3)	1.55-1.65	1.55-1.65	1.55-1.65
Viscosity (Pa s)	90-140	50-70	80-140
Pot life	-	-	90 minutes
Shelf Life	2 years	2 years	-

Chapter 4

RESULTS AND DISCUSSION

4.1 Tensile Properties of Adherend - Mild Steel

Fig.25 shows a typical stress strain curve produced experimentally for cold rolled mild steel. Cold rolled mild steel and hot rolled mild steel were used as adherends throughout this study. Thus, the aim of this experiment was to investigate these two types of adherend. The tensile properties of adherends are summarised in Table 7a. Table 7b shows the comparison of fracture strength of bonded joints using the cold and hot rolled steel and indicates that, since the difference between the elastic modulus was small, the fracture energies of the adhesives were essentially independent of the adherend material. Bell[61] bonded steel and carbon fibre reinforced plastic (CFPR) double cantilever beam with epoxies, showed in this work that the adverse adherend type used has a significant effect upon the plastic zone size and stress levels within the adhesive layer.

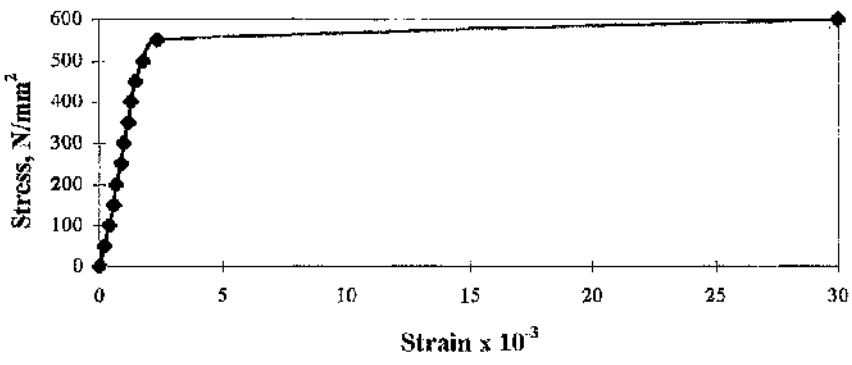

Fig.25 Stress strain curve for cold rolled mild steel adherend at room temperature

Table 7a Comparison of tensile properties of cold rolled mild steel and hot rolled mild steel.

Cold Rolled Mild Steel	0.2 % Proof Stress = 478 N/mm^2
Hot Rolled Mild Steel	Yield Stress = 200 N/mm^2

Table 7b Comparison of fracture strength of adhesives using two different steel adherends.

Adherend Type	**G_{IC} KJ/m^2 (Test no.)**
Cold Rolled Mild Steel	(1) 1.21
	(2) 0.78
	(3) 1.03
Hot Rolled Mild Steel	(1) 0.94
	(2) 1.12
	(3) 0.84

4.2 Tensile Properties of Bulk Adhesives

Calculations applied for bulk adhesives to produce stress strain curves are similar to that of adherends. Typical stress-strain curves of polymers can be seen in Figs.25a-c. Examples of the different curves obtained for F241, Araldite 2013 and XD 4416, were all tested at ambient temperature at a constant cross head rate of 0.5 mm/min. Each test was replicated three times. Comparing the three curves to the various stress strain curves in Fig.25d[60], it can be seen that F241 is a fairly tough material. Araldite 2013 and XD 4416, on the other hand were found to be relatively brittle materials. A summary of the three adhesives tensile properties can be seen in Table 8.

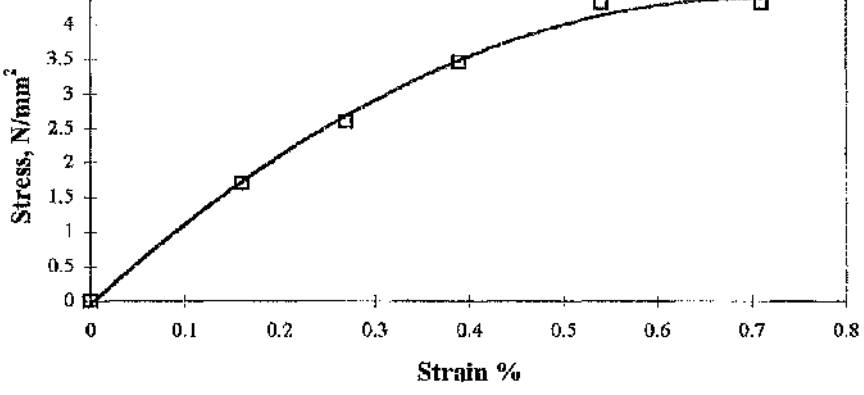

Fig.25a Stress-strain curve of F241

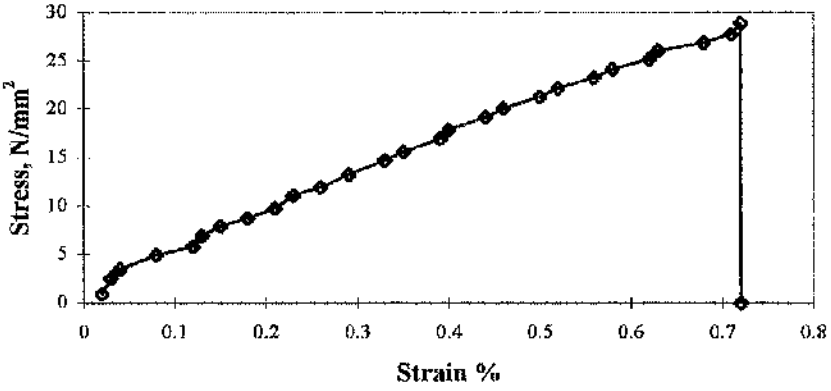

Fig.25b Stress-strain curve of Araldite 2013

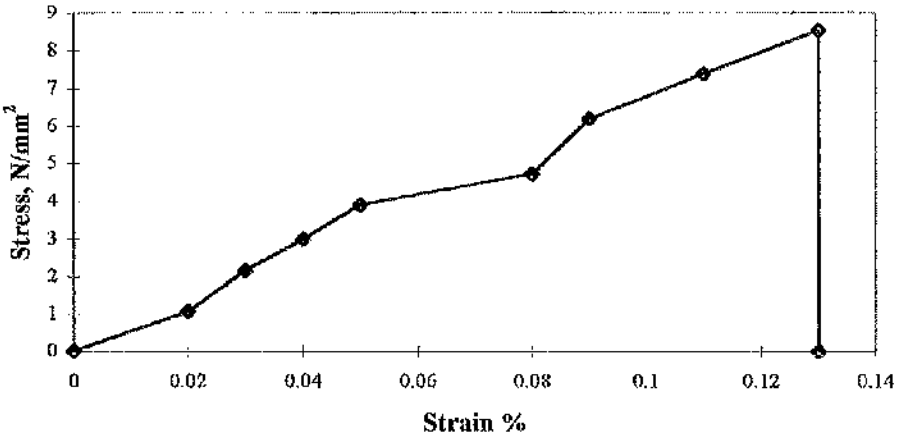

Fig.25c Stress-strain curve of XD 4416

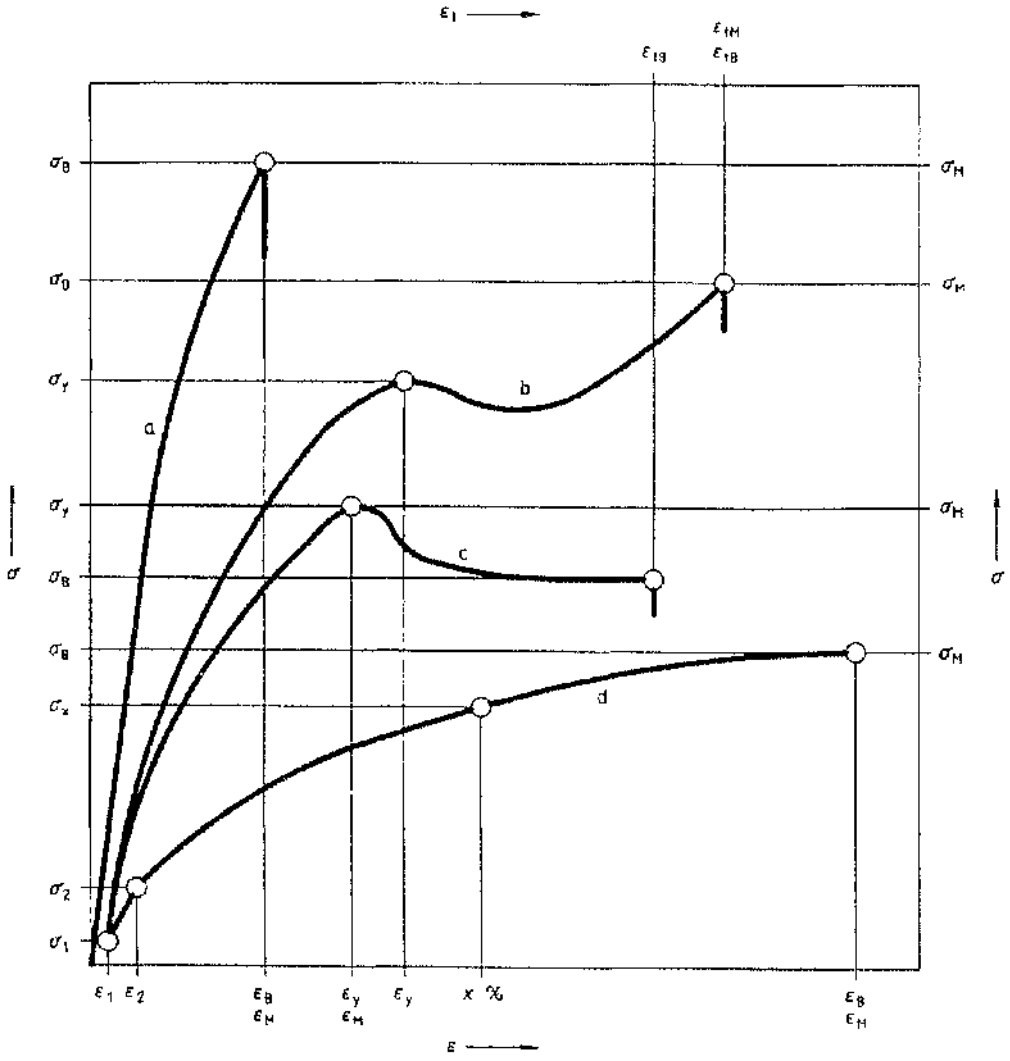

Curve a	Brittle materials
Curves b and C	Tough materials with yield point
Curve d	Tough materials without yield point

Fig.25d Typical stress/strain curves[60]

Table 8 Comparison of mechanical properties of the different types of adhesives

Adhesive	**Type**	**Young's Modulus (E) N/mm^2**	**Poisson's Ratio (ν)**
F241	Toughened Acrylic	3200	0.43
Redux 420	Two-part epoxy	14000	0.41
Aradlite 2013	Two-part epoxy	6711	0.54
XD 4416	Two-part epoxy	7237	0.4

4.3 Compliance of the Tapered Double Cantilever Beam

Full Size Specimens :

In this present study, the fracture toughness of F241, Redux 420 A/B, XD4416 and Araldite 2013 bonded joints were investigated. Table 9 shows the theoretical values of m for the standard geometry and this was used for F241, XD4416 and Araldite 2013. However for joints bonded with Redux 420, the theoretical value of m cannot be used due to the bending of the specimens during testing as shown in Fig.26. The plastic bending of the specimen causes the compliance to vary from the theoretical value.

Calculations of m :

$$m = \frac{dC}{da} = \frac{3a^2}{h^3} + \frac{1}{h}$$

Table 9 Theoretical m for full size specimen bonded with F241, XD4416 and Araldite 2013

	Theoretical m
Full size specimen	3.54 mm^{-1}

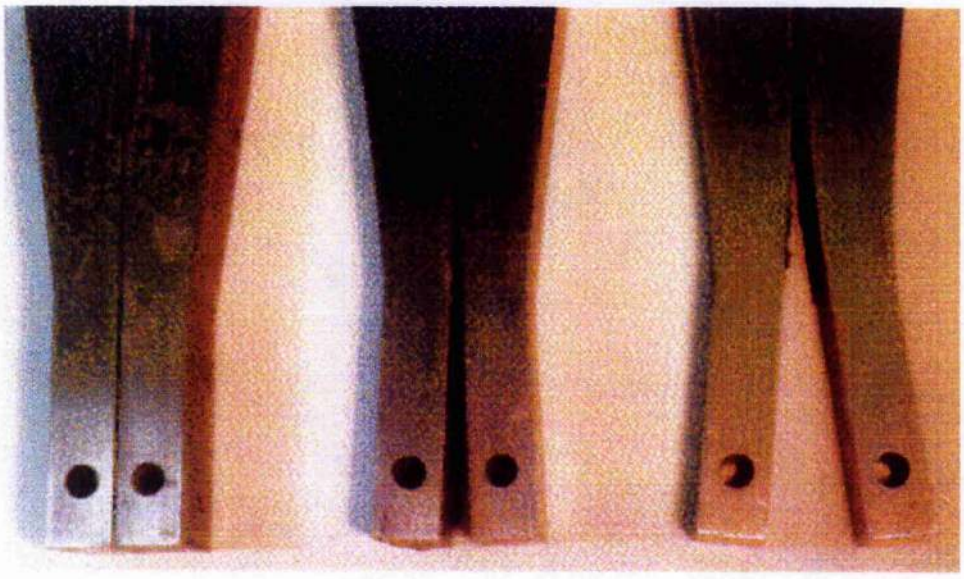

Fig.26 Joints bonded with Redux 420 A/B showing plastic deformation of the adherend.

Half Size Specimens :

Table 10 shows theoretical m for half size specimens which were used for joints bonded with F241, XD4416 and Araldite 2013. Since the specimens were reduced to half from the original size to enable temperature testing, the compliance of the half size specimens will also be changed. Therefore, it was necessary to correlate the fracture strength of the half size specimen with the full size specimens before performing temperature testing on the half size bonded joints.

Table 10 Theoretical m for half size specimens.

	Theoretical m
Half size specimen	7.08 mm^{-1}

Tables 11 and 12 below show a comparison of compliance and fracture strength of the joints between the full and half size specimens tested at room temperature. It can be seen from the tables that the fracture strength of both the full size specimens and half size specimens is in agreement. Although the compliance of the specimens has changed, the average fracture strength is approximately the same.

Table 11 Fracture parameters for full size TDCB specimens

Adhesives	**Loads (N)**	**Cal. G_{IC} KJ/m^2 m =3.54 mm^{-1}**	**Average G_{IC} KJ/m^2**
F241	3330, 3120, 3181	1.16, 1.02, 1.06	1.08
XD4416	400.4, 689.9, 702.8	0.017, 0.049, 0.052	0.04
Araldite 2013	2745, 2710, 2545.2	0.79, 0.77, 0.67	0.74

Table 12 Fracture parameters for half size TDCB specimens

Adhesives	**Loads (N)**	**Cal. G_{IC} KJ/m^2 m =7.08 mm^{-1}**	**Average G_{IC} KJ/m^2**
F241	1000, 1301, 1122	0.84, 1.42, 1.05	1.10
XD4416	148.8, 240.3, 255.6	0.02, 0.05, 0.05	0.04
Araldite 2013	946, 892, 938.4	0.75, 0.67, 0.73	0.72

The compliance of the tapered double cantilever beam has also been observed by Fenando *et al.*[11], using aluminium joints bonded with hot curing toughened epoxy. Excellent results between the theoretical and experiment results were obtained as can be seen in Table 13 .

Table 13 Compliance results[11]

	Theoretical m	Experimental m
Full size specimen	2.10 mm^{-1}	m = 2.05 mm^{-1}

4.4 Fracture Strength of Acrylic and Epoxy

Fig.27 shows a comparison of fracture strength of TDCB bonded joints, tested at ambient temperature. Three different cold curing adhesives were used for bonding the joints, namely F241, Araldite 2013 and XD 4416. It can be seen that F241 exhibits the highest fracture strength followed by Araldite 2013, while XD 4416 has the lowest fracture strength. It must be noted that XD 4416 should be post cured in order to achieve its maximum strength. In this present study, XD4416 was cured at ambient temperature. It was also observed that F241 is a softer adhesive compared to Araldite 2013 and XD4416, which are very brittle. Crack propagation of F241 was by tearing, where cavities caused by plastic flow linked up and the crack advanced by tearing producing rough peaks as shown in Fig.28. The plastic flow at the crack tip naturally turns an initially sharp crack into a blunt crack. Stress whitening was found on the rough fracture surface of the initiation region. The important thing that was noted was that the crack growth by tearing consumes a lot of energy which means the fracture strength was naturally higher.

Crack propagation in the epoxies Araldite 2013 and XD 4416 was in a much more brittle manner compared to F241.The fractured surface of Araldite 2013 was similar to that of a fractured chalk surface indicating a brittle adhesive, which frequently lead to brittle fracture at a low fracture strength because it was confined to a very small volume compared to the size of the specimen. Therefore, the amount of plastic energy absorbed was low. Due to the cavities coalescing to form secondary cracks, in the case of Araldite 2013, the main crack propagated in a zigzag manner, which can be seen in Fig.29. As for XD4416, crack propagation was in a relatively straight line manner, unimpeded by any porosity giving a smooth surface as shown in Fig30. Similar types of crack propagation of epoxies were also observed by Gledhill[62] and Kinloch[63].

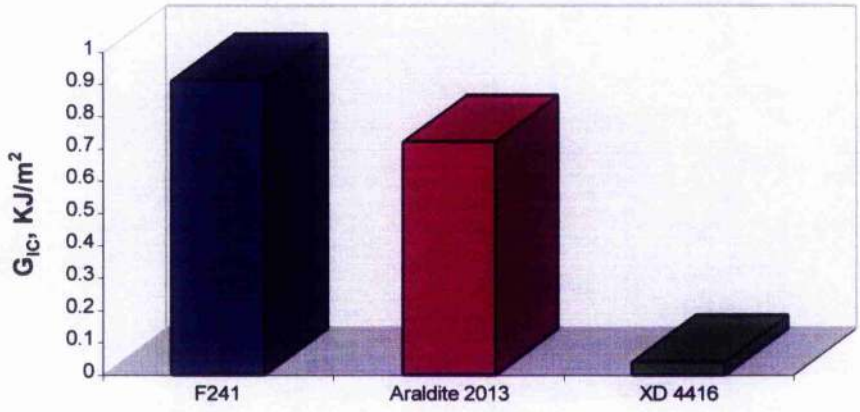

Fig.27 Comparisons of fracture strength of tapered double cantilever beam joints bonded with three different adhesives tested at ambient temperature

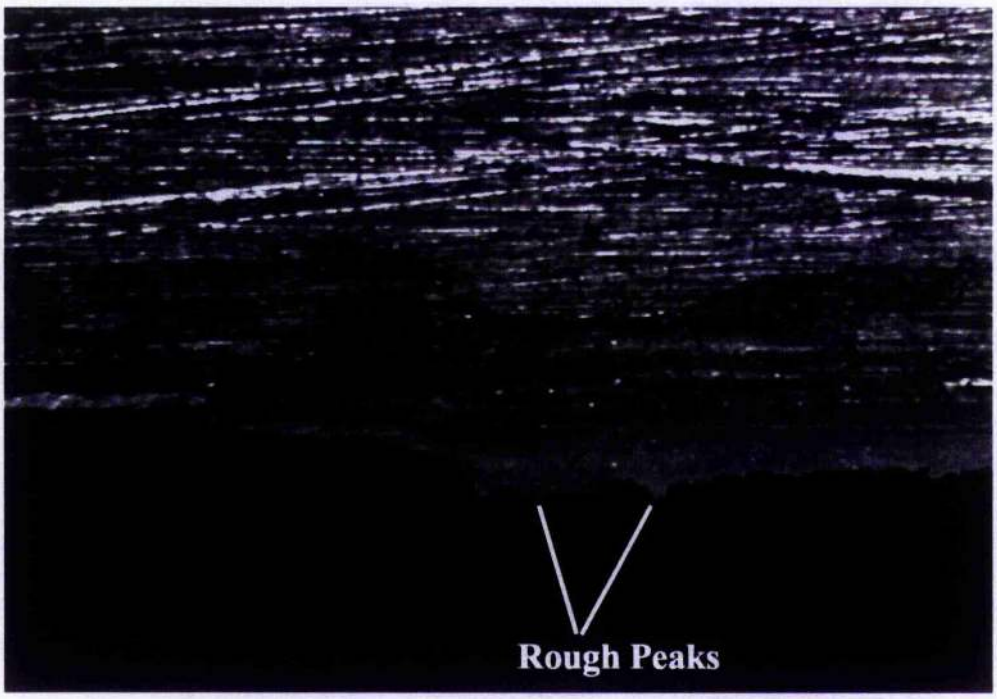

Fig.28 Crack propagation of joints bonded with Permabond F241

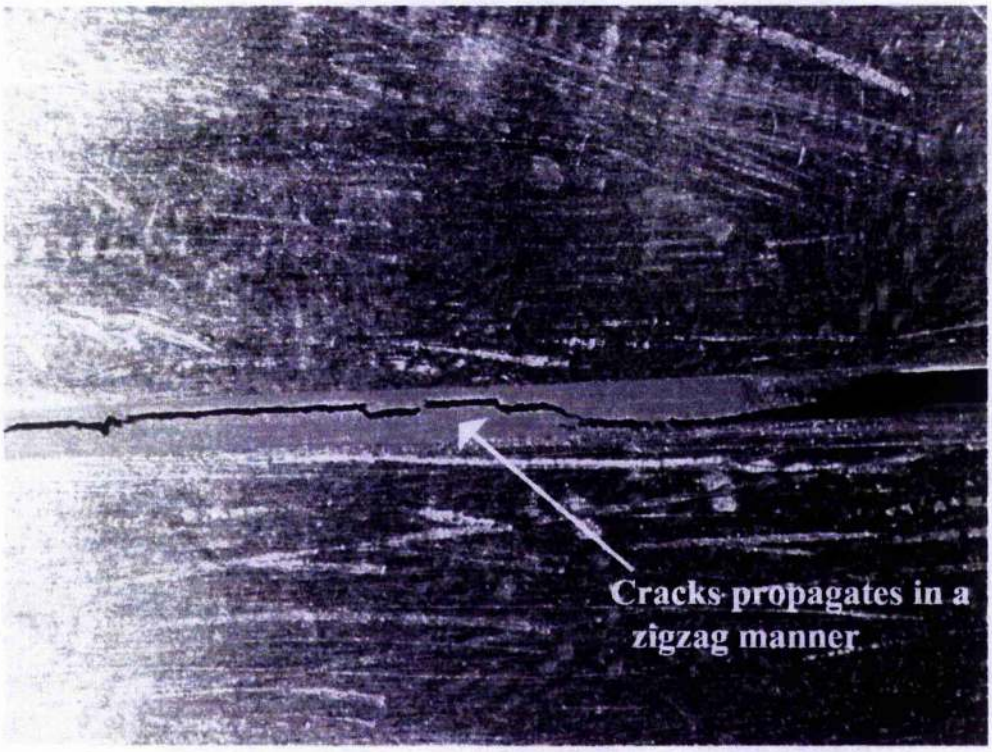

Fig.29 Crack propagation of joints bonded with Araldite 2013.

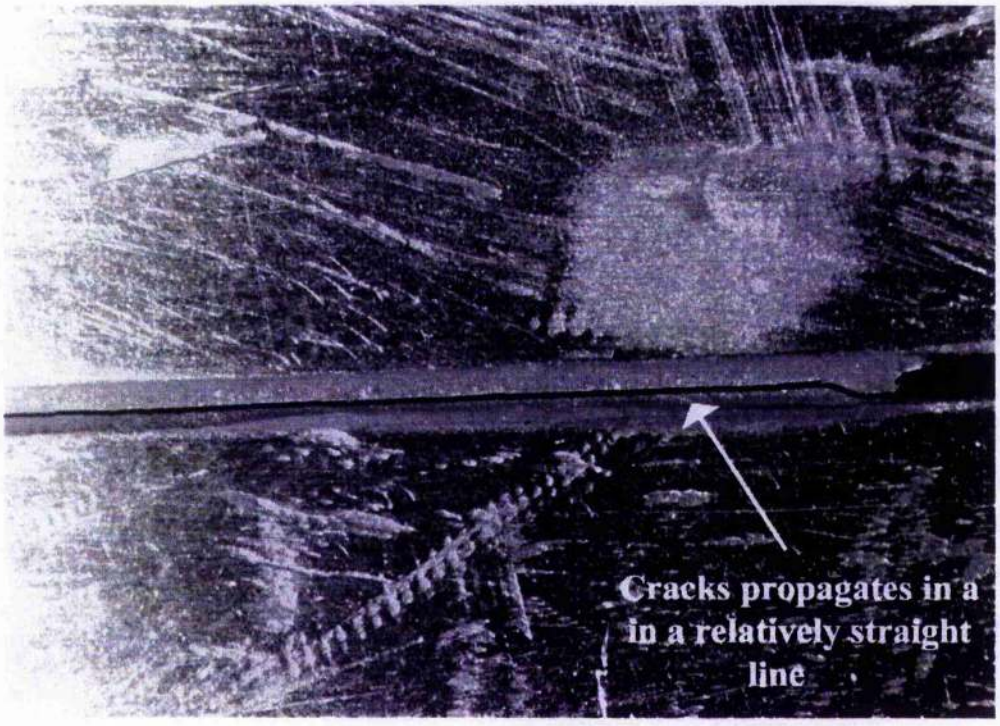

Fig.30 Crack propagation of joints bonded with XD4416

4.4.1 Micromechanisms of Failure

With the use of the stable test-pieces it is possible to relate features on fracture surfaces to particular types of crack propagation behaviour. When failure takes place by continuous propagation, as for F241, the fracture surfaces observed at the, slow fracture initiation region was filled with irregular cavities. This could have been caused by imperfect bonding. Stress concentrates around these cavities producing stress whitening on the fractured surface with only cohesive failure present, which can be seen in Fig.31. Debruyne[64] and Bascom[65] both furnished examples in the literature of situations where trapped air bubbles in the adhesive bond line furnished sites for high localised stress situations resulting in premature crack initiation and propagation to joint failure. Stress whitening is a process whereby small crack-like entities which are normal to the maximum principal tensile stress are formed during deformation. The presence of the white colour on the fracture surfaces of brittle adhesives has been taken as evidence of highly stressed areas around the cavities. The white coloration is thought to be due to layers of the material on the fracture surface possessing a different refractive index from the adhesive due to damage within the material. The white coloration is particularly noticeable on the fracture surface of F241 but the amount of coloration is considerably reduced on the fracture surface of the epoxies. This was because F241 has a lower modulus compared to epoxies and the colour of the viscous F241 was off-white. In Fig.32 the fast fracture end region of the fracture surface shows a relatively smoother surface with no stress whitening or crazing. Thus, it can deduced that the rapid fracturing speed at the end region of the bonded joint (constant cross-head speed) has a adverse effect on the appearance of the surface. The faster the fracture speed the less the time for stresses to build up around the cavities.

On the other hand, when failure takes place by continuous propagation, as in the epoxies, the fracture surfaces are relatively flat and featureless, suggesting little or no plastic deformation. Fig.33 shows a fractured surface from the initiation region of Araldite 2013. Weak bonds within the adhesive de-bond and combines together to form into a cavity and eventually coalesce with the crack. This causes the crack to propagate further in a zigzag manner and the process is repeated again. In the fast fracture end region, the fracture surface, as shown in Fig.34, was found to be slightly smoother compared to the slower fracture of the initiation region.

Propagation took place by a 'stick-slip' mode on the fracture surface of XD 4416. Crack arrest lines were observed faintly on the middle region, each one corresponding to a jump-arrest line, as seen in Fig.35. Distinct re-initiation marked the direction of crack propagation. Fig.36, shows the slow fracture initiation region of the XD 4416. The surface was observed to be smooth and reflective with embedded porosity. Similar to that of Araldite 2013, the crack spreads between a pair of atomic planes giving an essentially flat surface by cleavage. Towards the fast fracture region, in Fig.37, the surface was similar to that observed in the initiation region except that more jump-arrest lines were found towards the fast fracture end region. This behaviour was also seen by Young and Beaumont[66], Selby and Miller[67] and Phillips *et al.*[68], all using epoxy resins.

The initiation fracture surface of Redux 420 shown in Fig.38 involves cracks being impeded by porosity. This arises since when a crack meets an array of such porosity it becomes pinned and bows out between the porosity forming secondary cracks. The surface of the initiation region was also found to be a highly stressed region due to stress whitening present around the porosity indicating plastic deformation occurring around the crack tip. Failure of the adhesive was observed to be a combination of both cohesive and interfacial. The fast fracture surface, seen in Fig.39, was different to the initiation region. The fast fracture surface appeared to have little or no stress whitening, indicating a more brittle failure in this end region.

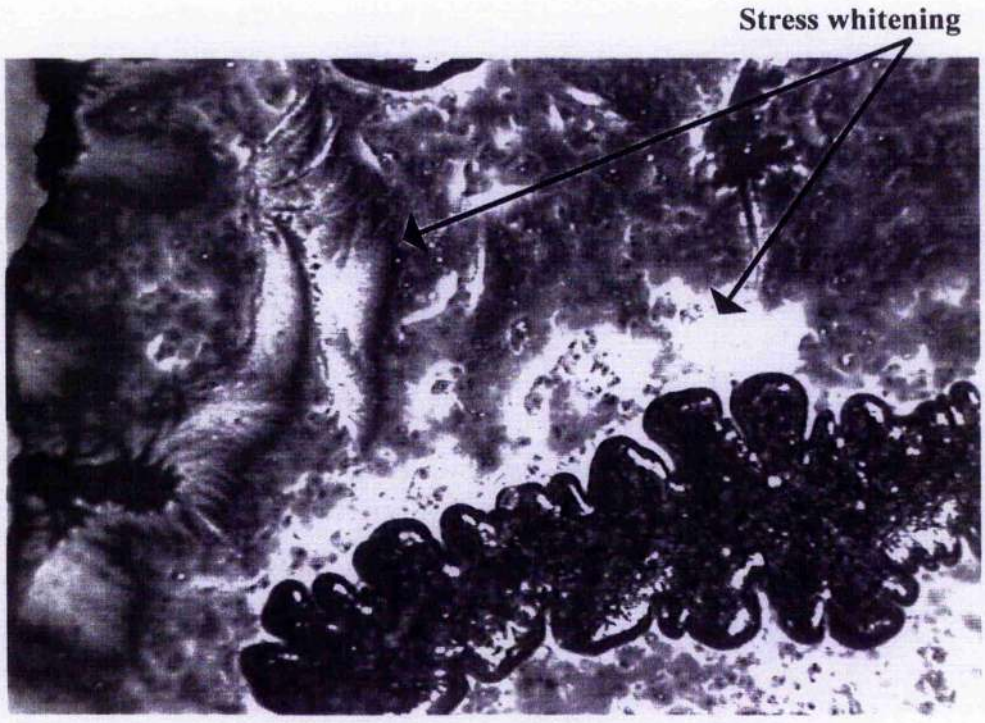

Fig.31 Initiation region of the fractured surface of acrylic F241 (30X)

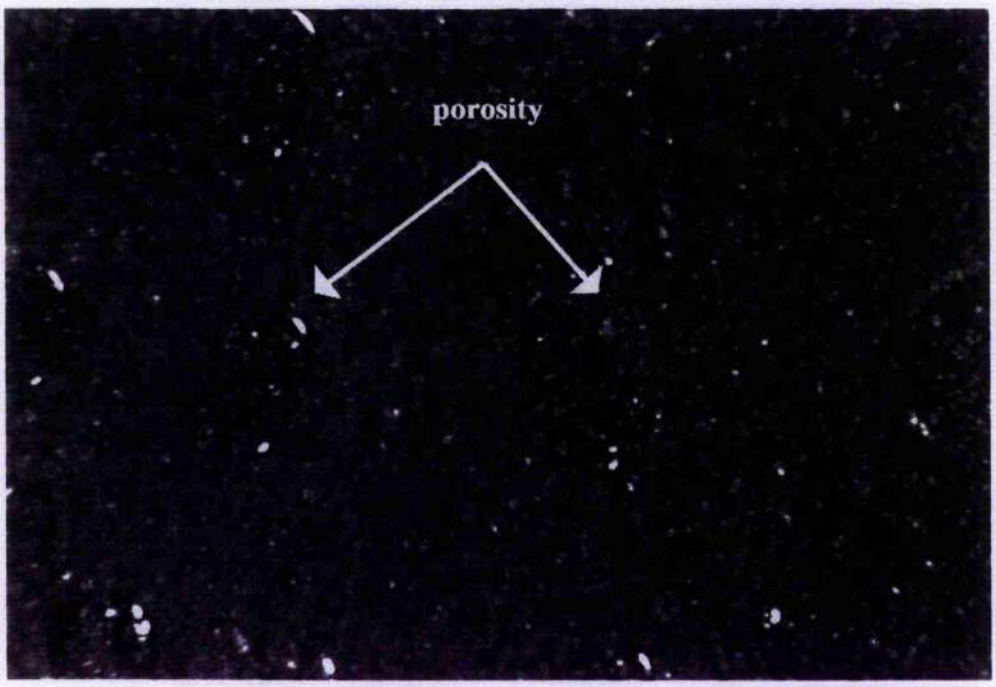

Fig.32 End region of the fracture surface of F241 (30X)

Fig.33 Initiation region of fractured surface of Araldite 2013 (20X)

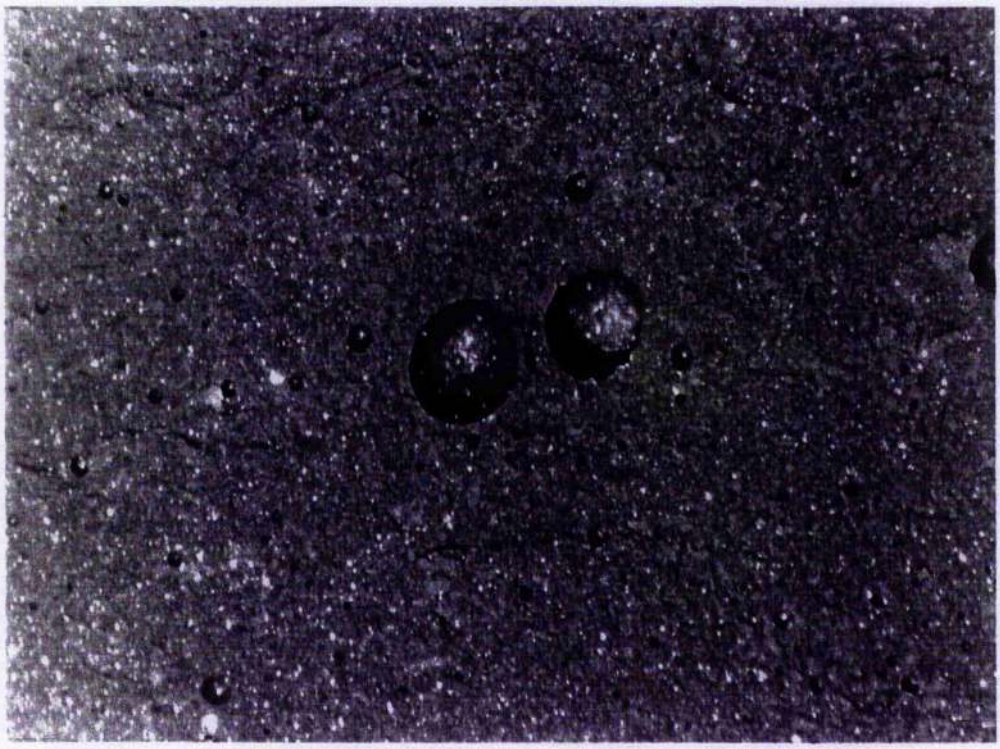

Fig.34 End region of fracture surface of Araldite 2013 (30X)

Fig.35 Fractured surface of XD4416 with marked river lines (20X)

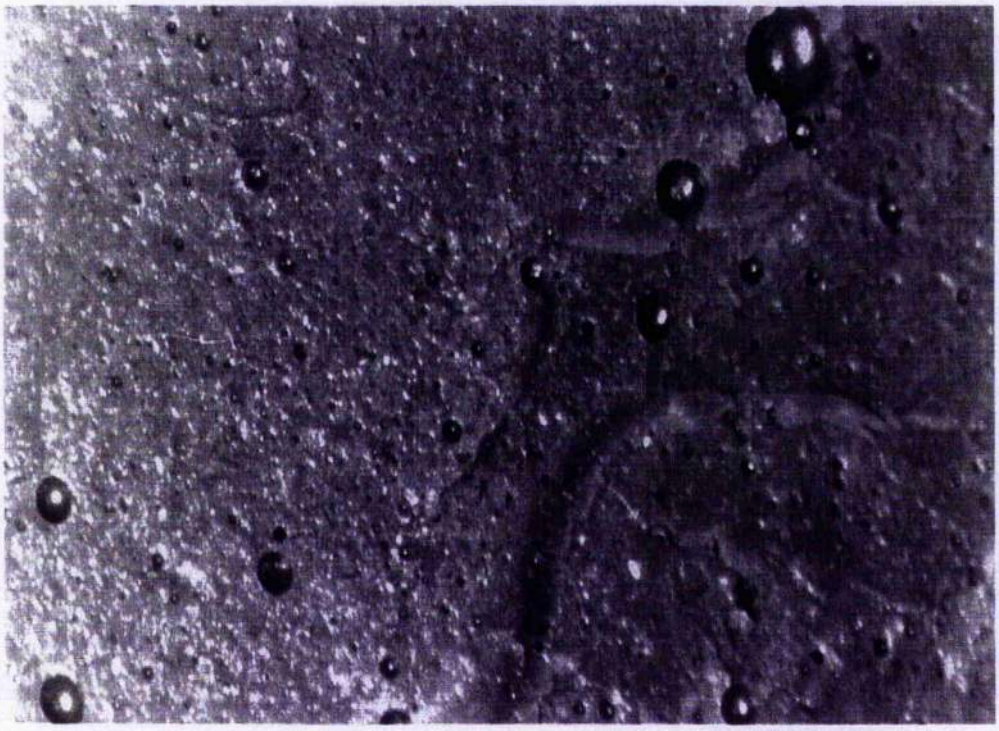

Fig. 36 Initiation region of fractured surface of XD4416 (20X)

Fig.37 End region of fracture surface of XD4416 (20X)

Fig.38 Initiation region of fractured surface of Redux 420 (30X)

Fig.39 End region of fracture surface of Redux 420 (30X)

4.5 Effect of Temperature on Fracture Strength

Temperature has an effect on the fracture strength on the bonded joints. This is readily seen in the graph of fracture strength for the different cold curing adhesives used for bonding the tapered double cantilever beams in Fig.40. The test temperature in most cases ranges from -40 °C to 60 °C. It was observed from the figure that F241 gave the best overall performance over the test temperature range. This indicates that it is most suitable for use in such adverse temperature environments. Mallick[69] tested CFRP/Al lap joints, at a temperature range of 20 °C to -55 °C, using different adhesives. It was also found that an acrylic adhesive exhibited the best lap joint strength and fracture strength. Lees[70] found good durability results with F241 using etched aluminium in 1982. This was based only a 3% loss in joint strength after 1000hr in 100 % RH at 45 °C

Araldite 2013, on the other hand, exhibited reasonable strength when tested at ambient temperatures but its strength decreased drastically when tested in both high and low temperature. XD 4416, being very brittle results in extremely low fracture strength when tested at ambient and -40 °C but had the highest fracture strength at 60 °C benefiting from its considerable ductility resulting from a post cure effect. This indicates that this adhesive is particularly suitable for use in this higher temperature environment. Work by Al-Hamdan[71] on steel/steel lap joints bonded with Ciba-Geigy epoxy 2004 tested over a range of temperature of -60 °C to 200 °C showed similar results. Joints were strongest in the region of 0-70 °C and at the lower temperatures, the adhesive became brittle but with a greater scatter in the results. In the current study, it was found that for epoxies, less scatter in results was observed as seen in Figs.46 and 54.

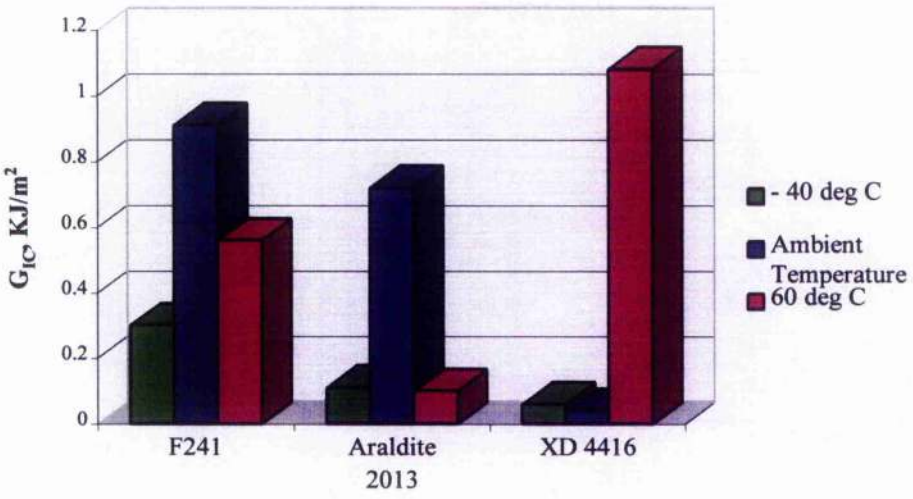

Fig.40 Effect of temperature on fracture strength of tapered double cantilever beam joints bonded with different adhesives

4.5.1 Permabond F241 Toughened Acrylic

F241 has a good ambient temperature fracture strength of approximately 0.9 KJ/m^2, as shown in Fig.41. As the temperature increases the adhesive viscosity reduces, it softens and becomes unable to sustain the load thus enabling it to flow and wet the surface causing the fracture strength to decrease to approximately 0.55 KJ/m^2. This explains the huge scatter in results, as seen in Fig.41, caused by unstable ductile tearing. The fracture surface at the higher test temperature can be seen in Fig.42. It appears to have more stress whitening lines shaped in contours, compared to those tested at ambient temperature which had less contoured white lines, as shown in Fig.43. At the low temperature, the adhesive became brittle leading to further reduction in fracture strength to 0.3 KJ/m^2. More stable crack growth with less scatter in results was observed as shown in Fig.41 and the fracture surface at the lower test temperature showed no stress whitening. Defined directional river marked or jump-arrest lines were, instead, observed on the fracture surface as shown in Fig.44. These river lines indicated the initiation and arrest of the crack during the process of crack propagation. The marked lines also indicated a more brittle adhesives when exposed to low temperature.

Fig.45 shows a comparison of the load versus displacement traces as a function of temperature for F241. The maximum load at point A of the three graphs seen in figure was used for calculating the fracture strength. It can be seen from the graph that when tested in ambient temperature it showed a mixture of stable and unstable continuous crack propagation in the tapered double cantilever beam. At the higher test temperature of 60 °C, it revealed a rather unstable ductile crack propagation caused by the softening of the adhesive. Clearly, when tested at the low temperature of -40 °C , unstable 'stick-slip' crack propagation was observed on the load-displacement trace which coincided with the marked lines found on the fracture surface.

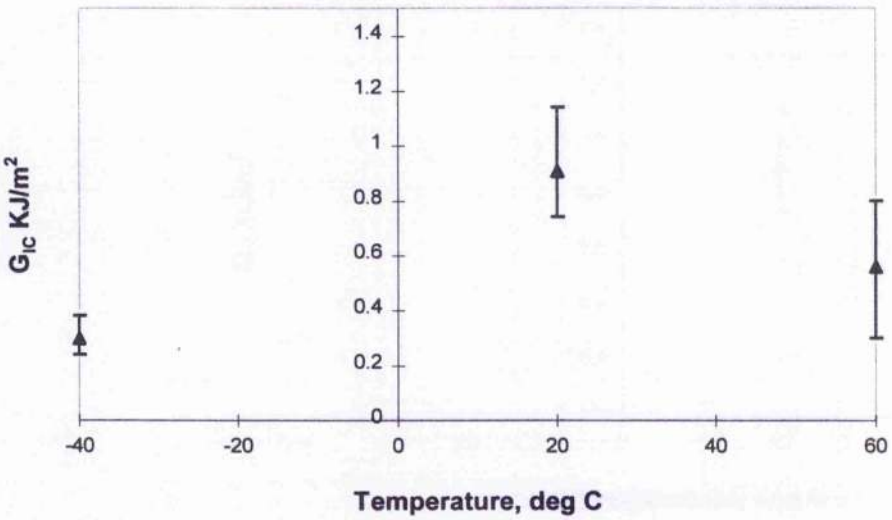

Fig.41 Effect of temperature on fracture strength of tapered double cantilever beam bonded with F241

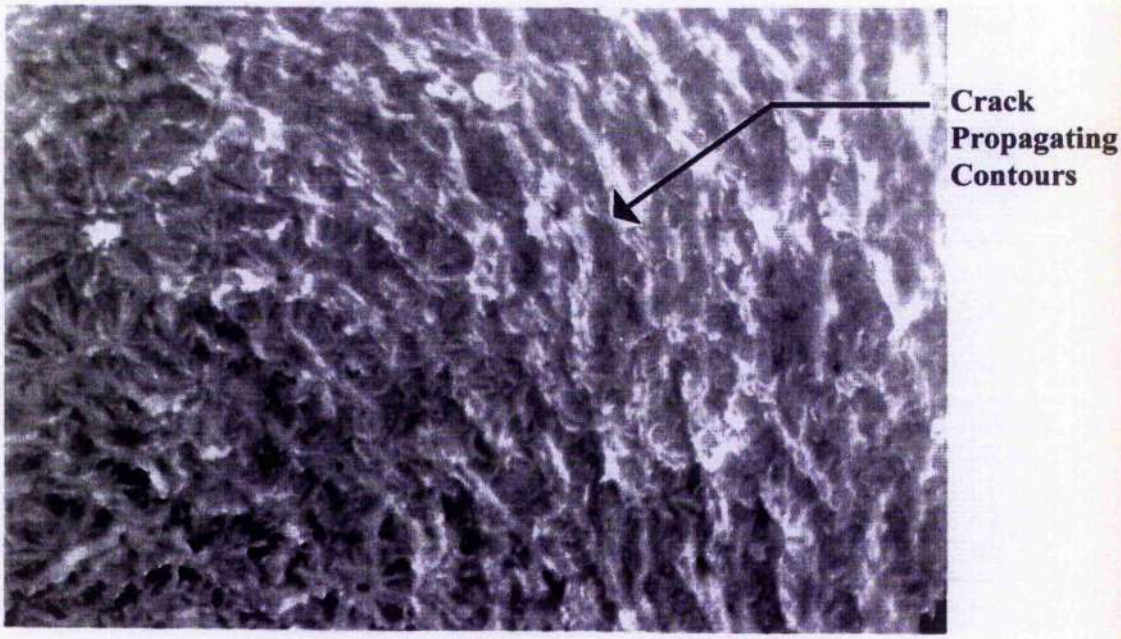

Fig.42 Fracture surface of F241 tested at 60 °C (20X)

Fig.43 Fracture surface of F241 tested at ambient temperature (20X)

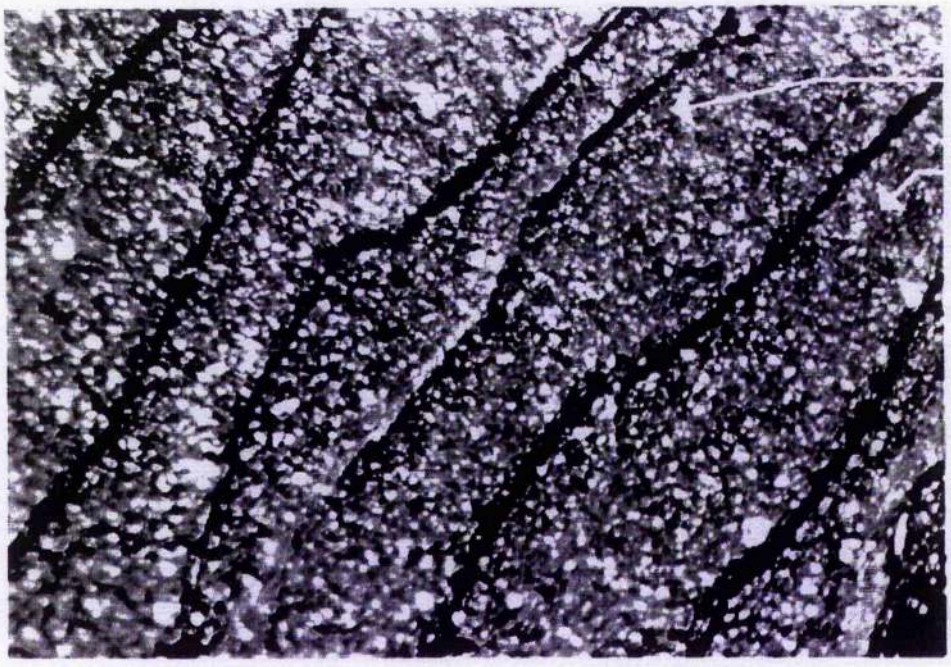

Fig.44 Fracture surface of F241 tested at -40 °C (20X)

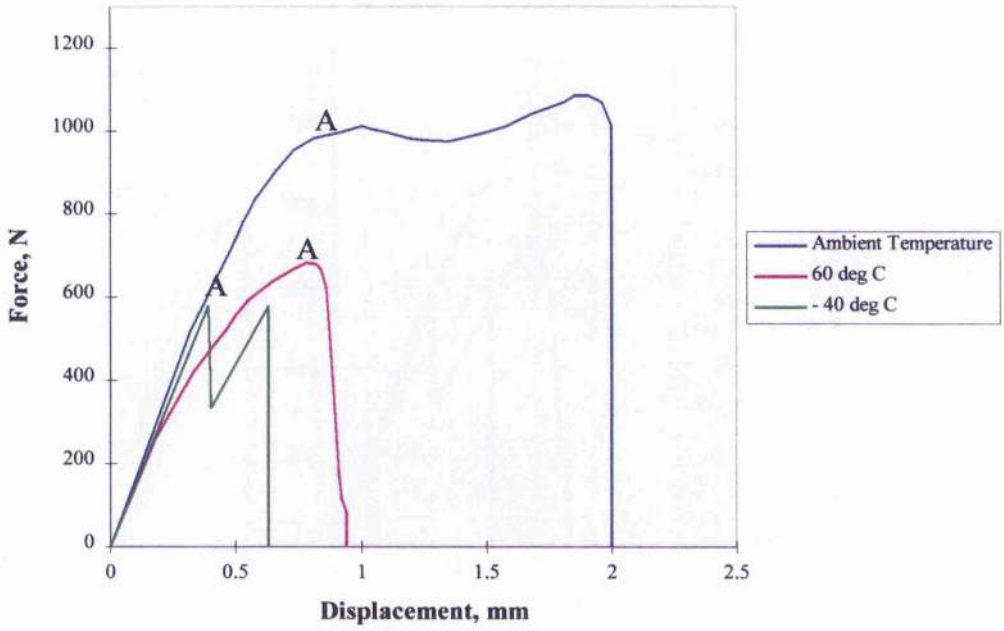

Fig. 45 Comparison of the load against displacement graphs for F241 tested at a series of temperatures.

4.5.2 Ciba Polymers Araldite 2013

Araldite 2013 adhesive was found to be extremely temperature sensitive when compared to that of F241. At ambient temperature, it had a fracture strength of approximately 0.7 KJ/m^2, but this dropped to less than half of this value when tested at the higher temperature of 60 °C, as shown in Fig.46. The results also appeared to have more scatter at ambient temperature compared to 60 °C and -40 °C. At the lower test temperature, the fracture strength was reduced from 0.7 KJ/m^2 to 0.45 KJ/m^2. This reduction was not as severe as when this adhesive was tested at the higher temperature.

The fracture surface of the initiation region tested at ambient temperature shown in Fig.47 was observed to be 'sand' rough and observed to be similar to that of the fractured surface of chalk. The fast fracture end region, shown in Fig.48, shows a slightly smoother and more reflective surface. The fracture surface from the higher test temperature is shown in Figs.49 and 50, where a combination of failure was observed. Interfacial failure was found in the initiation region (Fig.49) while towards the fast fracture end region, cohesive failure was observed (Fig.50) At the lower test temperature seen in Figs.51 and 52, only cohesive failure was observed. The fracture surface seem to be lot smoother than those tested at ambient temperature in the initiation region and fast fracture end region. The fast fracture region showed furrow like fracture lines parallel to the crack propagation direction. Stable crack propagation appears to have produced this surface.

Fig.53 shows a comparison of the load versus displacement traces as a function of temperature for Araldite 2013. The maximum load at point A of the three graphs seen in figure was used for calculating the fracture strength. It can be seen that when tested at ambient temperature this adhesive shows a mixture of stable and unstable continuous crack propagation, which explains the huge scatter in results. At the higher test temperature of 60 °C, where the fracture strength decreased drastically, there was unstable but slightly ductile crack propagation caused by the softening of the adhesives. When tested at -40 °C , stable continuous crack propagation was observed.

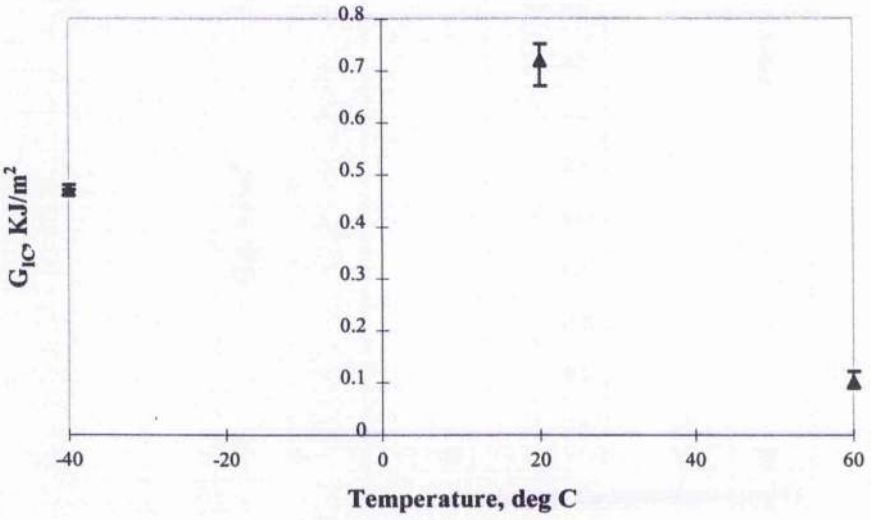

Fig.46 Effect of temeprature on fracture strength of tapered double cantilever beam bonded with Araldite 2013

Fig.47 Fracture surface of Araldite 2013 at initiation region tested at ambient temperature (20X)

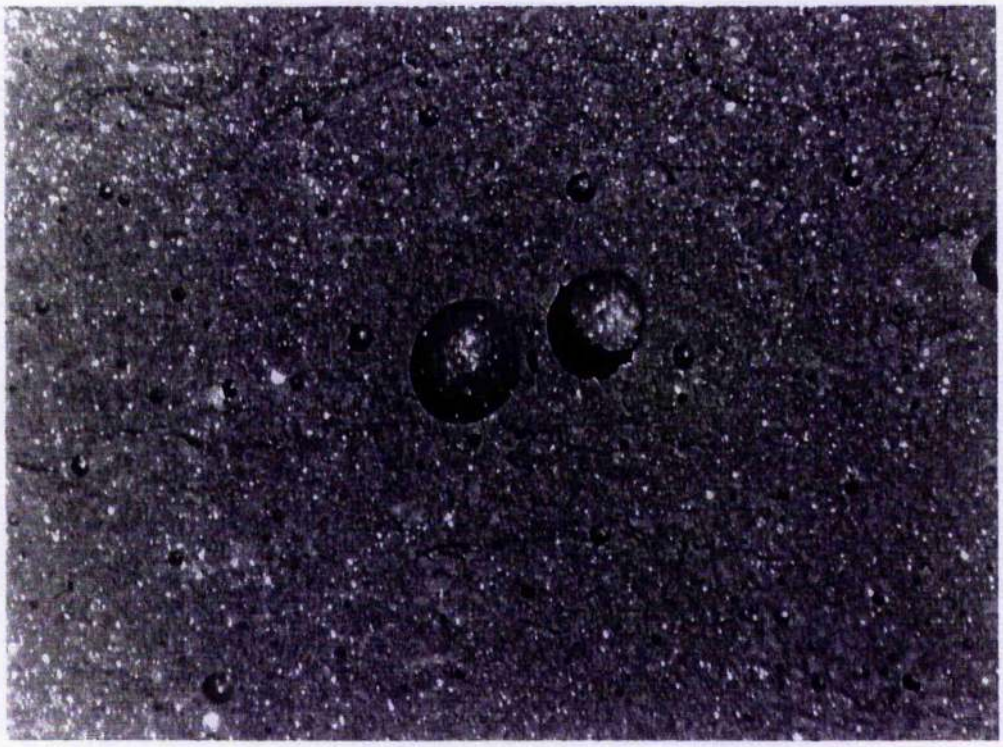

Fig.48 Fracture surface of Araldite 2013 at end region tested at ambient temperature (20X)

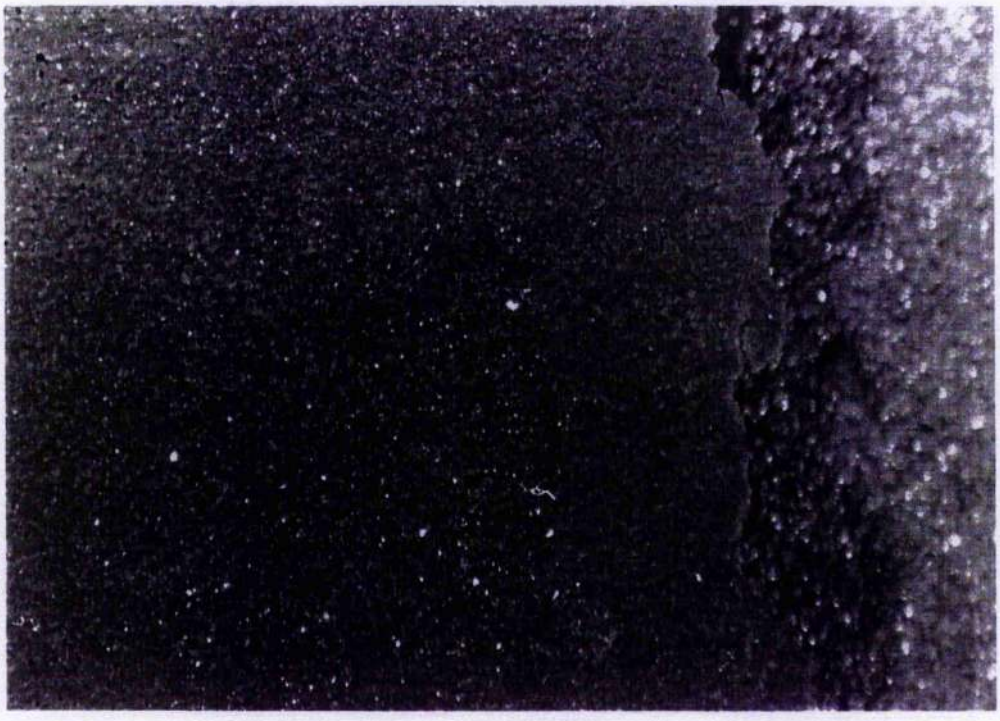

Fig.49 Fracture surface of Araldite 2013 at initiation region tested at 60 °C (20X)

Fig.50 Fracture surface of Araldite 2013 at end region tested at 60 °C (20X)

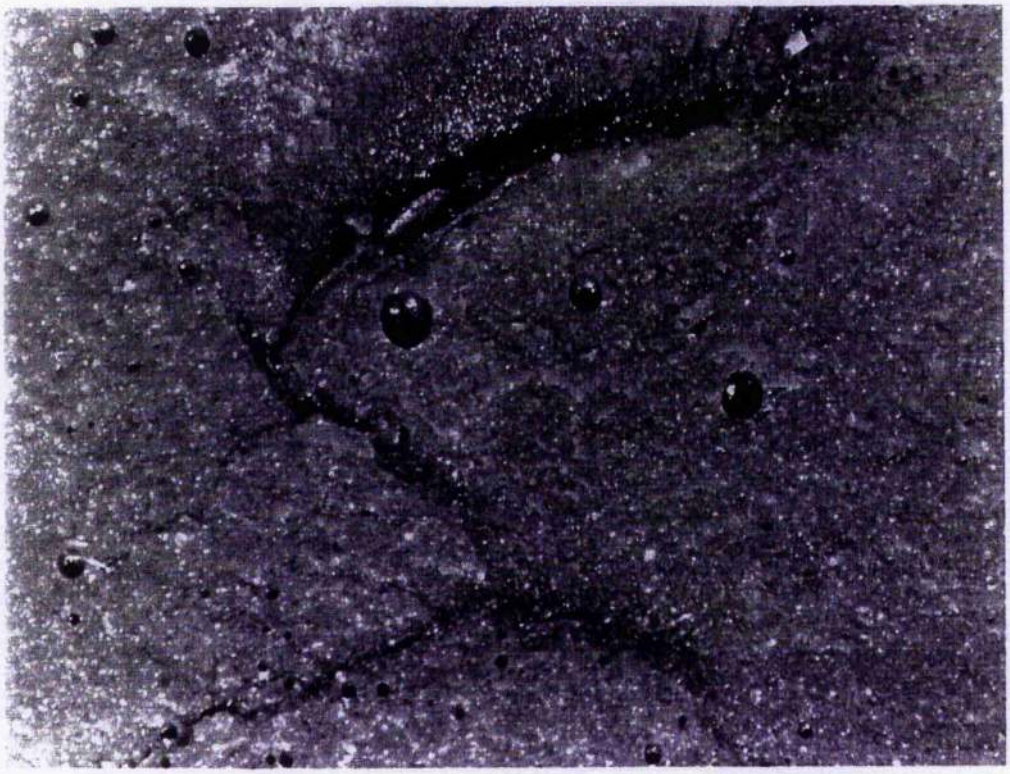

Fig.51 Fracture surface of Araldite 2013 at initiation region tested at -40 °C (20X)

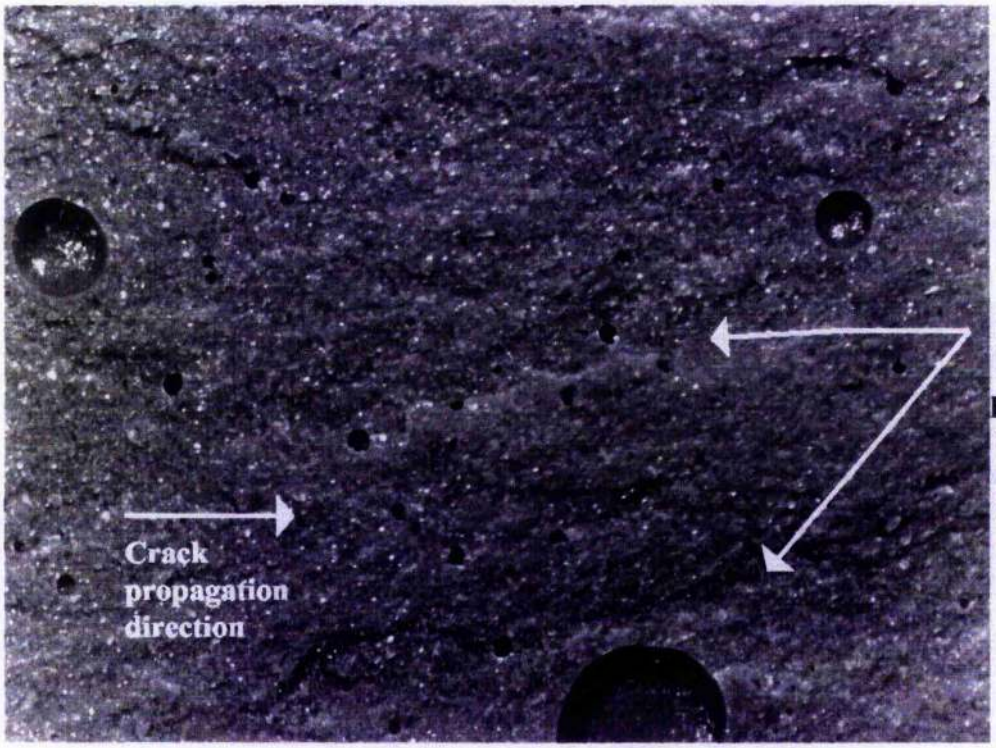

Fig.52 Fracture surface of Araldite 2013 at end region tested at -40 °C (20X)

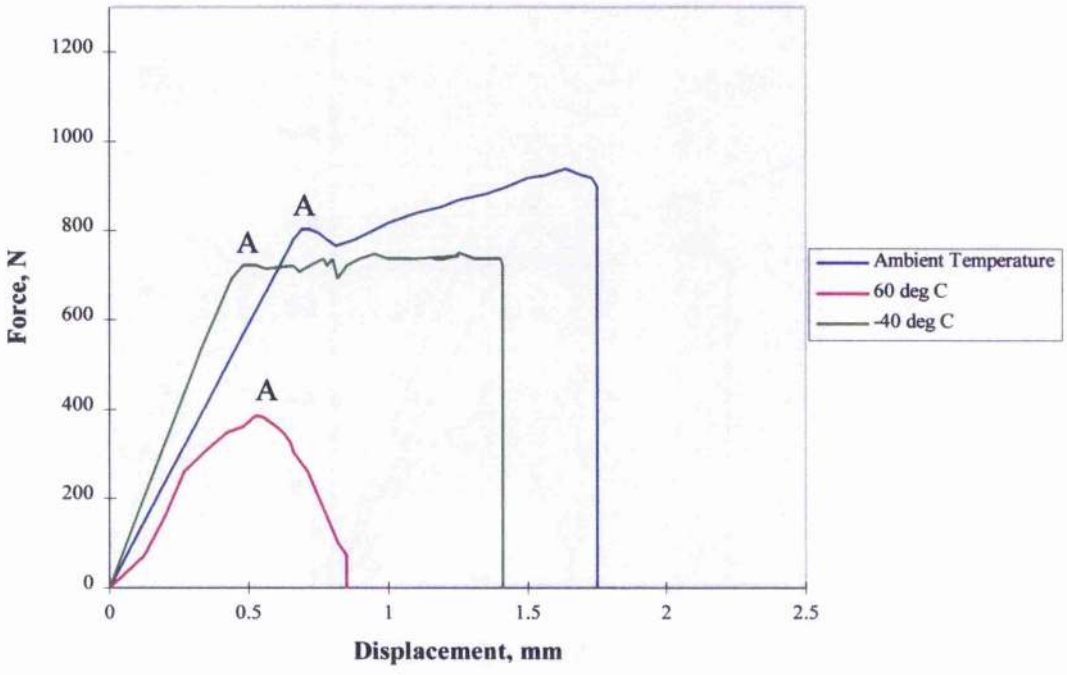

Fig.53 Comparison of the load against displacement graphs for Araldite 2013 tested at a series of temperatures.

4.5.3 XD 4416

Ciba Geigy two-part epoxy adhesive XD4416 is primarily intended for the use with warm curing and for optimum properties, a post cure treatment is required. In the current study, the adhesive was used with an ambient curing process temperature which results in only partial cure. Only at the test temperature of 60 °C does the adhesive becomes fully cured. The curing procedure adapted in this study have heavily affected the results for this adhesive.

This XD 4416 adhesive had a very low fracture strength of approximately 0.04 KJ/m^2 when tested at room temperature, as seen in Fig.54. At 60 °C, the fracture strength increased from 0.04 to 1.1 KJ/m^2.This phenomenon is a complete reverse of the temperature dependent behaviour of the other adhesives due to post cure effect. The results showed more scatter when tested at the higher temperature due to softening of the adhesive. At -40 °C, the fracture strength remained similar to that at ambient temperature. This suggests that this adhesive is highly suitable for use at the high temperature environment.

The fracture surface of the initiation region at ambient temperature is shown in Fig.55 and was observed to be smooth and slightly shiny. Towards the fast fracture region, in Fig.56, parallel crack propagation stress whitening lines were observed. Figs.57 and 58 show fracture surfaces tested at 60 °C, where it can be seen that the fracture surfaces were found to have an increase of stress whitening at the initiation region while at the end region, a smooth and reflective surface was observed. A totally different fracture surface was observed at -40 °C as shown in Figs.59 and 60, where there is a distinct

directional wave form. At the initiation region the waves were perpendicular to the crack propagation direction while at the fast fracture region the waves are parallel to the crack propagation direction.

Fig.61 shows a comparison of the load versus displacement traces for XD 4116 over the test temperature range. The maximum load at point A of the three graphs seen in figure was used for calculating the fracture strength. It can be seen that when tested at ambient temperature unstable ' stick- slip' crack propagation was observed. At 60 °C, with fracture strength increased more than four times over the ambient temperature value and revealed a mixture of stable and unstable crack propagation. As at ambient temperature, unstable crack propagation was observed when this adhesive was tested at -40 °C.

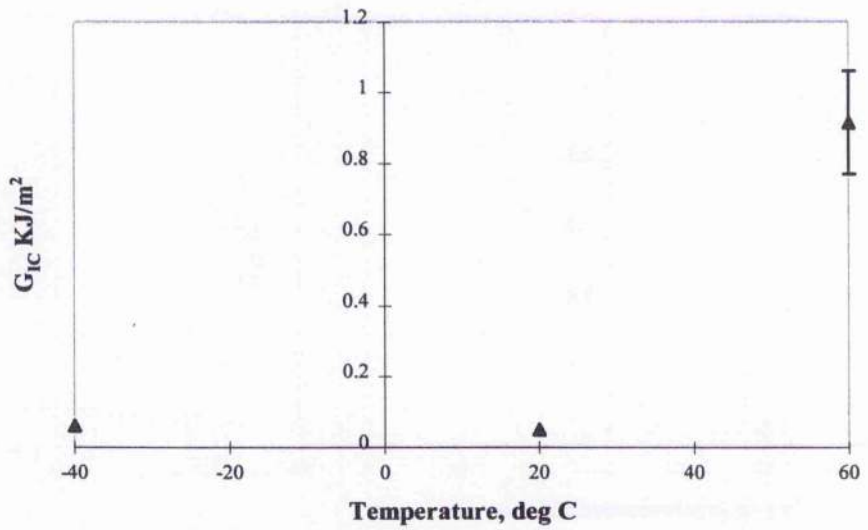

Fig.54 Effect of temperature on fracture strength of tapered double cantilever beam bonded with XD 4416

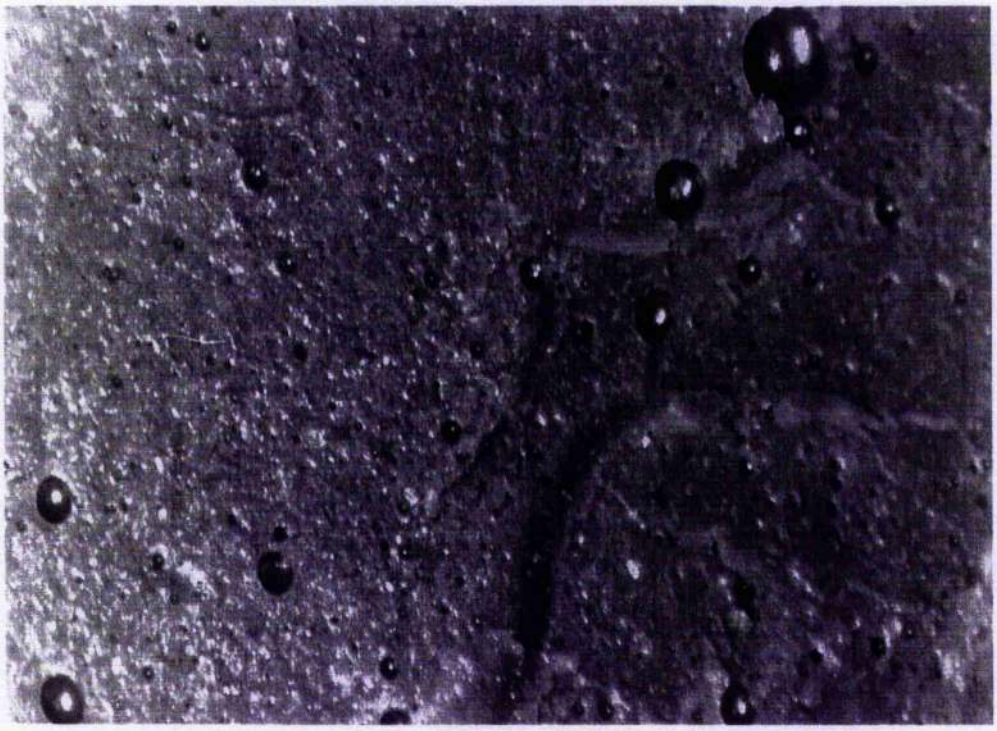

Fig.55 Fracture surface of XD4416 at initiation region tested at ambient temperature (20X)

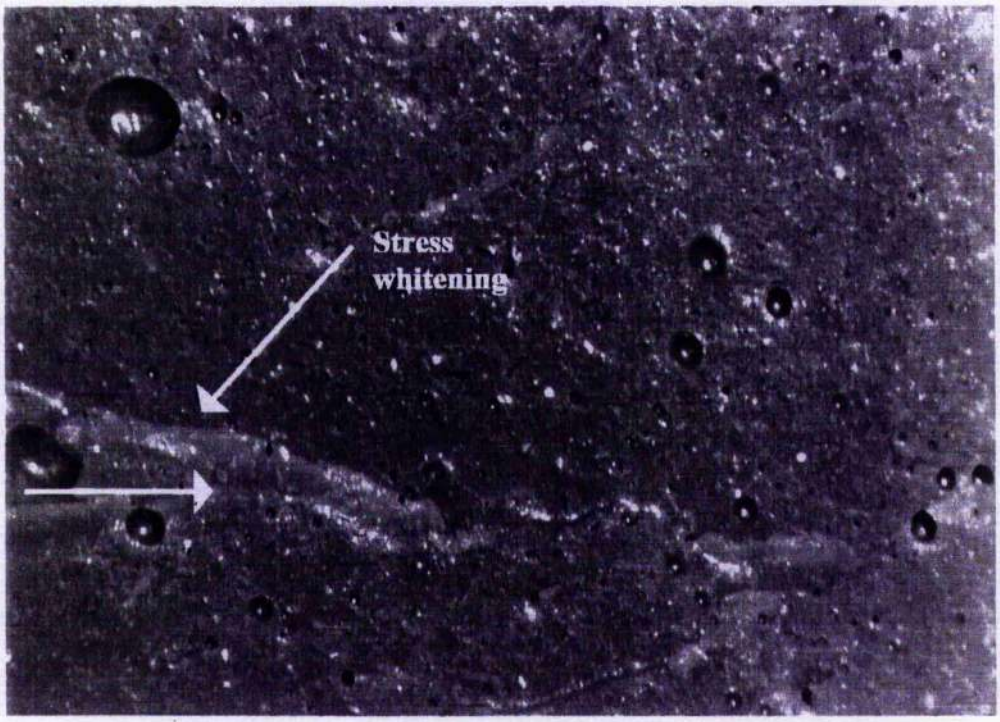

Fig.56 Fracture surface of XD4416 at end region tested at ambient temperature (20X)

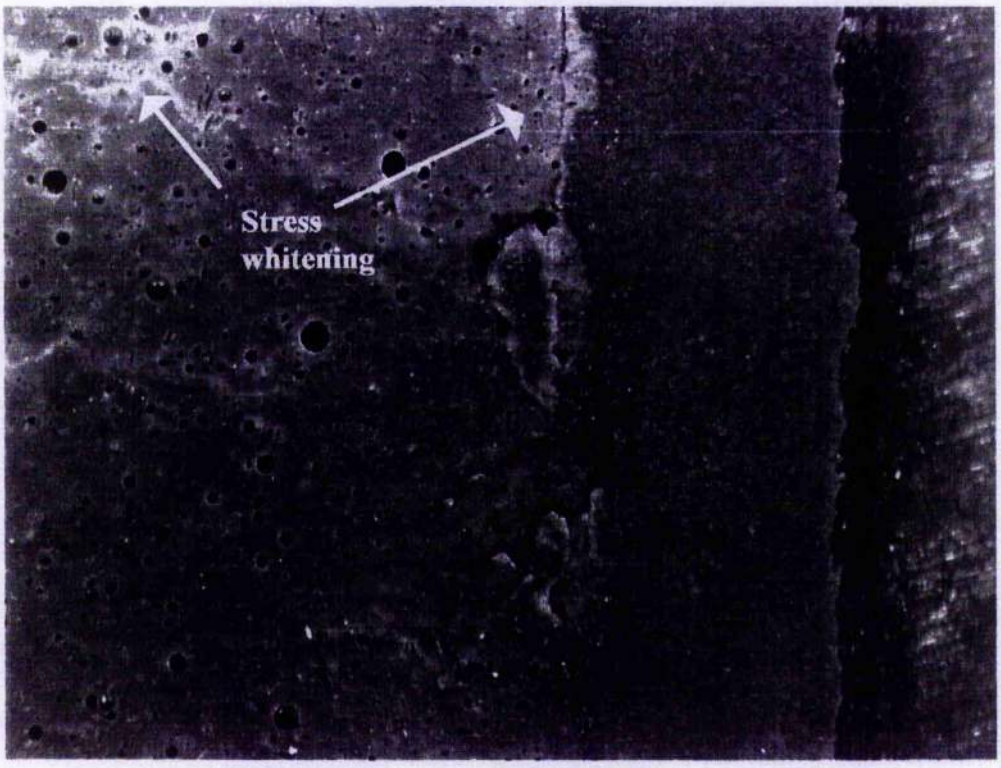

Fig.57 Fracture surface of XD4416 at initiation region tested at 60 °C (20X)

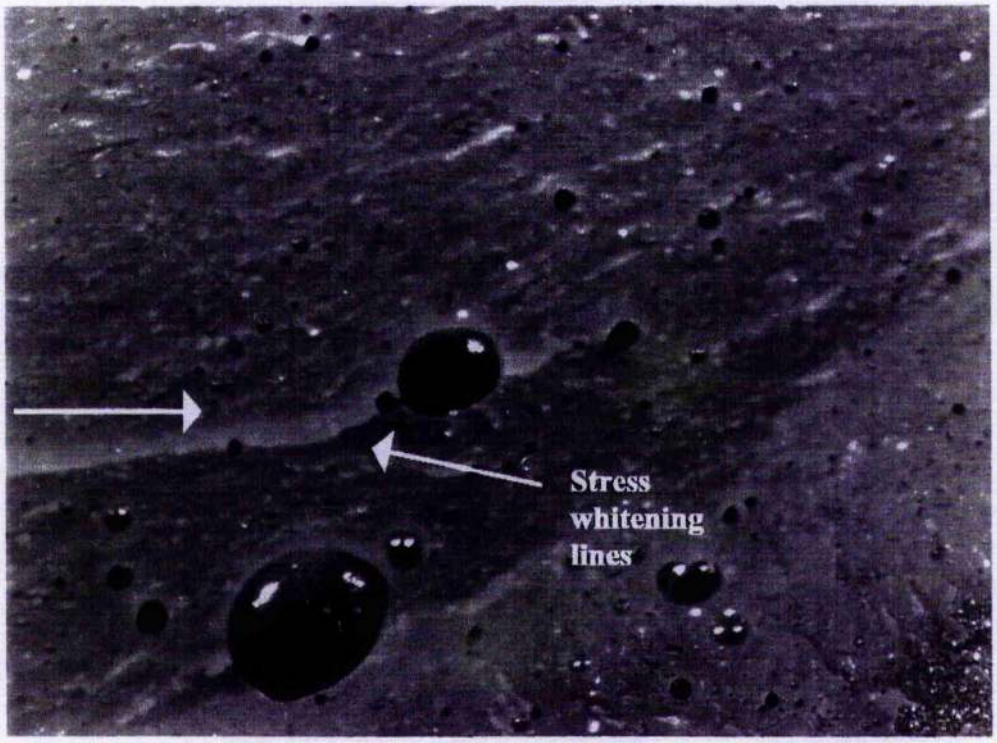

Fig.58 Fracture surface of XD4416 at end region tested at 60 °C (20X)

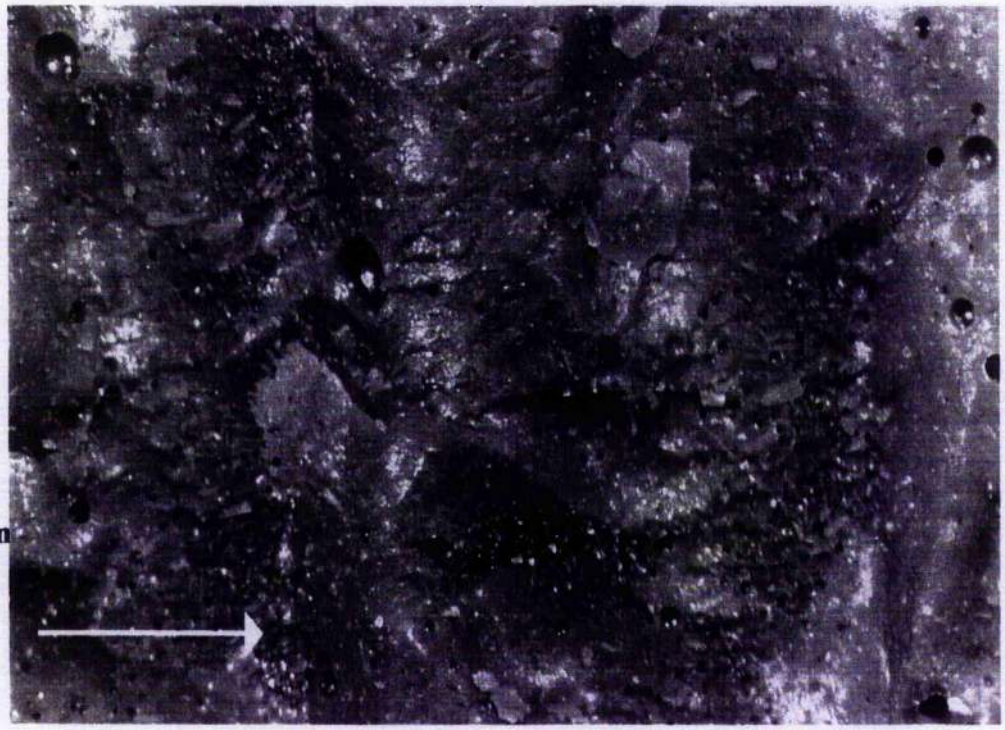

Fig.59 Fracture surface of XD4416 at initiation region tested at -40 °C (20X)

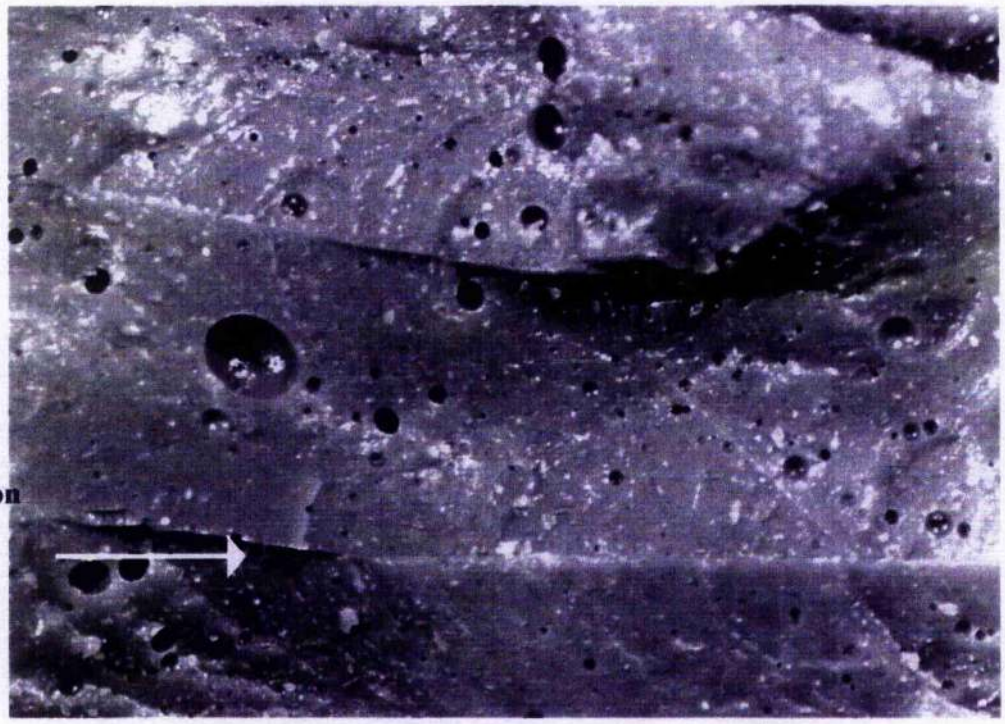

Fig.60 Fracture surface of XD4416 at end region tested at -40 °C (20X)

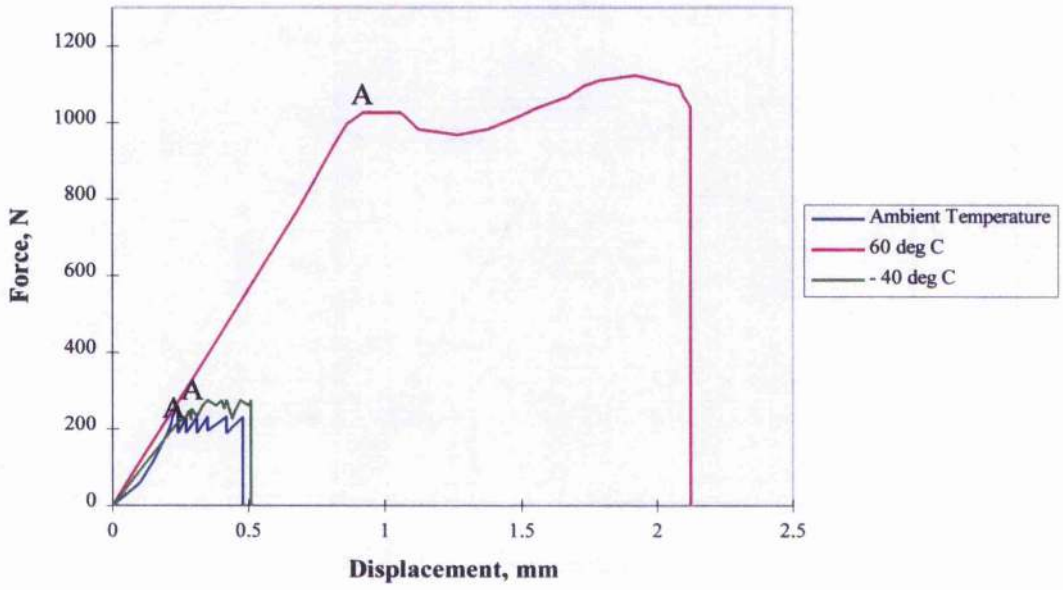

Fig.61 Comparison of the load against displacement graphs for XD 4416 tested at a series of temperatures.

4.6 Effect of Silane Coupling Agent on Fracture Strength

One method of improving the durability of adhesively bonded steel tapered double cantilever beam joints is to use a silane adhesion promoter. Silanes have been used for a number of years as primers or coupling agents[72], an early example of their use being to improve glass fibres and the resin matrix in glass-reinforced plastics. Silanes have been seen as an adhesion promoter, where the silane is applied to the substrate to be bonded to react with the substrate to form a more receptive surface for the adhesive and thus improve the bond strength. Fig.62 shows a comparison of two coupling agents namely Permabond Self Indicating Pretreatment (SIP) and Silquest A-187 which were evaluated for their effects on fracture strength. It can be seen that both Permabond SIP and A-187 produced a higher fracture strength compared to joints that were untreated. The surface treated with Permabond SIP recommended for F241 achieved the highest fracture strength. Work by Tod *et al.*[13] using mild steel single lap bonded joints showed that the correct choice of primer and adhesive combination has an adverse effect on strength and durability of a joint.

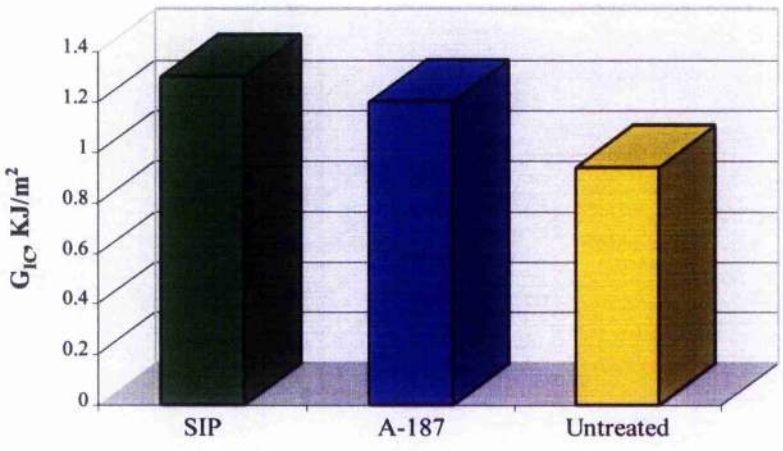

Fig.62 Comparison of fracture strength of both treated and untreated joints

The A-187 primer was applied to the steel surface using different concentration in water and ethanol. As can be seen in Fig.63, even this minor change had an effect on the fracture strength of the tapered double cantilever beam joints bonded with F241 and tested at ambient temperature. Of all concentrations studied, the 5% solution in water gave the highest fracture strength. It was observed that using water as a solvent gave the best results. However, during the drying of the specimens, the surface turns rusty and drying is slower than when ethanol is used, which dries rapidly with little or no traces of rust on the surface of the specimens. From the experiment it can be deduced that the concentration of the silane solution has an effect on the joint strength. Similar results were also obtained by Tod[13]. He found that an ethanol based solution, although essentially unaffected by 'solution age', produces bond strength significantly lower than the water based silane. Figs.64 and 65 show fracture surfaces for solutions with concentration in water and ethanol. Song[73] showed the peel strength of bonded joints was improved by applying three different silanes. The optimum strength varied with different silanes and concentration used.

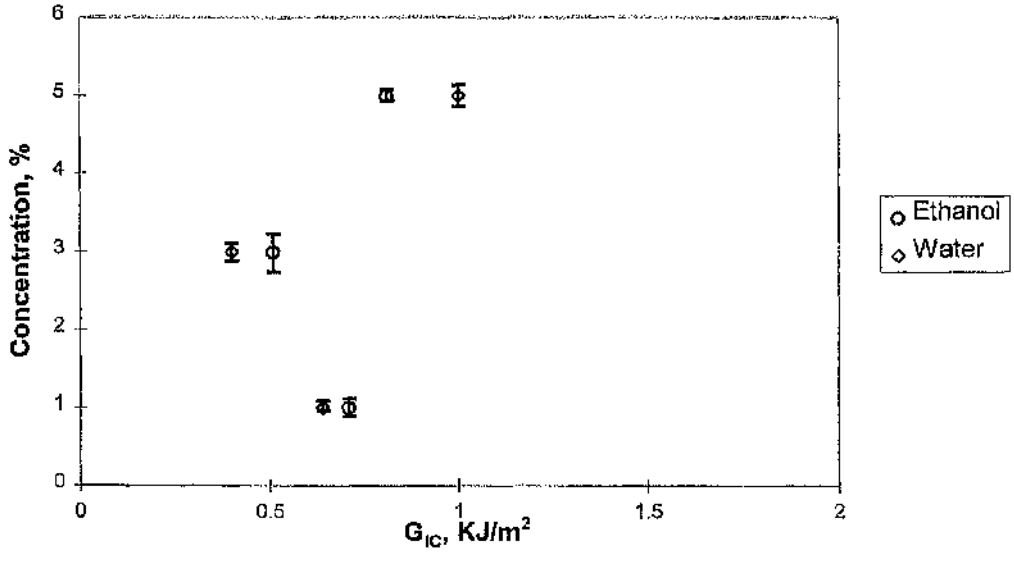

Fig.63 Effect of concentration of silane on fracture strength

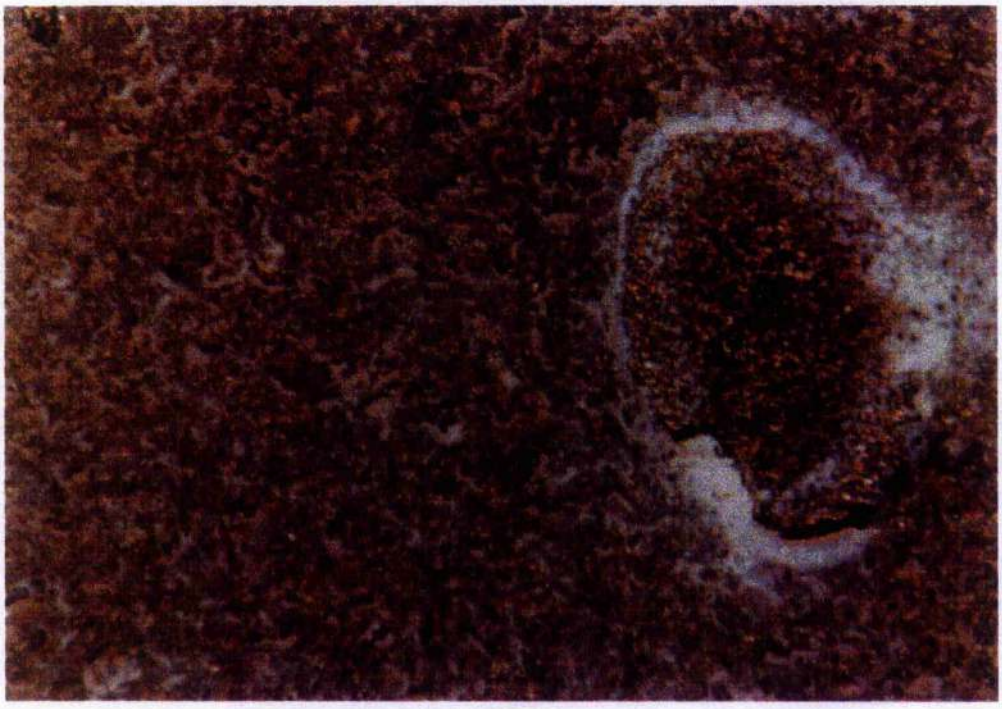

Fig.64 Fracture surface of F241 with silane coupling agent mixed with enthanol (20X)

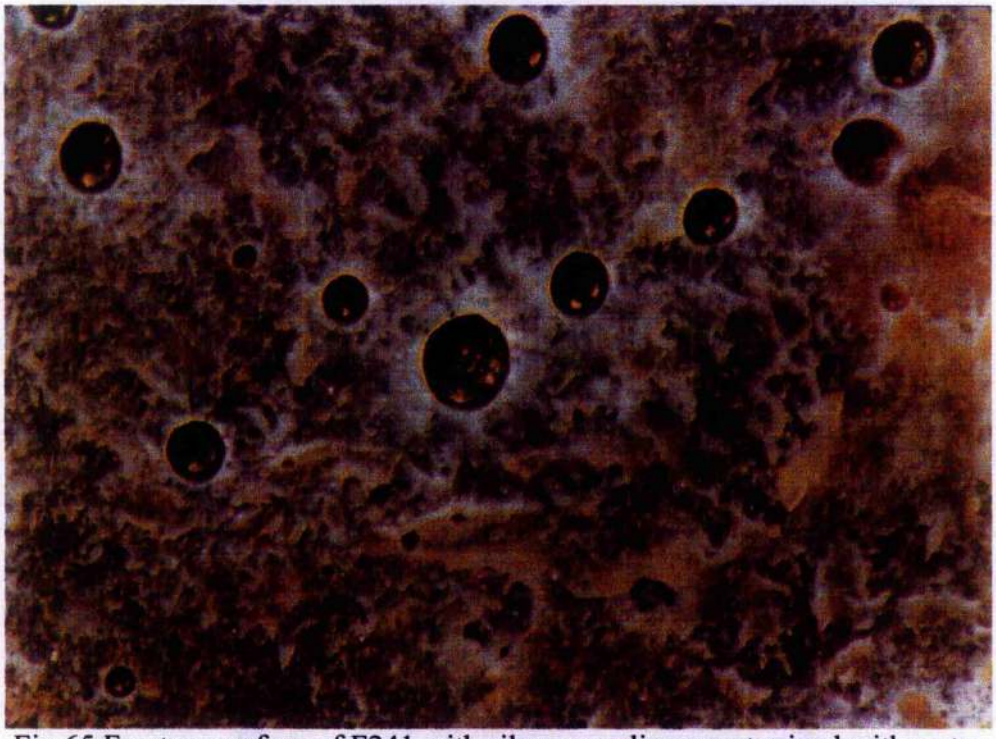

Fig.65 Fracture surface of F241 with silane coupling agent mixed with water (20X)

4.7 Fatigue Behaviour

The tapered double cantilever beam test specimen geometry was used to obtain the values of crack growth rate, da/dN, as a function of the maximum fracture energy release rate, Gmax and ΔG applied in the fatigue cycle. A sine wave loading form was employed at a frequency of 2 Hz. Gmax has be employed, as opposed to ΔG because the generation of surface debris, which prevents the crack from fully closing when it is unloaded, may give an artificially high value of Gmin. Thus, it has been suggested by Fernando[11] that it is better to use Gmax, instead of ΔG. Work by Sutton[74] implied that there is not a separate R ratio effect when characterising crack growth rate by ΔG. It is still unclear what mean stress effect needs to be taken account of when crack growth rate is correlated with Gmax.

Fig.66a-c, show the three different graphs of crack length versus number of cycles tested over a range of R ratios ranging from 0.13 to 0.17. The minimum load for each R ratio was kept constant throughout each experiments. The results showed that for each R ratio, three straight lines could be fitted to the data with the slope of lines representing the average fatigue crack growth rate. Comparing the data, it was observed that the deviation of the slope usually occurs at an initial crack length of approximately 100mm and then subsequently at approximately 140mm indicating that there is a possibility of crack growth rate dependence of the crack length. This change in crack growth rate occurred despite using a constant compliance geometry and a constant load range and maximum load.

Fig.67 show the crack growth rate data versus Gmax. The results showed a significant increase in crack growth rate when R ratio is decreased (maximum load increases). From the results reviewed from experiments conducted by Radon and co-worker[75], as well as the present study it is clear that ΔP and Pm are of considerable importance in influencing fatigue crack growth rate. It was also observed that the crack growth rate increases despite Gmax remaining constant for each of the three R ratios. The increase in crack growth rate may be due to non-linearity of the compliance curve. Jablonski[76] showed from his compliance curve that non-linearity usually occurs at a shorter crack length for lower yield strength adhesives. In this present study, Gmax was based on constant compliance. Thus, it can be concluded that the compliance may not always be constant. It is dependent on the adhesives used and the crack length. It is therefore important to obtain detailed compliance curves for the different adhesives used. Other possible explanations for the three regimes of crack growth rate include (i) the inadequacy of Gmax as the characterising parameter for fatigue crack growth rate (Knox[49] found a crack length/history effect), (ii) changes in the proportion of mode I loading and (iii) phenomenological changes in adhesive failure process.

From the test, it was also noted that catastrophic failure usually occurred at a critical length of approximately 196.6mm for the three R ratios. Only cohesive failure was observed on the fracture surface at all the different R ratios. Thus there was no dependence of the fatigue behaviour upon the surface pre-treatment when tested in a 'dry' environment. Similar failures were also obtained by other researchers where fatigue tests were conducted in 'dry' environments. They indicated that interfacial failure will increase with time of exposure to hostile environment[11,15].

Fatigue testing clearly shows the damaging effect of cyclic loading conditions compared to simply employing a constant rate of displacement to fracture the adhesive joint. Indeed, the value of the threshold fracture energy release rate, Gth, was far lower than the value of adhesive fracture energy, G_{IC}, which was obtained under monotonic loading, i.e. the value of Gth is about 0.25 KJ/m^2, whilst the value of the adhesive fracture energy, G_{IC}, is about 1.02 KJ/mm^2.

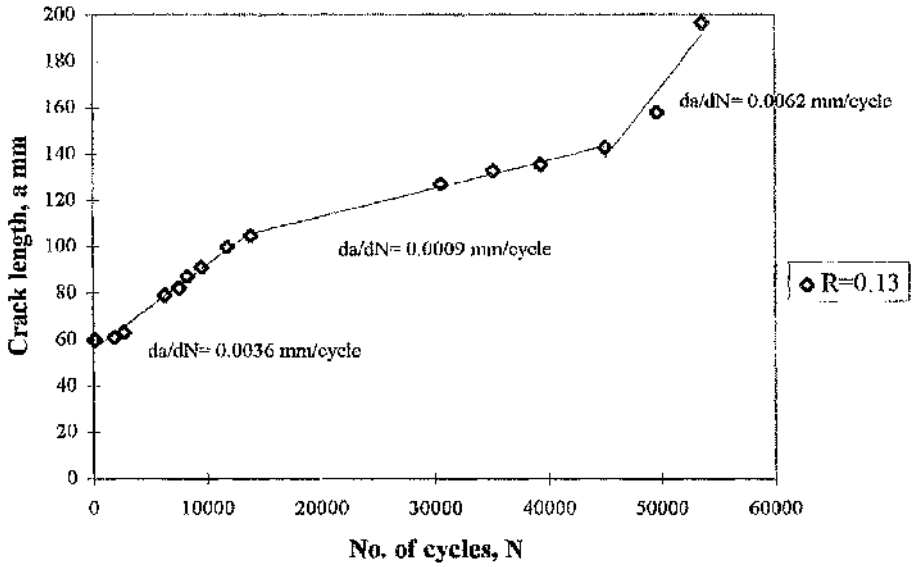

Fig.66a Crack length versus no. of cycles

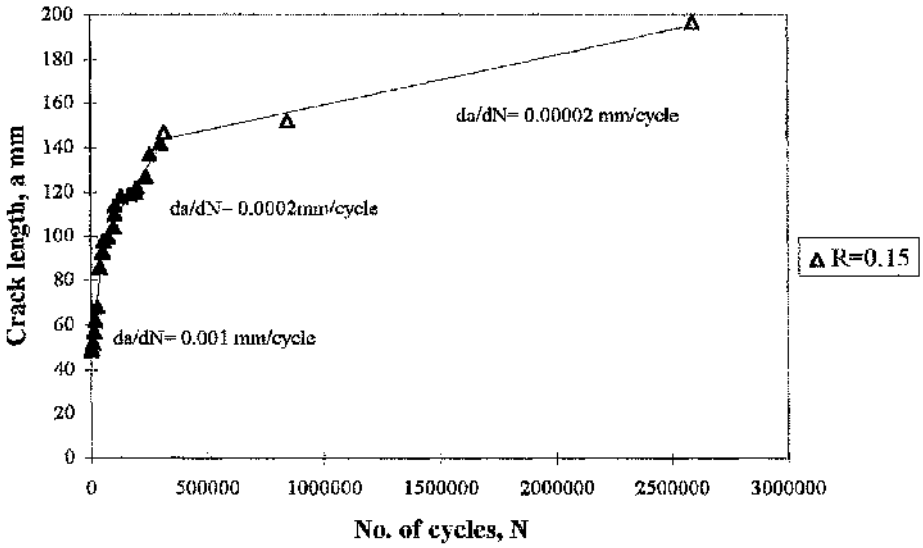

Fig.66b Crack length versus no. of cycles

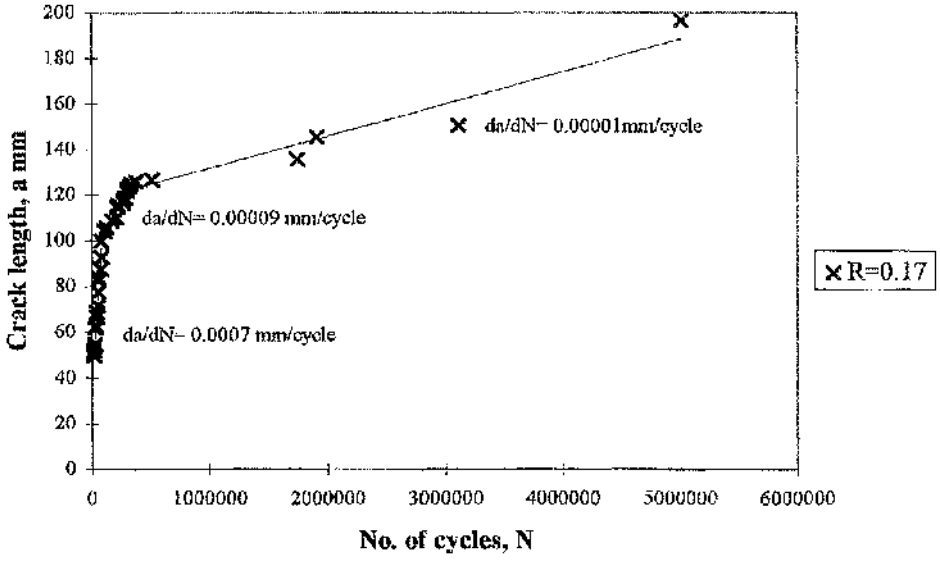

Fig.66c Crack length versus no. of cycles

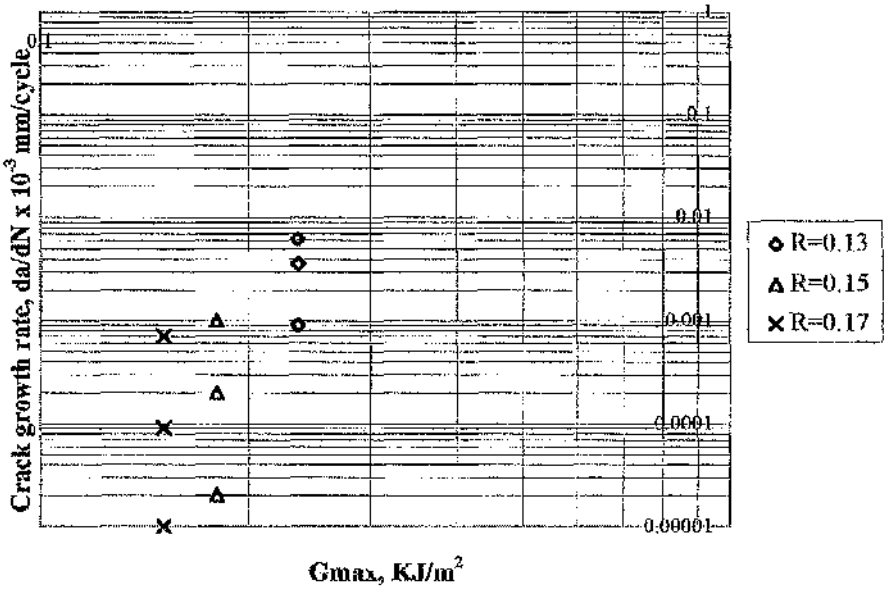

Fig.67 Crack growth rate versus Gmax for F241 tested in a "dry" environment for a series of R ratios.

Chapter 5

CONCLUSIONS

Fracture strength of cold curing adhesives

The different forms of cold curing adhesives that are commercially available have been identified and discussed. Comparing the three adhesives, the best results when tested in ambient temperature, were obtained from joints bonded with F241 followed by Araldite 2013. XD4416 exhibited the lowest fracture strength due to the post curing effect.

The loci of joint failure for the three cold curing adhesives were observed to be cohesive throughout the adhesive layer. Crack propagation was observed to take place by a 'stick-slip' mode on the fracture surface of XD 4416, indicating a very brittle adhesive which results in such low fracture energy release rate.

Effect of temperature of fracture strength of cold curing adhesives

Temperature has an effect on the fracture strength of the cold curing adhesives. The results clearly showed huge sensitivity to test temperature. In the vicinity of room temperature, F241 and Araldite 2013 adhesives exhibited high toughness, but as the temperature was increased to 60 °C the toughness reduced drastically. The toughness of XD4416 increased rapidly due to the enhanced curing at this temperature. This indicates that this adhesive is particularly suitable for use in higher temperature environment. At the low temperature of -40 °C, all of the adhesives exhibited low toughness.

Effect of silane coupling agents

The measured fracture toughness F241 on mild steel adherend was improved by incorporating of organosilanes as pre-bond primers. Experimental parameters such as the nature of the solvent employed to prepare the initial organosilane solution, the concentration of the primer solution and the choice of primer and adhesive. have been shown to be of important. Two different silane primers namely Permabond self indicating pretreatment (SIP) and A-187 were evaluated and compared. SIP was found to exhibit the highest fracture strength. And 5% solution of A-187, in water was found to give the excellent fracture strength.

Fatigue behaviour

A fracture mechanics approach has been successfully used to examine the cyclic fatigue behaviour of the bonded joints. As previously reported, cyclic fatigue tests conducted in a dry environment led to joint failure at far lower loads, and far lower values of the maximum fracture energy release rate, Gmax, applied in the fatigue cycle compared to the value of the adhesive fracture energy, Gmax, determined from monotonically loaded fracture tests[11].

The locus of joint failure was observed to be cohesive throughout the adhesive layer tested in the 'dry' environment. The effect of the R ratio on the fatigue crack initiation has been investigated but in the limited experimental programme the effect of changing R is combined with changes in Gmax and ΔG. It has not been possible to disassociate these variables. Crack growth rates were observed to decrease with crack length under nominally constant Gmax conditions.

Chapter 6

RECOMMENDATION FOR FUTURE WORK

It is clear that over the past decade there have been important developments in the understanding of fracture mechanics of adhesively bonded connections. It has been proven to be particularly useful for such aspects as characterising the toughness of adhesives, identifying mechanisms of failure and estimating the service life of 'damaged' structure being in the form of cracks, air filled voids, de-bonds rise from environmental attack and fatigue loading.

Nevertheless, there are still areas in the application of fracture mechanics to the failure of adhesive joints which are far from fully understood such as the various types of loading condition and environments which may adversely effect the service life of a bonded connection. Adhesive joints are frequently expected to perform satisfactorily under service conditions which include dynamically and statically applied loads under exposure to hostile marine environments. Thus, it is of prime importance to be able to develop and recommend suitable adhesive systems which will possess an adequate service life under these operating conditions. If the aims of reducing uncertainty of adhesive bonding are to be achieved, the following work are suggested for future studies :

(1) Durability test of TDCB bonded joints immersed in salt water over a period of time
(2) Fatigue test of TDCB bonded joints immersed in salt water over a period of time

(3) Effect of primer on durability and fatigue test of TDCB bonded joints

(4) Detailed examination of the fatigue crack growth phenomena under nominally constant Gmax conditions.

Appendices

Fatigue Crack Growth Rate Data

P max = 1.5 KN
P min = 0.2 KN

P max = 1.3 KN
P min = 0.2 KN

P max = 1.2 KN
P min = 0.2 KN

R=0.13		R=0.15		R=0.17	
a	No. of cycles	a	No. of cycles	a	No. of cycles
60	109	48.6	870	49.6	16005
61	1845	49	3785	51.6	17675
63	2700	52	11048	53.6	22199
79	6288	57	13136	54.6	25785
82	7532	62	19070	61.6	32372
87	8246	68	27800	62.6	40310
91	9528	86	38453	66.6	43884
100	11815	93	47874	68.6	45456
105	13866	98	54182	71.6	51465
108	24517	100	73979	77.6	53502
127	30540	104	97884	82.6	55745
133	35155	110	103859	83.6	60784
135.5	39352	114	105099	87.6	75108
143	45085	118	128649	92.6	78471
158	49661	119	169103	99.6	83590
196.6	53661	120	193379	104	106872
		122	199382	105.6	123503
		127	238796	108.6	170337
		137	252784	109.6	208605
		142	301016	114.6	215884
		147	316124	115.6	221186
		152	846861	116.6	267362
		196.6	2594119	117.6	269138
				118.6	278704
				121.6	294326
				122.6	299197
				123.6	318027
				124.6	337038
				125.6	373403
				126.6	505576
				135.6	1744844
				145.6	1908568
				150.6	3111533
				196.6	5012901

Input Data : **Pmax = 1.5**

Pmin = 0.2

Pmean = 0.85

R ratio = 0.13

R=0.13					
No. of cycles, N	**Crack length, a mm**	**dN**	**da**	**da/dN**	**Gmax**
1845	61	1736	1	0.576	0.236
2700	63	855	2	2.34	0.236
6288	79	3588	16	4.46	0.235
7532	82	1244	3	2.41	0.235
8246	87	714	5	7	0.236
9528	91	1282	4	3.12	0.236
11815	100	2287	9	3.94	0.240
13866	105	2051	5	2.44	0.236
24517	108	10651	3	0.282	0.236
30540	127	6023	19	3.15	0.236
35155	133	4615	6	1.3	0.236
39352	135.5	4197	2.5	5.96	0.236
45085	143	5733	7.5	1.31	0.236
49661	158	4576	15	3.28	0.235
53661	193.6	4000	38.6	9.65	0.235

Input Data : **Pmax = 1.3**

Pmin = 0.2

Pmean = 0.75

R ratio = 0.15

R=0.15					
No. of cycles, N	**Crack length, a mm**	**dN**	**da**	**da/dN**	**Gmax**
3785	49	2915	0.4	1.37	0.176
11048	52	7263	3	4.13	0.176
13136	57	2088	5	23.9	0.173
19070	62	5934	5	8.43	0.174
27800	68	8730	6	6.87	0.173
38453	86	10653	18	16.9	0.173
47874	93	9421	7	7.43	0.169
54182	98	6308	5	7.93	0.173
73979	100	19797	2	1.01	0.173
97884	104	23905	4	1.67	0.173
103859	110	5975	6	10	0.173
105099	114	1240	4	32.3	0.173
128649	118	23550	4	1.7	0.172
169103	119	40454	1	0.247	0.173
193379	120	24276	1	0.412	0.173
199382	122	6003	2	3.33	0.1763
238796	127	39414	5	1.27	0.173
252784	137	13988	10	7.15	0.173
301016	142	48232	5	1.04	0.173
316124	147	15108	5	3.31	0.173
846861	152	530737	5	0.0942	0.175
2594119	196.6	1747258	44.6	0.255	0.195

Input Data : **Pmax = 1.2**

Pmin = 0.2

Pmean = 0.7

R ratio = 0.17

R=0.17					
No. of cycles, N	**Crack length, a mm**	**dN**	**da**	**da/dN**	**Gmax**
17675	51.6	1670	2	12	0.1512
22199	53.6	4524	2	4.42	0.1514
25785	54.6	3586	1	2.8	0.1515
32372	61.6	6587	7	11	0.1511
40310	62.6	7938	1	1.26	0.1509
43884	66.6	3574	4	11.2	0.1508
45456	68.6	1572	2	12.7	0.1512
51465	71.6	6009	3	5	0.1513
53502	77.6	2000	6	30	0.1510
55745	82.6	2243	5	22.3	0.1508
60784	83.6	5039	1	2	0.1509
75108	87.6	14324	4	2.8	0.1511
78471	92.6	3363	5	15	0.1510
83590	99.6	5119	7	13	0.151
106872	102.6	23282	3	1.29	0.1508
123503	105.6	16631	3	1.8	0.1504
170337	108.6	46834	3	0.64	0.1510
215884	114.6	7279	6	8.2	0.1509
221186	115.6	5302	1	1.89	0.1507
278704	118.6	57518	3	0.52	0.1507
294326	121.6	15622	3	1.92	0.152
299197	122.6	4871	1	2.05	0.1508

318027	123.6	18830	1	0.53	0.1508
337038	124.6	19011	1	0.53	0.1509
373403	125.6	36365	1	0.0275	0.1509
505576	126.6	132173	1	0.0756	0.150
1744844	135.6	1239268	9	0.0726	0.150
1908568	145.6	163724	10	0.611	0.151
3111533	150.6	1202965	5	0.0416	0.151

References

1. Hashim, S.A., Winkle, I.E., Knox, E.M. and Cowling, M.J, 'Adantages of adhesive bonding in offshore and marine application', Chapter 19, Integrity of offshore structures - 5, Eds Faulkner, D., Cowling, M.J., Incecik, A. and Das, P.K., Published by EMAS, 1993
2. Kemp, P.W. 'Some practical applications', Proc. Int. Conference on Structural Adhesive in Engineering, IMech.E.,London, 1989
3. Semerdjiev, S., 'Metal to metal adhesive bonding', Business Book Limited, London, 1970
4. Lees, W.A. 'Bonding of composites', Bonding and repair of composites, Proc. RAPRA 1989, Butterworths, 1989
5. Lee, W.A., 'Adhesive in engineering design', London: Region Council, 1984
6. Aitken, D.F., Blit, M.A., 'Engineer's Handbook of Adhesive', Brighton Machinery publishing, 1972
7. Bascom, W.D., Cottington, R.L and Timmons, C.O., 'Fracture design criteria for structural adhesive bonding - Promise and Problem', Naval Engineers Journal, August 1976
8. Mostovoy, S. and Ripling, E. J., 'Adhesion science and technology', Plenum press, New York, 1975, p514
9. Mostovoy, S. and Ripling, E.J., 'Flaw tolerance of a number of commercial and experiment adheisve' Material research laboratory, Inc.
10. ASTM standards D3433-93, Standard test method for fracture strength in cleavage of adhesives in bonded metal joints, p218
11. Fernando, M., Harjoprayitno, W.W. and Kinloch, A.J., 'A fracture mechanics study of the influence of moisture on the fatigue behaviour of adhesively bonded aluminium alloy joints.' Int. J. Adhesion and Adhesives 16, 1996, p113-119
12. Pocius, A.V., 'Adhesion and Adhesives Technology An introduction', Hanser publishers, 1997

13. Tod, D.A., Atkins, R.W. and Shaw, S.J., 'Use of primers to enhance adhesive bonds', Int. J. Adhesion and Adhesives, 12, 3, July 1992, p159-163
14. Gledhil, R.A, Shaw, S.J. and Tod, D.A., 'Durability of adhesive bonded joints employing organosilane coupling agents', Int. J. Adhesion and Adhesives, 10, 3, July 1990, p192-198
15. Kinloch, A.J., 'Adhesion and Adhesives' Science and Technology, Chapman & Hall, 1994
16. Lees, W.A., 'Recent development in composite bonding with particular reference to large structures and unprepared surfaces', Technical Director, Permabond Division, National Starch and Chemical Limited, 1989
17. Handbook of Adheisves, Skeist, 1990
18. Zalucha, D.J., Adhes. Age, 15(2):21, 1972
19. Minford, J.D., unpulished work, Aluminium co. of America
20. Minford, J.D., 'Durability of adhesive bonded aluminium joints, Treatise on Adhesion and Adhesives (Patrick, R.L. *ed.*), Marcel Dekker, New York, 3, 1973, p91-92
21. Minford, J.D., Adhesive bonded aluminium joints, Treatise on Adhesion and Adhesives (R.L. Patrick, ed.). Marcel Dekker, New York, Basel, 3, 1973
22. Critchlow, G.W. and Brewis, D.M., 'Influence of surface macro-roughness on the durability of epoxide-Aluminium joints', Int. J. Adhesion and Adhesives, 15, 3, 1995
23. Maxwell, J.W., Trans Am. Soc. Mech. Engs. 67:104, 1945
24. Boroff, E.M. and Wake, W.C., Trans. Inst. Rubber Ind. 199,210, 1949
25. Perrins, L.E. and Pettett, K., Plastic and Polymer 39:391, 1971
26. Packham, D.E., Adhesion - 7 (Alner, D.J. and Allen, K.W. *eds.*), Transcripta Books, London, 1973, p51
27. Chen, J.M., Sun, T.S. and Venables, J.D., Natl. SAMPLE Sump. Exhib. 22:25, 1978

28. White, H.W., Godwin, L.M. and Elliatroglu, R.J., J. Adhes. 13:177, 1981
29. Evans, J.R.G. and Packham, D.E., J. Adhes. 11:177, 1979
30. Eick, J.D., Good, R.J., Newman, A.W. and Fromer, J.R., J.Adhes. 3:23, 1971
31. Knott, J.F., 'Fundamentals of fracture mechanics', Butterworths, London, 1969
32. Williams, J.G.,' Stress analysis of polymer' 2nd edition, Ellis Horwoud, Chichester, 1980
33. Gent, A.N., Rubb Chem. Technol. 47, 1974
34. Kinloch, A.J. and Shaw, S.J.,' Developments in adhesives - 2' edited by Kinloch, A.J., Applied Science Publishers, London, 1981
35. Anderson, G.P., Bennett, S.J. and Devries, K.L, 'Analysis and testing of adhesive bonds', Academic press, New York and London, 1977
36. Irwin, G. R. (1973) Applied Material Res. 3, 65
37. Giffith, A.A. (1920). Phil. Trans. Roy. Soc. A221, 163
38. Orowan, E. (1948) Report. Prog. Phys. 12, 183
39. Mostovoy, S. and Ripling, E.J., Appl. Polymer Sci, 10, 1966, p1351
40. Westergaard, H. M. (1939) J. Appl. Mech. 30, 232
41. Ripling, E.J., Mostovoy, S., and Patrick, R.L., Materials Research and Standards, 4, 3, 1964, p129-138
42. Irwin, G.R., Treatise on Adhesion and Adhesives, vol.1, R.L. Patrick, Ed., Marcel Dekker, Inc., 1967, p223-268
43. Mostovy, S. and Ripling, E.J., Polymer Science and Technology, 9B, 1975, p513-561
44. Trantic, G.G., Journal of Composite Materials, 6, 1972, p371-385
45. Gilman, J.J., Fracture, B.L. Averbach *et al. eds.*, Massachusetts Institute of Technology Press, Cambridge, Mass., 1959, p193-224
46. Ripling, E.J., Mostovoy, S., and Corten, H.T., Journal of Adhesion, Vol.3, 1971, p107-123

47. Broutman, L.J. and McGarry, F.J., J. Applied Polymer Sci, 9, 1965, p609
48. Bascom, W.D, Cottington, R.L. Jones and Peyser, P., J.Appl. Polymer Sci, 19, 1975, p2545
49. Knox, E.M., Cowling, M.J. and Hashim, S.A., 'Fatigue performance of adhesively bonded steel connections for marine structures', SAE, Structural Adhesives in Engineering IV, 1995
50. Albrecht, P., Journal of structural engineering, ASCE 113, 1987
51. Martin, D.M., PHD, Thesis, University of Dundee
52. Falcon, A.S. and Miller, J.E., J. Appl. Polym Sci., Polym Symp. 32:247, 1977
53. Herczeg, A., Ronay, G.S. and Simpsom, W.C., Surface chemical characteristics of epoxy resins, Nat. SAMPE Tech. Conf. On Aerospace Adhesives and Elastomers, p221, 1970
54. Bishop, J.A., Sim, E.K., Thompson, G.E. and Wood, G.C., 'The adhesively bonded aluminum joint: The effect of pre treatment on durability', J. Adhes. 26:237, 1988
55. Waldman, A., 'Silane coupling agents improve performance', Osi specialities Inc. Tarrytown, N.Y.
56. Walker, P., Wilson, A.D, Nicholson, J.W. and Prosser H.J., 'Surface Coating', Elsevier, Applied Science Publishing,1987
57. Shaw, S.J.,Todd, D.A. and Griffith, J.R. and Lee L.H., 'Adhesives, sealant and coatings for space and harsh environments', Plenum, 1988
58. BS 18 : 1987 British Standard : Method for Tensile Testing of Materials
59. Jeandrau. J. P., 'Analysis and design data for adhesively bonded joints', Int. J. Adhesion and Adhesives, 11, 2, April 1991
60. BS 2782 : Part 3 : Method 322 : 1994 : ISO 527-2:1993 : Plastics-Mechanical properties
61. Bell, A.J., Kinloch, A.J. and Wang, Y., 'Effect of adherend type upon the adhesive mode I fracture energy of DCB joints'

62. Gledhill, R.A., Kinloch, A.J., Yamini, S. and Young, R.J., Polymer 19, 1978
63. Kinloch, A.J., Shaw, S.J., Tod, D.A. and Hunston, D.L., Polymer 24, 1983
64. DeBruyne, N.A., 'The extent of contact between glue and adherend, Bull. no.168,Tech. Service Dept., Aerospace Research Ltd., Duxford, Cambridge, 1956
65. Bascom, W.D., 'The origin and removal of microvoids in filiment wound composites', NRL Report 6268, 1965
66. Young, R.J. and Beaumont, P.W.R., J. Mat. Sci., 11, 1976
67. Selby, K. and Miller, L.E., J. Mat. Sci., 5, 1970
68. Philips, D.C., Scott, J.M. and Jones. M., J. Mat. Sci., 13, 1978
69. Mallick, V. 'Stress analysis of metal/CFRP adhesive joints subjected to the effects of thermal stress', PHD thesis, University of Bristol, 1989
70. Lees, W.A., 'Advances in adhesives, Application, Materials, and Safety', (Brewis, D.M. and Comyn, J. *eds.*), Warwick Publishing, Birmingham, 1982
71. Al-Handan, H. 'Thermal stress in bonded joints', MSc thesis, University of Bristol, 1989
72. Plueddemann, E.P. 'Silane Coupling Agents' Plenum, New York, NY, USA, 1982
73. Song, S.M., Park, C.E., Yun, H.K., Oh, S.Y. and Park, J.M., 'Adhesion improvement of epoxy resin to alloy 42 lead frame by silane coupling agents', J.adhesion sci. Technol., 11, 6, 1997
74. Sutton, S.A., 'Fatigue crack propagation in an epoxy polymer',
75. Arad, S., Radon, J.C. and Culver, L.E., 'Fatigue crack propagation in polymethy/methacrylate; The effect of the mean value of stress intensity factor' I. Mech. Eng. Sci. 13, 2, 1971
77. Jablonski, D.A., 'Fatigue crack growth in structural adhesives', J. Adhes. 11:125, 1980